

An Underwater Neutral-Buoyancy Telerobot for Zero-Gravity Simulation with Attitude Control and Automatic Balancing

by

KURT D. EBERLY

S.B. Aeronautics and Astronautics, Massachusetts Institute of Technology
(1989)

Submitted to the Department of Aeronautics and Astronautics in partial fulfillment of the requirements for the degree of

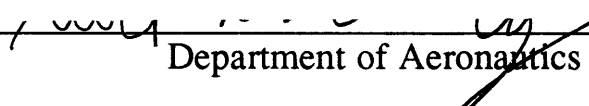
MASTER OF SCIENCE IN AERONAUTICS AND ASTRONAUTICS

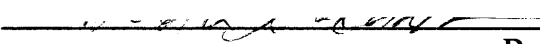
at the

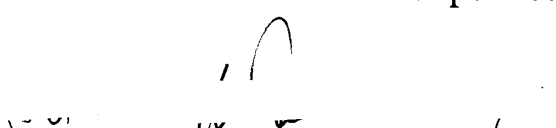
MASSACHUSETTS INSTITUTE OF TECHNOLOGY

September 1991

©1991, Massachusetts Institute of Technology

Signature of Author 
Department of Aeronautics and Astronautics
August 28, 1991

Certified by 
Professor Harold L. Alexander
Thesis Supervisor

Accepted by 
Professor Harold Y. Wachman
Chairman, Department Graduate Committee



Aero

An Underwater Neutral-Buoyancy Telerobot for Zero-Gravity Simulation with Attitude Control and Automatic Balancing

by

Kurt D. Eberly

Submitted to the Department of Aeronautics and Astronautics in partial fulfillment of the requirements for the degree of Master of Science in Aeronautics and Astronautics

Abstract

This thesis documents the design, construction, and testing of a neutral-buoyancy robot to be used as a zero-gravity simulator for space robotics research in the Laboratory for Space Teleoperation and Robotics (LSTAR). The robot was primarily designed to support the development of autonomous, vision-based vehicle navigation and control. In a secondary role, it was also designed to support research of operator-vehicle visual interfaces to provide verification of results obtained from virtual-environment experimentation.

The robot design was based on neutral-buoyancy robots previously built by the Space Systems Laboratory. Several design improvements were undertaken to remedy problems discovered during past neutral-buoyancy testing. The most notable of these improvements is the design of an automatic balancing subsystem.

An attitude control system was implemented to demonstrate the controllability of the robot. The performance of the control system was evaluated through the measurement of system response to the application of step inputs. The control system was found to be fast and powerful.

A program of pool testing and checkout was administered upon construction of the robot. The robot design was found to be successful in producing a neutral-buoyancy simulation testbed for space robotics research that improved upon past SSL vehicle designs.

Thesis Supervisor: Harold L. Alexander
Title: Bradley Career Development
Assistant Professor of Aeronautics and Astronautics

Acknowledgements

I would like to thank myself, first of all, for not succumbing to my inherently lazy leanings.

I thank my parents for their unwavering spiritual and financial support during my whole stay at MIT. Every son should be so lucky.

Thanks go to Sandy for being involved and caring. Best of luck in all things smutty!

Thanks to the whole nefarious crew at the ole LSTAR. In particular, I offer my undying gratitude to Harald and Paul, who really put out some hard wares. Also, thanks to Mike for the software and the music, Matt for his help and for having good dreams and for not being bashful about describing them. Rob, thanks for the advice and the excellent food - a rare combination.

Thanks go the former SSL'ers, namely Jud and Russ and Dave, for answering my pesky questions about why, why, why, and, occasionally, why not.

Thanks to all the N^o6ers, especially Daniele, for keeping me getting too nerdy. Resist ye temptation, my sisters and brothers, guided by the light of Saint Anthony.

Thanks to Don and Earle, without whose expertise and caring STAR would not have happened.

Thanks to the LMP guys, Kevin and Fred, for their help. Thanks especially to Keving for slaving over a hot lathe making the ducts.

Thanks to Ping for all of her extraordinary help.

Dedication

This thesis is dedicated to the memory of Joseph Han Joon Shinn.

Table of Contents

List of Figures.....	9
1 Introduction.....	12
1.0 Introduction.....	12
1.1 Background.....	13
1.2 Thesis Overview.....	15
2 System Design.....	16
2.0 Research Goals.....	16
2.1 Requirements.....	17
2.1.1 Autonomous Vehicle Navigation and Control.....	17
2.1.2 Operator-Vehicle Visual Interface Research.....	20
2.1.3 Other Requirements.....	21
2.2 Partition of System.....	23
2.2.1 Computer/Electronics.....	23
2.2.2 Propulsion.....	24
2.2.3 Balancer.....	24
2.2.4 Vision.....	25
2.2.5 Sensor.....	27
2.2.6 Power.....	28
2.2.7 Pressure.....	28
2.2.8 Structure.....	29
3 Subsystem Design.....	31
3.1 Computer/Electronics.....	31
3.1.1 Computer.....	32
3.1.2 QNX Operating System.....	33
3.1.3 Electronics Bus.....	34

3.1.4	PC-bus to STD-bus Interface Circuit	35
3.1.5	A/D Conversion Circuit	40
3.1.6	Medium-Power Switching Circuit	40
3.1.7	Thruster Motor Control Circuits.....	41
3.1.8	Balancer Motor Control Circuit.....	43
3.1.9	Network Hub Card	45
3.1.10	Patch Board.....	45
3.2	Propulsion	47
3.2.1	Motor Driver Circuit.....	47
3.2.2	Thruster Duct	50
3.2.3	Construction	52
3.3	Balancer	58
3.3.1	Sizing.....	58
3.3.2	Actuation.....	59
3.3.3	Electronics.....	60
3.3.4	Balancer Motor Driver Circuit	60
3.3.5	Enclosure	61
3.3.6	Construction	63
3.4	Vision.....	65
3.4.1	Camera System Design.....	65
3.4.2	Enclosure	68
3.5	Sensors	70
3.5.1	Angular Rate Sensors.....	70
3.5.2	Accelerometers	71
3.5.3	Sensor Mount.....	71
3.6	Power.....	73
3.6.1	High-Current Power	74
3.6.2	Low-Current Power	75
3.6.3	Battery Chargers	77
3.7	Pressure.....	80

3.8	Structure.....	83
3.8.1	Pressure Vessel	86
3.8.2	Computer/Electronics Drawer	93
3.8.2	Battery Drawers.....	96
3.8.3	Rear Structure.....	101
3.8.4	Side Mounting Structures	101
3.8.5	Top/Bottom Mounting Structures	106
3.9	Control Station.....	106
4	Control Systems	113
4.1	Balancer Control System	113
4.1.1	Hardware.....	113
4.1.2	Implementation	114
4.2	Attitude Control System	116
4.2.1	Hardware.....	116
4.2.2	Implementation	116
5	Results.....	118
5.1	Testing	119
5.1.1	February 9, 1991.....	118
5.1.2	June 8, 1991.....	119
5.1.3	July 6, 1991	119
5.1.4	July 20, 1991	120
5.1.5	August 3, 1991	120
5.1.6	August 17, 1991	121
5.2	Attitude Control Data.....	121
6	Conclusion.....	125
	References.....	127
	Appendix A	
	Drawings.....	130

Appendix B

Electronics.....	143
B.1 STD - Bus.....	143
B.2 A/D Card.....	144
B.3 D.C. Driver Card	145
B.4 Rate Sensors.....	146
B.5 Accelerometers.....	147

Appendix C

Software.....	148
A.1 Balancer Control Code	148
A.2 Attitude Control Code	158

List of Figures

Figure 3.1	PC-bus to STD-bus Interface: STD Card	36
Figure 3.2	PC-bus to STD-bus Interface: PC Card.....	39
Figure 3.3	Thruster Motor Controller Circuit.....	42
Figure 3.4	Balancer Motor Controller Circuit.....	44
Figure 3.5	Patch Board.....	46
Figure 3.6	Thruster Motor Driver Circuit.....	49
Figure 3.7	Motor Driver and Heat Sink Assembly	51
Figure 3.8	Thruster Duct Cross Section.....	53
Figure 3.9	Electric Thruster Motor With Modifications.....	54
Figure 3.10	Thruster Assembly Without Grilles.....	56
Figure 3.11	Thruster Assembly With Grilles	57
Figure 3.12	Balancer Motor Driver Circuit	62
Figure 3.13	Balancer Assembly	64
Figure 3.14	Balancer Assembly and PVC Tube	66
Figure 3.15	Photograph of Balancer Assembly and PVC Tube.....	67
Figure 3.16	Sectional View of Camera and Housing.....	69
Figure 3.17	Detail of Rate Sensor Mounting	72
Figure 3.18	Sensor Subsystem Assembly	72
Figure 3.19	High-Current Power System Layout.....	76
Figure 3.20	Low-Current Power System Layout.....	78
Figure 3.21	Photograph of Battery Recharger Case	79
Figure 3.22	Side Section View of Regulator Second Stage	81
Figure 3.23	Top and Bottom Views of Modified Second Stage.....	82
Figure 3.24	Pressure Subsystem Layout	84
Figure 3.25	Rear View of Pressure Vessel.....	87

Figure 3.26	Side View of Pressure Vessel.....	88
Figure 3.27	Rear Section View of Pressure Vessel Compartments.....	89
Figure 3.28	Electronics Drawer	94
Figure 3.29	Top View of Electronics Drawer Layout	95
Figure 3.30	Photograph of Interior of Electronics Drawer.....	97
Figure 3.31	Photograph of STAR With Opened Electronics Drawer ..	97
Figure 3.32	Battery Drawer Layout.....	98
Figure 3.33	Photograph of Opened Battery Drawer.....	99
Figure 3.34	Photograph of STAR with Opened Battery Drawer.....	100
Figure 3.35	Rear Box Tube Structure	102
Figure 3.36	Front View of Side Mounting Structure.....	103
Figure 3.37	Side View of Side Mounting Structure.....	104
Figure 3.38	Bottom View of Side Mounting Structure	105
Figure 3.39	Side View of STAR Thruster and Balancer Layout	107
Figure 3.40	Rear View of STAR Thruster and Balancer Layout	108
Figure 3.41	Top View of Top Mounting Structure	109
Figure 3.42	Bottom Mounting Structure.....	110
Figure 3.43	Photograph of Left Side of STAR	111
Figure 5.1	Integrated Rate vs. Time.....	122
Figure 5.2	Control Command vs. Time	123
Figure 5.3	Angular Rate vs. Time.....	123
Figure A.1	Balancer Motor Disk	130
Figure A.2	Balancer Lead Screw Mounting Disk.....	131
Figure A.3	Balancer Weight.....	132
Figure A.4	Camera Housing Tube Flange	133
Figure A.5	Camera Housing Front Disk	134
Figure A.6	Camera Housing Back Disk	135
Figure A.7	Coaxial Pass-Through Plate for Electronics Door.....	136
Figure A.8	Connector Hole Details	137

Figure A.9 Battery Compartment Door.....	138
Figure A.10 Electronics Compartment Door.....	139
Figure A.11 Electronics Compartment Door Connector Hole Layout .	140
Figure A.12 Battery Compartment Door Connector Hole Layout.....	141
Figure A.13 Electronics Compartment Door Connector Hole Layout .	142

1.0 Introduction

At present, every orbital system employs humans for physical tasks such as construction, servicing, inspection, and repair of its components. In the future, it is hoped that remotely-controlled, freely-flying space robots will be capable of performing these tasks, decreasing costly and dangerous astronaut-EVA time. These space robots are envisioned to be controlled in one of three ways: automatically; via human teleoperation; or by some combination of the two. Initially, the human teleoperation mode of control is likely to be spatially local -- meaning that the remote operator is within several kilometers of the robot -- in order to eliminate the effects of communication delays resulting from large transmission distances. This implies that, for orbital teleoperation tasks, the operator is located in a space vehicle, such as NASA's shuttle, while controlling a robot nearby. It is hoped, however, that research will eventually focus on teleoperator control of orbital robots from the surface of the Earth. This would require a complex human-robot interface that would somehow compensate for the unavoidable seconds-long communications delay.

Due to the extreme impracticality of performing space telerobotic research in the environs of outer space, ground-based simulation has become the accepted mode of experimentation. Of the many ground-based systems available, neutral-buoyancy simulation provides the closest approximation to outer space possible. Neutral-buoyancy simulation is performed by making the simulated system -- such as a telerobot, a human in EVA-suit, or a satellite -- be neutrally buoyant underwater. Also, through appropriate relative placement of the center of gravity and the center of buoyancy of the system, a neutral-attitude condition is imposed. In this way, full six degrees of freedom are attained.

Obviously, the simulated system's motion dynamics are quite different from reality due to the high viscosity of water. For example, humans

performing EVA tasks in neutral-buoyancy simulation can move their bodies by flapping their arms and legs -- a possibly dangerous discrepancy when training astronauts. For vehicle control research, water introduces damping to the system; thus, a control system which is stable during neutral-buoyancy simulation may be unstable when reproduced in outer space. Despite these difficulties of working in a viscous medium, neutral-buoyancy simulation is viewed as an invaluable research tool for space systems development.

1.1 Background

Since 1983, the Space Systems Laboratory (SSL) under Professor David Akin at the Massachusetts Institute of Technology has been a pioneer in the development of teleoperated space robot simulators for neutral-buoyancy research. Hardware testing was performed at MIT's Alumni Pool, while most experimentation was carried out during an annual trip to NASA-Marshall's neutral-buoyancy facility in Huntsville, Alabama. The SSL performed its space telerobotics research using three neutral-buoyancy vehicles, which are described here briefly to provide the reader with some understanding of the present state-of-the-art in neutral-buoyancy simulators.

The first vehicle to be built was the Beam Assembly Teleoperator (BAT), which was built in 1983 [1,2]. To perform the beam-assembly operations for which it was designed, BAT used two manipulators: one five degree of freedom dextrous manipulator, which was slaved to a remote master arm controlled by the operator; and one one fixed grasping arm. BAT was capable of supporting remote operator vision feedback research with its two separate camera systems: a fixed, belly-mounted stereo camera system; and a tilt-and-pan stereo camera pair that could be slaved to a head-tracking linkage attached to the operator.

The second vehicle developed in the SSL was the Multi-mode Proximity Operations Device (MPOD), built in 1984 [3]. MPOD was designed with an onboard control panel to allow for control by a SCUBA-wearing driver. This allowed for comparisons between on-board control and teleoperation

from a pool-side control station. It was outfitted with a docking probe which, when used with a satellite mockup on the pool's wall, permitted docking tasks to compare the two control modes. Later in its development, MPOD was fitted with the Three-Dimensional Acoustic Positioning System (3-DAPS) [4] for navigation with the ultimate goal of performing autonomous docking. 3-DAPS measured the transmission delays of synchronized acoustic pulses to provide vehicle position updates. Generated by eight thumpers arranged on the pool walls, the acoustic pulses were detected by four hydrophones attached to the vehicle.

The third vehicle constructed at MIT by the SSL was named the Apparatus for Space TeleRobotic Operations (ASTRO), built in 1986 [5]. While not having any of the features of the earlier two vehicles, such as manipulators, extensive vision systems, or position sensing, ASTRO was intended to research various control schemes. Closed-loop depth control was to be effected using pressure transducers to sense depth; closed-loop attitude damping was achieved using rate gyros to sense rotation. While never implemented, closed-loop angular velocity control of each of ASTRO's thrusters was possible since each thruster motor was constructed with an optical encoder to sense shaft rotation.

In 1990, Professor Akin accepted a professorship at the University of Maryland, taking the three telerobotic vehicles discussed above with him. Professor Harold Alexander assumed leadership of neutral-buoyancy research at MIT with the formation of the Laboratory for Space Teleoperation and Robotics (LSTAR). To provide a testbed for further space teleoperation research, a new neutral-buoyancy vehicle was mandated. To prepare a preliminary vehicle design, Professor Alexander administered a graduate design class (16.601 - Advanced Space Robotics) at MIT in the spring semester of 1989. The final design reports from each student, while far from complete, were valuable as a starting point for the design of the new vehicle, named the Submersible for Telerobotic and Astronautical Research (STAR).

This thesis documents the design, construction, and testing of STAR. The design phase extended from September, 1989, through January, 1990. At this time, construction of the vehicle's structural components was started

and lasted until December, 1990. From January, 1991, up to June, 1991, construction, integration, and testing of all subsystems occurred simultaneously. June 8, 1991, saw the first pool test integrating the various subsystems. Further development and testing of the vehicle continued through the summer of 1991 up to the time of this writing.

1.2 Thesis Overview

Chapter two describes the design of STAR. The first section discusses how the system requirements were derived from the research goals of the LSTAR. The second section of Chapter two introduces the system's nine subsystems. In Chapter three, the design and construction of each subsystem is detailed, beginning with a discussion of similar subsystems used in the SSL vehicles. The final choice of subsystem design is then presented, followed by a description of any pertinent construction details. Results of subsystem testing follow, accompanied by photographs of the hardware.

Chapter four presents the two control systems that were developed and tested by the time of this writing. Section one details the balancer control system. Section two illustrates the vehicle attitude control system.

Chapter five describes the program of testing and checkout which sought to verify the operational status of STAR and subsequent suitability for neutral-buoyancy experimentation. Data taken during testing of the attitude control system is presented and analyzed. Conclusions drawn from the STAR project are presented in Chapter six.

2.0 Research Goals

STAR was designed as a testbed to support the research goals of the LSTAR. Thus, it is pertinent to identify those goals here in order to provide an understanding of STAR's design from the highest level.

The LSTAR's current research goals include: developing visual operator interfaces for improved vehicle teleoperation; determining the effects of different visual interface system designs on operator performance; and achieving autonomous vehicle navigation and control [6]. Future goals include determining the effects of different operator-vehicle interfaces on operator performance of telemanipulation tasks, and automatic coordination of vehicle motion with telemanipulation. The LSTAR is interested in using two modes of space robotic vehicle simulation to meet its research goals. The first is virtual-environment simulation, wherein a dynamic model of the remote vehicle and a graphical model of its visual environment are combined to create the illusion of controlling a real vehicle. The second mode is neutral-buoyancy simulation, which was discussed in Chapter 1.

Virtual-environment simulation permits well-controlled human subject experimentation, making it ideal for studying the relative merits of various operator-vehicle interfaces. As a result, in the LSTAR research plan, virtual-environment experimentation is to be used to work towards the first two of the three above-stated goals. However, once results from virtual-environment studies have been obtained, they are to be confirmed with neutral-buoyancy experimentation supported by the STAR vehicle. The third of the above-stated goals, which is to achieve autonomous vehicle navigation and control, is to be researched solely with STAR.

Thus, STAR was designed primarily to support the development of autonomous vehicle navigation and control; in a secondary role, it was also

designed to support research of operator-vehicle visual interfaces, in order to provide verification of results obtained from virtual-environment experimentation. These two research goals were used to determine the requirements presented in the following section. Throughout the design process, however, thought was also given to making STAR versatile and expandable, so that the above-mentioned future research goals may be met with a minimum of vehicle redesign.

2.1 Requirements

The STAR system requirements, based on the two broad design goals identified in Section 2.0, are presented in the following two sub-sections.

2.1.1 Autonomous Vehicle Navigation and Control

The design requirements for STAR's primary design goal are presented below. Each requirement is accompanied by a discussion of the rationale behind its formulation.

Submersibility

To fulfill its goal of providing a testbed for the development of autonomous vehicle navigation and control, STAR must be capable of uninterrupted, submerged operation for a period of six hours. This time requirement was determined to be the maximum amount of testing time that could be performed at both MIT's Alumni Pool and NASA-Marshall's neutral-buoyancy tank during one day. All subsystems exposed to water must be corrosion-resistant in a chlorinated, fresh-water environment. STAR must be capable of full operation to a maximum depth of 40 feet (18 psi ambient gauge pressure), a condition which is imposed to allow for the possibility of experimentation with STAR at the NASA-Marshall neutral-buoyancy facility.

Neutral Buoyancy

STAR must be capable of being neutrally-buoyant to provide a realistic simulation of the zero-torque condition found in orbital space. If neutral buoyancy is not achieved and maintained, it would then be

necessary to expend control effort to keep STAR from changing elevation. This scenario is unacceptable, as any navigation or control system designed without STAR being neutrally-buoyant will not be directly applicable to space hardware. If, for example, significant amounts of control effort must be expended to maintain a vertical position by counteracting the non-zero disturbance force in the vertical plane, the remaining control effort may not be adequate for stable vehicle control; however, a similar control system in space, free of disturbances, might very well achieve stability.

Rotational Balancing

To provide a realistic simulation of the rotational freedom present in outer space, the STAR vehicle must be rotationally balanced. The term “rotationally balanced” refers to the condition wherein a neutrally-buoyant vehicle has no preferred rotational orientations. Similar to the above discussion of the neutral-buoyancy requirement, rotational balancing is essential to the development of vehicle control systems that have direct applicability to outer space systems. If the vehicle is stabilized by its buoyancy, the results of neutral-buoyancy experimentation would not be applicable to outer space systems because this stability would no longer be available.

Propulsion

Development of a control system for a vehicle with six degrees-of-freedom is simplest and easiest when actuation is available in each degree-of-freedom. Control system complexity increases dramatically when each degree-of-freedom can not be controlled. For this reason, it is required that STAR have bi-directional actuation in each of its six degrees-of-freedom. Since any control system developed for STAR will be implemented in software, the propulsion actuation is further required to be readily computer-controlled.

Sensing

Development of STAR’s real-time, autonomous control system will depend on accurate, fast calculation of the vehicle state. The state vector will include position, orientation, linear velocity, and angular

velocity. For speed and accuracy, it is desirable to measure directly as many of the state variables as possible using various sensors. In order to maintain the integrity of the space simulation, it is desired to only use sensors that could operate in outer space. As a result of this caveat, gravity-sensing instruments, such as accelerometers and pendula, are unacceptable. While it is desirable to feed-back as much state information as possible, there are no sensors available to measure some state variables, such as linear velocity. The linear velocity portion of the state vector must be calculated indirectly by taking the derivative of the position data. Thus, STAR's sensors must provide position, orientation, and rotational velocity measurements.

Computation

Computing will be necessary for a variety of tasks on STAR. Of primary importance, it must support the control system, which will be implemented with software. Control system support includes several tasks, such as reading sensor data, computation of immeasurable state vector variables, computation of the control algorithm, and outputting propulsion commands. In addition to control system tasks, computation will be needed to monitor onboard power and pressure systems, as well as record and store data from various sources for experimentation and de-bugging. Computational hardware must be sized such that the above tasks can be completed as often as necessary, while still providing enough speed to perform the computations necessary for stable real-time, closed-loop vehicle control.

Power

As stated earlier, STAR must be capable of uninterrupted, submerged operation for a period of six hours. Hence, the sizing of the power requirement is driven by the power loads of all subsystems over this period of time.

Communication

Once the goal of autonomous vehicle control is achieved, STAR will be capable of completely autonomous operation, obviating the need for communication with remote stations. During control system

development, however, communication between onboard computers and remote, poolside computers is indispensable as a development tool. The ability to observe control system performance, de-bug software, and implement control system changes (such as gain adjustment) from a remote station is extremely useful for control system development.

Control Station

As discussed in the previous paragraph, a simple control station will be necessary for the development and testing of STAR's mechanical components as well as the testing and monitoring of STAR's control system. Since all subsystems will be computer-controlled, the control station must include a computer capable of communicating with the onboard computer (see above paragraph).

2.1.2 Operator-Vehicle Visual Interface Research

The requirements driven by STAR's secondary research goal of supporting operator-vehicle visual interface experimentation are presented below. Operationally-speaking, the only difference between this secondary goal and the primary goal is that STAR will be controlled via human teleoperation, rather than by an autonomous control system. As a result, many of the requirements for this goal are nearly identical to the requirements stated above in Section 2.1.1, and, therefore, they will not be restated here. However, there are some important differences between similarly-titled requirements presented here and those of the last sub-section. These must be noted and accounted for in vehicle design. Also, there are several wholly new requirements presented in this sub-section.

Communication

To support teleoperation experimentation, STAR must be capable of being completely human-controlled from a remote control station. To achieve this, operator commands must be communicated from the control station to STAR. Since our goal is to verify experimental results obtained from virtual environment simulation, it is necessary to approximate the operator-vehicle interface that was used with the virtual environment; otherwise, comparisons between neutral-

buoyancy results and those from virtual environments will be invalidated. To enable the STAR system to approximate the widest variety of operator-vehicle interfaces, STAR's communications must be as fast as possible. This requirement arises from the fact that it is easy to match, with software, the delay between operator command and vehicle actuation present on STAR to the delay found in the virtual environment if the virtual environment delay is longer than that of STAR. However, if STAR's actuation delay is longer than the virtual environment delay, then STAR's delay becomes the limiting factor in control system speed, and the virtual environment speed must be slowed to accommodate this delay, which, obviously, is undesirable.

Vision

As was stated in the preceding paragraph, our goal requires STAR's operator-vehicle interface to mimic that used in virtual environment experimentation as closely as possible. Since the LSTAR's virtual environment experimentation utilizes human vision exclusively as feedback to the operator for vehicle control [7,8], STAR must be equipped with similar vision-feedback capabilities. This translates into a need for onboard cameras. These cameras' video signals will be sent to the operator via umbilical.

Control Station

The need for STAR's operator-vehicle interface to match the one used in virtual environment simulation has already been stated. Since a control station has already been developed for, and used with, virtual environment experimentation by graduate students Anna Cinniger and Matthew Machlis, it has been decided, in the interests of compatibility and expediency, to require that STAR utilize the same control station for human control.

2.1.3 Other Requirements

Operational Requirements

There are several requirements driven not by research goals, but rather by consideration of the research facilities available to the

LSTAR at MIT. There are several requirements imposed by the fact that the LSTAR's laboratory facilities, which will be used to develop STAR, are approximately one-half mile away from the swimming pool where testing will occur. Vehicle design is affected in several ways by this fact. The vehicle must be designed to fit onto a cart for transportation to and from the pool. Vehicle sizing is constrained such that the vehicle-cart combination must fit into an elevator door measuring 4 in. wide by 87 in. deep by 86 in. high. This same size constraint applies to the control station. A further consideration is efficient use of testing time. The swimming pool to be used for testing can only be reserved far in advance for limited periods of time. Considering this fact, along with the necessity of hiring a lifeguard, it is important to make efficient use of pool-testing time. Efficient use of pool-testing time means having STAR in the water for as much of the testing period as possible, or, equivalently, minimizing the amount of time that is spent preparing STAR for entry into the water once it has arrived at the pool, and minimizing the amount of time that is spent preparing STAR for transportation back from the pool after it has been removed from the water.

Safety

Divers equipped with self-contained underwater breathing apparatuses (SCUBA) are necessary to support neutral-buoyancy experimentation. Performing tasks such as modifying vehicle buoyancy, monitoring onboard subsystems, observing vehicle performance, assisting with vehicle submersion and removal, and providing collision avoidance, these divers are typically in close proximity to the vehicle during its operation. As a result, the vehicle is required to be incapable of causing diver injury, both during normal operation and during all conceivable failure modes.

Expandability

To meet future research goals, STAR must be designed to allow the expansion of its capabilities with a minimum of redesign effort. From an examination of LSTAR's future research goals, it is evident that STAR will require the addition of a dextrous manipulator. Thus,

STAR's subsystems must be designed to facilitate the addition of a manipulator.

2.2 Partition of System

The next step in the design process is to partition the system into smaller, more easily managed subsystems. This partition is done in such a way as to ensure that all of the requirements of the last section will be met. The subsystems are presented below and discussed briefly. A detailed presentation of each subsystem design, as well as construction details, is contained in Chapter 3.

2.2.1 Computer/Electronics

STAR's computer/electronics subsystem will be used for a wide variety of vehicle tasks. The task of autonomous vehicle navigation is extremely computationally-intensive. In particular, the vision-based position sensing (see Subsection 2.2.4) necessary for autonomous control is very complex. To ensure that vehicle position is updated frequently enough for stable control, it is logical to provide a computer dedicated solely to the task of calculating instantaneous vehicle position using the machine vision system. The remaining tasks, which include implementation of the autonomous control system, and monitoring and controlling the various onboard subsystems, will be supported by a different computer. Obviously, these two computers must communicate quickly and easily to effect stable control. To achieve this, they will be networked together. Included in this computer network will be the remote control station computer. The control station computer will handle the A/D conversion of the operator's commands, allow for surface debugging of onboard systems and software, and download software to the onboard computers.

Thus, there is a need for three networked computers: one vision-based position calculation computer, one vehicle control and subsystem control computer, and one control system computer. However, the need for additional computers is anticipated to meet future goals. The addition of a manipulator will require a dedicated computer for the calculation of the

complex kinematic equations used to control manipulators. Thus, STAR's computing system must be expandable to include additional computers.

Interfacing vehicle subsystems with the controlling onboard computer to enable monitoring and controlling tasks will require a variety of digital electronic interface circuits. Since each of these digital interface circuits must be supplied with similar power and data connections to the computer, a common power and data bus is desirable to save space and complication.

2.2.2 Propulsion

Our stated propulsion requirement is bi-directional actuation of each vehicle degree of freedom. To simulate the small bi-directional thrusters used on space vehicles, a variable speed, bi-directional electric motor and hydrodynamic propeller combination will be used. Hereafter, this combination of electric motor and propeller will be referred to as a single thruster. Care must be taken in choosing the number of thrusters, as well as their placement, to provide independent, bi-directional actuation of each degree-of-freedom. In this way, cross-coupling terms between degrees-of-freedom will not be present in STAR's dynamic equations, greatly simplifying any control algorithm.

To satisfy the safety requirement, STAR's thrusters must be shielded to protect divers from injury. To this effect, each thruster will include a duct, which is co-axial with the motor shaft, with grilles covering each end. This duct-grille combination will prevent divers' hands from being sucked into the thrusters' propellers.

2.2.3 Balancer

STAR's structure subsystem (see Section 2.2.8) will be designed so that, on paper, the completed vehicle will be neutrally-buoyant and rotationally-balanced. For a variety of reasons, however, such as last-minute redesign, measurement errors, inaccurate machining, and inaccurate modeling, STAR will not be neutrally-buoyant nor rotationally-balanced when first placed in water.

The balancer subsystem's sole purpose is to expedite the process of fulfilling STAR's rotational balancing requirement before each pool session. In the past, the SSL's vehicles were manually balanced by divers prior to each pool test by attaching lead weights and foam floats to appropriate places on the vehicles' structures. This process was often difficult and time-consuming. Since another of our requirements is that pool time be used efficiently (see Operational Requirements in Subsection 2.1.1), manual balancing is unacceptable.

Thus, the balancer subsystem must be capable of allowing remote adjustment of the relative locations of STAR's center of mass and center of buoyancy. To allow remote operator control of this process, the actuation must be computer-controlled. In addition to remote operator control of the balancer subsystem, it was decided that STAR should also have the ability to autonomously balance itself; this would represent a step in the process to make the vehicle as autonomous as possible. In order to do this, gravity sensors must be added. While it was stated earlier that such sensors would not be used for autonomous vehicle control in order to maintain the integrity of the simulation, there is no reason not to use these sensors for autonomous balancing since the balancing process is outside of the actual simulation; it is merely part of the construction of the simulation. Subsection 2.2.5, which presents the sensor subsystem, contains a more detailed discussion of gravity sensing.

2.2.4 Vision

As stated in Subsection 2.1.2, STAR must be equipped with onboard video cameras for visual feedback during teleoperator control of the vehicle. Since our goal requires that STAR's operator-vehicle interface mimic that used in virtual environment experimentation as closely as possible, the following two camera configurations are necessary: a fixed, stereoscopic belly-mount camera pair; and a tilt-and-pan stereoscopic camera pair. Stereovision is necessary in both configurations to enable the remote operator to use head-mounted video displays, which are used extensively in virtual environment experimentation. The tilt-and-pan configuration allows the pointing of the onboard camera pair to be slaved to a head-tracking system attached to the remote operator.

In Subsection 2.1.1, it was stated that STAR must have some means of sensing vehicle position if autonomous navigation is to be possible. Several position-sensing methods are currently in use. Traditionally, acoustic positioning has been popular for underwater teleoperated vehicles. In the SSL, the only vehicle to have position-sensing capabilities was MPOD, which used an acoustic positioning system called 3-DAPS (see Chap.1). 3-DAPS measured the transmission delays of synchronized acoustic pulses to provide vehicle position updates. While some successes were reported with MPOD [4], acoustic positioning is undesirable since it has no applicability to the non-transmitting vacuum of outer space. Two other options that have been used for docking tasks in outer space with some limited success are laser- or radar-based navigation. These methods measure a laser beam or radar signal reflected from a known target to give position information. While these systems are suitable for docking tasks, they may be deficient when used to control a telerobotic vehicle, as they may not provide both coverage, which is required for navigation, and precision, which is needed for manipulation.

Machine vision navigation, which utilizes edge and/or point analysis of digitized video signals to identify the size and shape of objects in the video frame, provides good precision scaling, meaning it is increasingly precise as vehicle-target distance decreases. This is desirable, since high precision is needed for close-in manipulation tasks. In addition, machine-vision systems are capable of using a wide variety of targets. In terms of applicability to outer space systems, machine vision sensing is directly portable to the space environment. For these reasons, machine vision was chosen as the method of vehicle navigation for STAR.

To allow the machine vision camera to remain pointed at the stationary vision target during vehicle motion, a tilt-and-pan mount must be developed for the camera. A three-dimensional target must also be developed for use with STAR in an underwater environment. The target must be three dimensional to enable the machine vision system to differentiate between translation and rotation. Consideration must be given to target color and texture in order to make the target highly visible in pool water, and highly contrasted with a pool wall for background.

Thus, STAR's vision subsystem will consist of the following: one belly-mounted stereo camera pair and one tilt-and-pan stereo camera pair for teleoperation experimentation; one tilt-and-pan monocular camera for machine vision position sensing; and a three-dimensional, underwater target to support machine vision navigation.

2.2.5 Sensor

The sensor subsystem can be divided into two categories: sensors used to support autonomous vehicle control; and sensors used for automatic vehicle balancing. For the first category, the stated requirement is to directly sense as many of the subvectors contained within the vehicle state vector as possible. The position and orientation subvectors will be sensed using the machine vision system described above in Subsection 2.2.4. The linear velocity subvector is not directly measurable; hence, it will be calculated indirectly by differentiating the position data. The only remaining subvector is that of rotational velocity. To sense the three elements of this subvector, three rate sensors will be used, one sensor for each axis. The second category of sensors is to be used in conjunction with the balancer subsystem to autonomously balance the vehicle (see Subsection 2.2.3). Autonomous balancing requires sensing the direction of gravity in a vehicle-fixed coordinate frame. This gravity vector is then used to determine the orientation of the vehicle with respect to the Earth. To return an accurate gravity vector, three accelerometers will be used, with one sensor oriented along each axis.

There is one additional sensor that will be integrated into STAR: a pressure sensor to measure vehicle depth underwater. This sensor is not mentioned with the other two categories because it is not driven by any of STAR's requirements. Its purpose is to aid in the development of STAR's subsystems. For example, when testing and debugging the machine vision navigation system, it may be useful to initially use the depth sensor to control vehicle depth, thereby removing one translational degree of freedom from the vehicle. Another application of the depth sensor is to prevent vehicle collisions with the pool bottom by providing vehicle depth information to the remote operator during teleoperation control of STAR.

2.2.6 Power

The power subsystem may also be divided into two categories according to load: power supplied to electrical motors (thruster motors and balancer motors), and power supplied to computers, electronics, and sensors. This division is logical due to the very different power needs of the two categories. Electrical motors draw large, varying amounts of current; when this current load is high, the inevitable voltage drop in the supplied power is not harmful to the motor. In comparison, computers, digital electronics, and electrically-powered sensors are very delicate. Their current load is small, and any variation in supply voltage can be harmful or fatal to these circuits. Thus, it is prudent to divide the power subsystem into two separate parts, one to supply high-current power to the propulsion and balancer subsystems, and one to supply low-current power to the computer/electronics subsystem, the sensor subsystem, and the vision subsystem.

STAR's power can not be supplied from a remote source via umbilical to the vehicle for two reasons: first, it is very dangerous to pass electrical power through diver-occupied water; second, it is desired for STAR to eventually be capable of completely autonomous operation. As a result, onboard rechargeable batteries are a logical choice for power, having been proven capable and reliable in past SSL vehicles. The number, electrical potential, and size of the batteries will be determined by analysis of subsystem electrical loads over the desired operation time of six hours. The division of the power subsystem that was discussed in the first paragraph of this subsection can be easily implemented by using separate batteries for each partition.

To fulfill the safety requirement, STAR's power subsystem must be incapable of injuring divers, even in conceivable failure modes. Thus, the batteries must be fused to prevent the buildup of potential in the water surrounding the vehicle in the event of external wiring shorts. Computer-controlled relays must be used between the batteries and subsystem loads to allow remote shut down of the power subsystem.

2.2.7 Pressure

In the past, the SSL has pressurized all the motors, electronics compartments, battery compartments, relay enclosures, and camera enclosures on its three vehicles to make them waterproof. This over-pressure inside each container was achieved by using a SCUBA tank and regulator, which had been modified to produce an output pressure which was always slightly higher than the ambient water pressure at depth. One of the major departures in STAR's design from past vehicles' designs is that STAR's electronics, battery, and camera containers will not be pressurized. As a result of this design decision, the only volumes on STAR that must be pressurized are the thruster motor casings. The reason that the motors must be pressurized is to prevent their weak shaft seals from leaking. Thus, STAR must be provided with a pressure system to maintain the internal pressure of each thruster motor at a level slightly higher than its surrounding water pressure over the required operational time of six hours.

To satisfy the requirement of being expandable to serve future needs, STAR's pressure system must have enough capacity to supply an underwater manipulator. This would entail pressurizing approximately seven joint motors, and supplying up to two pressure-cylinder-actuated end-effectors.

2.2.8 Structure

STAR's structure must be designed to meet many different requirements. Most importantly, however, STAR's structure must integrate the relatively large and massive electronics and power subsystems in such a way that allows the other, smaller subsystems to be placed appropriately. While enabling this subsystem integration, STAR's structure must, in the final analysis, result in a neutrally-buoyant and rotationally-balanced vehicle. Further, to meet its operational requirements, STAR's overall dimensions, plus those of its transport cart, must not exceed the size limitations imposed by LSTAR's freight elevator and MIT's pool entrance. The materials used for STAR's structure must be chosen to withstand the corrosiveness of chlorinated pool water. To satisfy the requirement of expandability, STAR's structure must be designed to support a manipulator. Also, to expedite subsystem redesign and expansion, all subsystem mounts,

enclosures, and connectors should be fastened mechanically (i.e., with bolts) where permissible, rather than with welds or adhesives, to permit the disassembly of subsystems for easy component repair or replacement.

The detailed designs of STAR's subsystems are presented in this chapter. To explain the rationale behind important design decisions, a discussion of options, trade studies, and analysis accompanies each subsystem presentation. Many of these discussions center around designs used in the past on SSL vehicles, as these vehicles represent a rich source of information on successful, and unsuccessful, uses of various technologies.

3.1 Computer/Electronics

It was worthwhile to study the computer/electronics systems used in past SSL vehicles before beginning the design of STAR's subsystem. IBM PC-clone microprocessors were used without fail on all three SSL vehicles. In-house and manufactured electronic circuit cards were interfaced to the microprocessor via PC-bus. The operating system used for all microprocessors was Microsoft's Disk Operating System (DOS). The operating system and all vehicle software was kept on non-volatile random access memory (NOVRAM) or floppy disk. The onboard computer communicated to the remote control station computers via serial link, usually a fiber-optics cable. Since DOS made no provisions for networking, a serial communications protocol named the Pilot-Vehicle Communications System (PiVeCS) was written by Robert Sanner while a graduate student in the SSL [9].

Through discussions with students who had worked with the SSL vehicles, several problem areas in the computer/electronics subsystems were identified. The small size of the foam/fiberglass boxes used to contain the subsystems inhibited maintenance and limited expansion. The inability to change vehicle software once the vehicle was placed in the water retarded software development. There were several problems associated with using DOS for the operating system: it was slow, it could not support multi-tasking, and it had no provision for linking more than two computers. The

fiber optics cable used for serial communications between the onboard and control station computers was highly unreliable. STAR's computer/electronics subsystem was designed to avoid these pitfalls where possible.

3.1.1 Computer

There is a very large variety of microprocessors and bus formats available today. For STAR, an IBM PC-clone computer was chosen for several reasons. First, a PC-type computer was chosen to allow use of the QNX operating system, which requires a PC computer. The use of QNX was desired because it would solve many of the problems associated with past computer systems (see Subsection 3.1.2). Second, there is a great variety of affordable software available for PC platforms. Third, the cost of PC computers was much less than that of STD computers with similar performance; this results from the fact that PC computers are targeted at consumers rather than industry.

The specific computer chosen for STAR was the Little Board/386, manufactured by Ampro Computers Inc., of Sunnyvale, CA. This computer was chosen for several reasons. First, the Little Board provided powerful computing power in a very small package. A 32-bit, 20 MHz 80386 microprocessor system was contained on a single board; the entire package measured 5.75" x 8.0" x 1.1." This small size was attractive since vehicle requirements dictated the eventual need for three separate onboard computers. Second, Ampro computers were found to be very reliable during use in past SSL vehicles. Third, the Little Board required only 10 - 12 W of power; a low power load was desirable since STAR was to be powered by batteries. Finally, the operating temperature range of the Little Board was very wide (0 - 70° C). A wide operating temperature range was necessary for all components of STAR's computer/electronics subsystem because these components were to be subjected to elevated ambient temperatures resulting from the subsystem being sealed inside one compartment without ventilation.

The Ampro Little Board was purchased with a compact, 2-slot passive backplane capable of accommodating two PC-bus cards. This backplane

was used to hold the QNX network card and a card containing the PC-bus part of the PC-bus to STD-bus interface circuit. The QNX card was needed to control the Ampro board's communications with the QNX network; the PC-bus part of the interface circuit was necessary to allow PC-bus to STD-bus communication. See Subsection 3.1.4 for further discussion of this interface circuit.

In Subsection 2.2.1, it was stated that STAR will eventually need three onboard computers. At the time of this writing, however, only one computer had been placed on board; this computer provided adequate computing capability for the program of subsystem development and testing that was followed to this point.

3.1.2 QNX Operating System

The QNX operating system is manufactured by Quantum Software Systems Ltd. of Kanata, Ontario, Canada. QNX was deemed a very important choice for STAR's computer system because its use provides solutions to several of the problems associated with past computer systems that were outlined in the opening discussion of Section 3.1. Specifically, QNX addresses the following problems: the inability to download software from a remote computer; the slow serial communications; and the lack of multi-computer linking.

Unlike DOS, QNX is an operating system that supports true networking of various computer nodes. This architecture consists of a set of cooperating administrator tasks with which user programs and other administrators communicate via messages. These messages are passed between tasks on separate nodes in the same way that messages are passed between tasks internal to one computer. This allows for easy coordination of tasks running on separate computer nodes, something that is impossible when using DOS, since DOS runs independently on each computer, oblivious to tasks running on another computer. Also, any node in the QNX network may assume complete remote control of any other node. This allows tasks to be downloaded from one node to another, solving the problem of downloading software to STAR's onboard computer from the remote control station computer. STAR's computer nodes were linked by coaxial

cable. This cable was chosen to provide reliable communications, eliminating the problem of unreliability present with fiber optic cable.

To perform vision-based, closed-loop vehicle control, the operating system must be capable of fast inter-task communication and fast task-switching between vision processing tasks, estimation-calculation tasks, control algorithm tasks, and motor command tasks. QNX was designed as a "real-time" operating system, capable of greater than 7200 task switches per second. This speed was deemed more than sufficient to support STAR's control tasks.

3.1.3 Electronics Bus

Interfacing vehicle subsystems with the controlling onboard computer to enable monitoring and controlling tasks required a variety of digital interface circuits. For example, for the computer to read the angular rate sensors, which output an analog voltage range, an analog to digital (A/D) conversion circuit was needed. Since each of these digital interface circuits needed to be supplied with power and a data connection with the computer system, a common power bus and a common data bus were logical choices to support STAR's digital circuitry. Additionally, a common data bus between microprocessors permits direct data-transfer; also, microprocessor RAM can easily be supplemented by placing memory cards on the bus.

There were two choices of standard digital circuit buses available that provided both power and data connections to digital circuit cards. These were the PC-bus and the STD-bus. Since, in Subsection 3.1.1, a PC computer was chosen, the PC-bus seemed to be the likely choice since it was readily compatible with the computer. Despite this fact, however, the STD-bus was chosen to support STAR's digital circuits. The primary reason for the choice of the STD-bus was space-efficiency. First, the aspect ratio of the STD-bus cards was nearly one, compared to an aspect ratio of approximately three for the longer PC-bus cards, making the shape of the STD-bus much more space-efficient than the PC-bus. Second, the STD-bus wasted considerably less space between cards on the bus than the PC-bus. The STD-bus was also chosen for its availability in rack-mount configuration. Since the STD-bus is used primarily in industrial

applications, it was available in a compact, 19" standard rack-mounted configuration. The PC-bus, on the other hand, was only available as one part of a computer chassis, which placed little emphasis on space-efficiency.

The STD-bus purchased for use was manufactured by the Pro-Log Corporation of Monterey, California. The model chosen was the BX26R, which is a standard 19" rack mount bus with slots for 26 cards. A list of specifications for this model is contained in Appendix B.

3.1.4 PC-bus to STD-bus Interface Circuit

Since the STD-bus was chosen to support STAR's digital circuits, interface circuitry was necessary to allow the PC-computer to control and exchange data with the STD-cards. This interface was not available commercially; hence, the interface was designed by Professor Harold Alexander and constructed by LSTAR graduate students Harald Weigl and Michael Valdez. The interface consisted of one circuit mounted on an STD-card and one circuit mounted on a PC-bus card. The STD-card was placed in one slot of the STD-bus and connected via 50-pin ribbon cable to the PC-card, which was placed in one slot of the 2-slot backplane attached to the Ampro Little Board. Since the need for three onboard computers was outlined in Subsection 2.2.1, the interface circuit was designed to allow up to three separate microprocessors to communicate with the same STD-bus. Thus, all three computers could access the same STD-bus circuit cards. The interface circuit was also designed to allow the user to assign priorities to the three onboard computers; this is extremely useful for control system development, where certain tasks can not wait for other tasks to be completed before being performed.

A circuit diagram of the STD-bus part of the PC-bus to STD-bus interface circuit is shown in Figure 3.1. While the circuit diagram is presented here on two pages, the circuit was wired onto one STD-card. Referring to page one of the two-page circuit diagram, several features of the circuit will be noted. The circuitry in this figure was devoted to controlling the service requests of the three microprocessors. The signals numbered one in this diagram were associated with the highest priority computer; those labeled

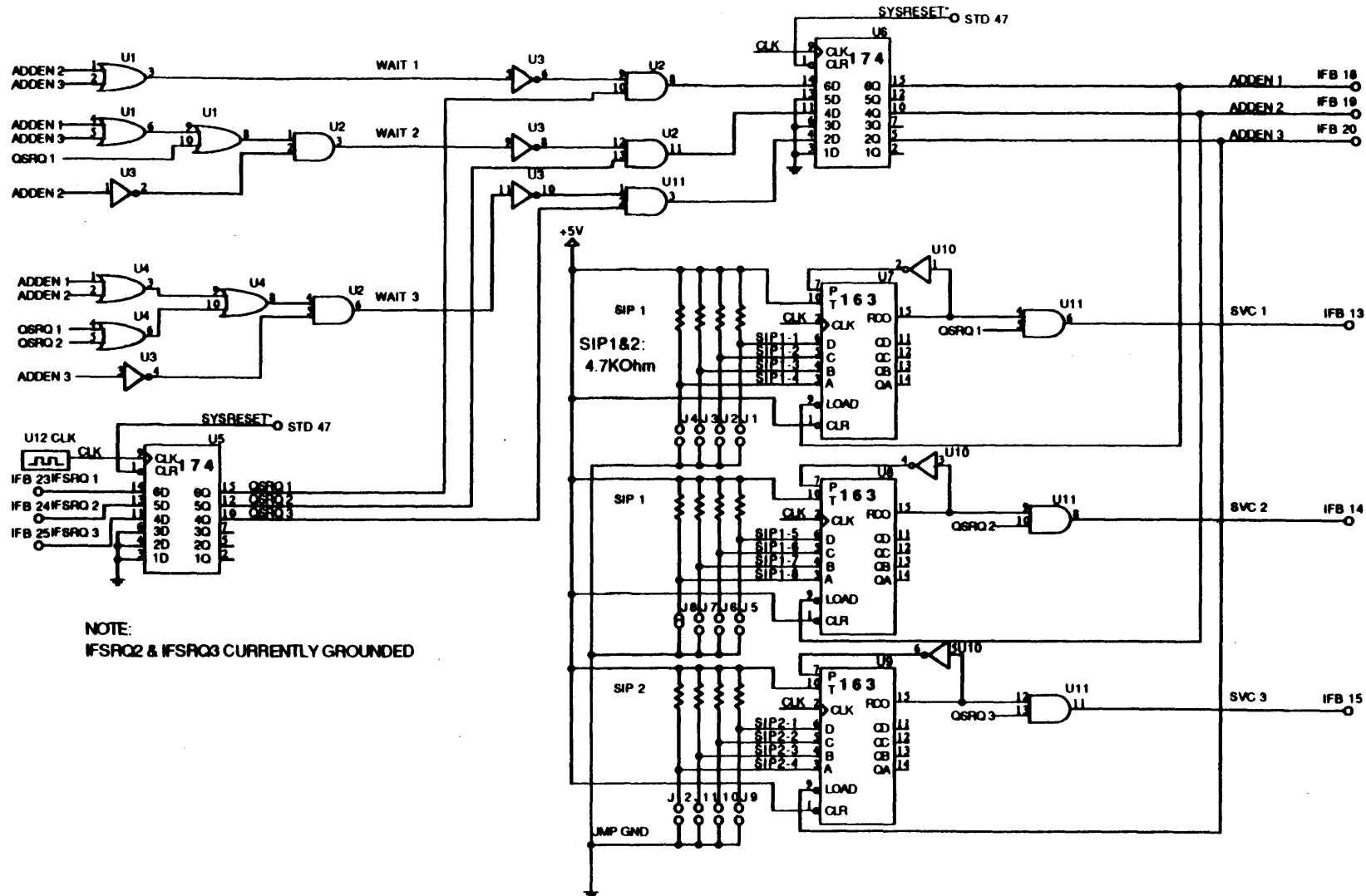


Figure 3.1 PC-bus to STD-bus Interface: STD Card Circuit Diagram

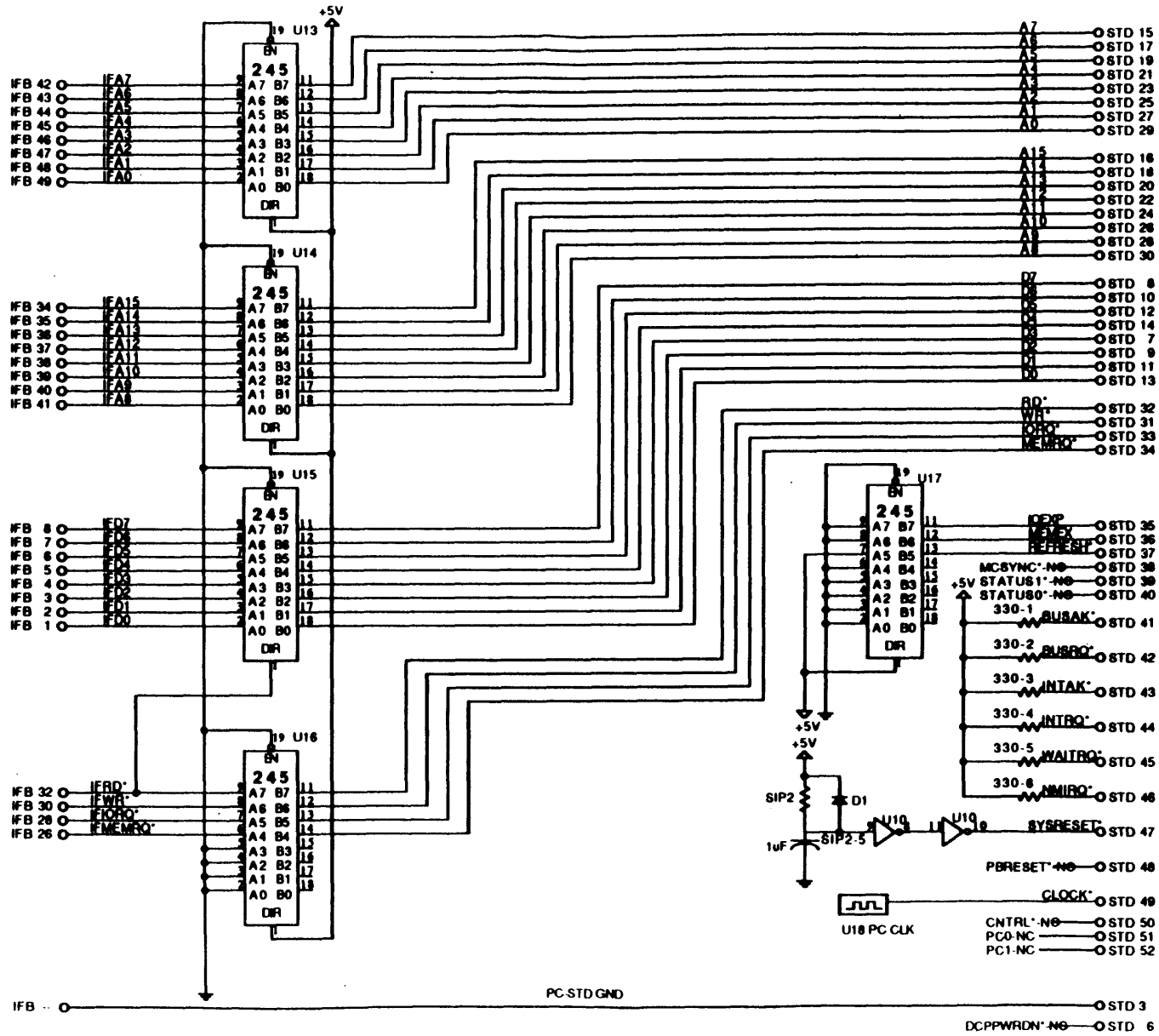


Figure 3.1 PC-bus to STD-bus Interface: STD Card Circuit Diagram

2 and 3 belonged to the computers with the second and third priority, respectively. The signals IFSRQ1, IFSRQ2, and IFSRQ3 were the service request signals from the three computers. Two of the signals, IFSRQ2 and IFSRQ3, were grounded because only one computer was being used at the time of this writing. These signals were gated with the left LS174 D flip-flop. The upper left corner of the page consists of combinational logic that used previous service request information along with the prioritization of the computers to determine the three WAIT signals. These three WAIT signals indicated which computer must wait on its service request until a previous request has finished. These WAIT signals were then combined logically with the clocked service request signals; the three signals resulting from this combination were then clocked themselves, producing the three address-enable signals at the upper right corner of the diagram. These address-enable signals were then fed into the three LS163 timer chips in the center of the diagram. These chips used jumpers J1 through J12 to allow the user to define the delay between the assertion of the address-enable signals and the assertion of the service signals, SVC1, SVC2, and SVC3, which are shown on the right side of the diagram. This delay was necessary to allow the setup time on the data bus to pass before the data was read. The second page of the STD-bus card circuit diagram merely consists of LS245 line drivers which were used to drive the bus signals.

Figure 3.2 is a circuit diagram of the PC-bus part of the interface circuit. This circuit was wired onto a PC-bus card; this card was placed in one of the two slots in the Ampro computer backplane PC-bus. The upper left corner of this circuit was concerned with converting the four PC-bus control signals - I/O READ, I/O WRITE, MEMORY READ, MEMORY WRITE - to the four STD-bus control signals - namely, I/O REQUEST, MEMORY REQUEST, READ, WRITE - which are shown in the upper center of the diagram. The three address-enable signals from the STD-bus interface card were combined with the three service signals from the STD-bus interface card to produce the I/O CHANNEL READY signal shown at the upper right of the circuit diagram; I/O CHANNEL READY is used to put the PC microprocessor into a "sleep" mode as desired. Again, an LS163 timer chip was used to insert a delay between the service notice and the commencement of the bus operation. The LS688 chips were used to

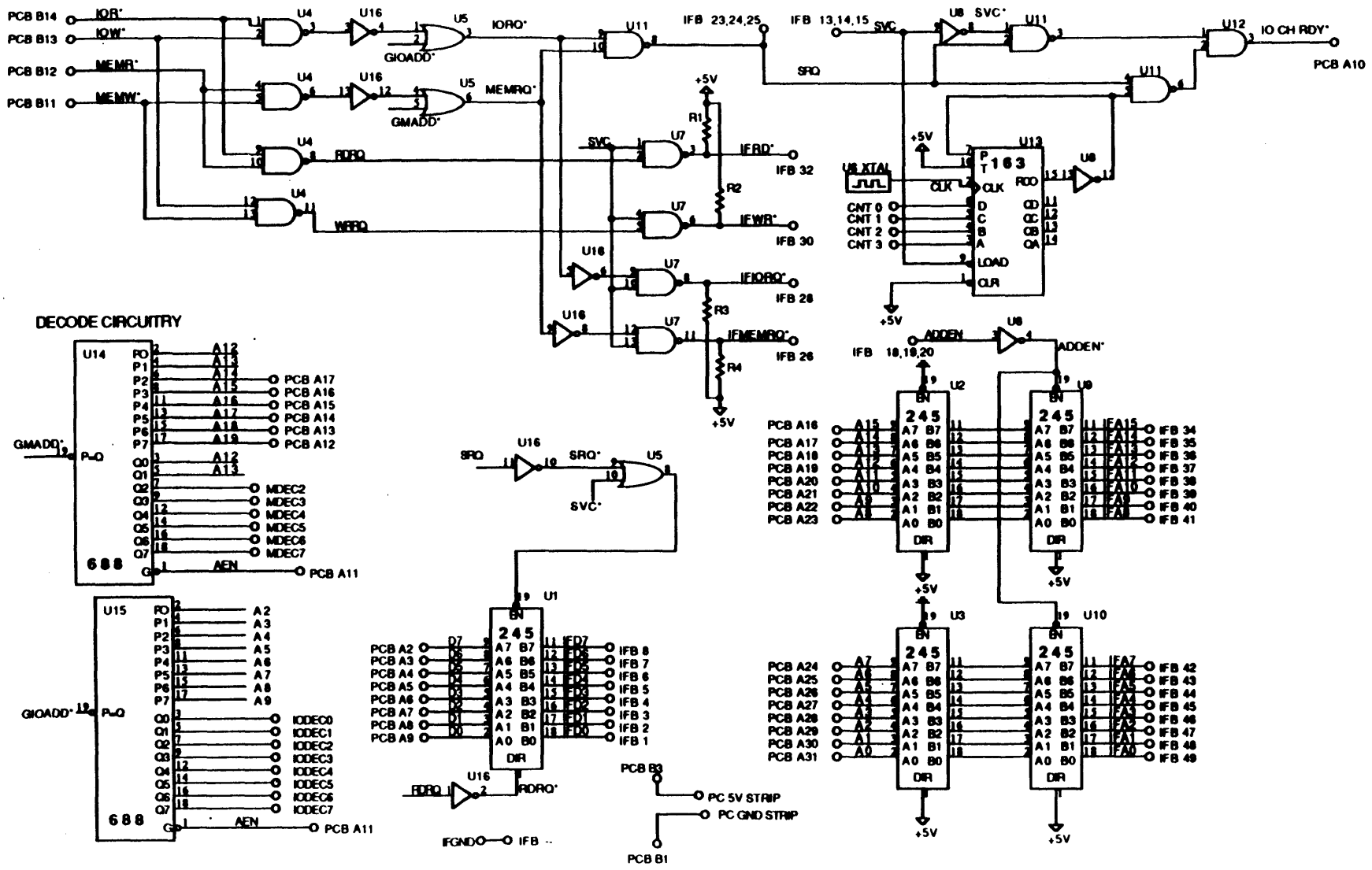


Figure 3.2 PC-bus to STD-bus Interface: PC Card Circuit Diagram

decode the memory and I/O signals. The LS245 chips were again used to drive the bus signals.

The following five Subsections present the various digital circuit cards used with the STD-bus.

3.1.5 A/D Conversion Circuit

A general-purpose A/D conversion circuit card was purchased and installed onto the STD-bus. Manufactured by Pro-Log Corporation of Monterey, California, the RTI-1260 circuit was used to digitize the analog sensor signals such that they were capable of being read by the computer. The RTI-1260 card was capable of converting an analog DC voltage range of 0 - 10V. The A/D resolution was 12 bits, meaning that the 0 - 10V range was quantized into 4096 levels. Thus, the sensors were read as follows: after receiving a request from the computer along the PC-bus, the RTI-1260 sampled the analog sensor signals that were connected to input ports of the card; these sensor samples were then quantized to a 12-bit representation, which was placed onto the STD-bus; the computer then read this 12-bit number after receiving notification of its presence on the STD-bus by the A/D card. A list of specifications for the RTI-1260 card is contained in Appendix B.

3.1.6 Medium-Power Switching Circuit

A medium-power DC driver card was purchased and installed on the STD-bus for the purpose of enabling computer control of the power relays. This card was manufactured by the Pro-Log Corporation of Monterey, California. The power relays are discussed in detail with the power subsystem in Section 3.6. This driver card converted TTL-level signals sent to the STD-bus from the computer system to latched, negative true, open-collector DC drive signals. This conversion was very useful, as it allowed the remote operator to turn vehicle power on and off from the remote control station computer. Also, since the driver card was controlled merely by sending TTL signals from the computer to the appropriate STD-bus addresses, future autonomous control systems would be capable of turning on and shutting down vehicle power. While this

capability enables another step towards complete autonomous operation, it is also important for safety considerations. A list of specifications for the RTI-1260 card is contained in Appendix B.

3.1.7 Thruster Motor Control Circuits

Two STD-bus circuit cards were designed and constructed for the purpose of controlling the angular velocity of the electric thruster motors. Each card contains 4 National Semiconductor LM629 motion-control processor chips, one chip dedicated to each thruster motor. These chips were designed to perform the intensive, real-time computational tasks required for angular velocity control of the thruster motors.

Unfortunately, at the time of this writing, the incremental shaft encoders that were to provide shaft position feedback to the LM629's were not yet mounted. This fact made closed-loop control impossible. Since this control system was already designed, however, the design is presented in Chapter 6. Since closed-loop control was impossible, the motor control circuits were used to convert the motor command signals from the computer system into two open-loop pulse-width-modulated (PWM) signals: forward, and reverse. These two signals were then output to the motor driver circuit (see Subsection 3.2.1) for amplification.

Figure 3.3 shows a diagram of the thruster motor control circuit. Two identical copies of this circuit, each wired to its own STD-bus card, were used to control the eight thruster motors. It is a very simple circuit, consisting of only the LM629 motion control chips and a small amount of supporting circuitry. The LM629 chips received commands from and sent data to the computer system one byte at a time through the signals MD0 - MD7, shown on the left side of each chip. These I/O processes were controlled by the MEMORY WRITE (MWR) and MEMORY READ (MRD) signals shown on the lower left of each chip. The LM629's had two output signals: SIGN, which was designed to control motor direction, and MAGNITUDE (MAG), which was the PWM signal used to control the magnitude of motor actuation. To interface with the motor driver circuit, these two signals were converted using combinational logic into a PWM

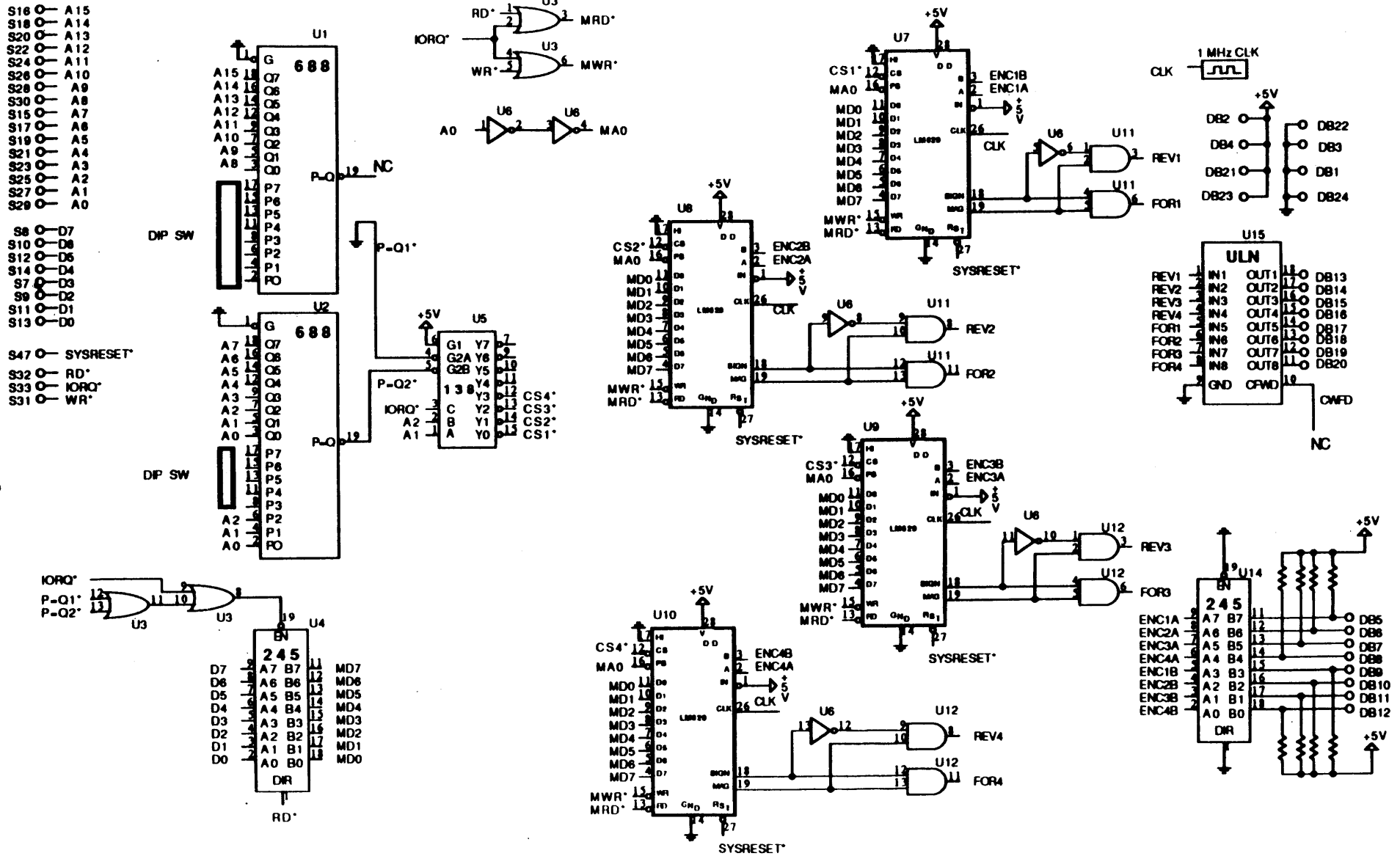


Figure 3.3 Thruster Motor Controller Circuit

forward signal, and a PWM reverse signal, labeled REVERSE (REV) and FORWARD (FOR) on the circuit diagram.

Since there were no encoder signals available to the LM629 chips, the ENCODER A (ENCA) and ENCODER B (ENCB) pins shown at the upper right corner of each chip were grounded. Grounding these pins supplied the LM629 with a constant zero-position feedback signal. This enabled the magnitude of the PWM forward and reverse signals to be easily controlled by issuing a non-zero position command from the computer. Any non-zero position command was converted to servo error since the shaft position was always held to zero. Negative error was produced by commanding a negative position. A non-zero proportional gain was then used to make the magnitude of the PWM forward and reverse signals proportional to the servo error. In this way, the LM629 chips used simple computer position commands to produce open-loop PWM motor command signals in the absence of feedback from shaft encoders.

3.1.8 Balancer Motor Control Circuit

A motor control circuit was designed and built to control the linear position of the balancer weights (see Section 3.3) by controlling the angular position of the electric balancer motors. This circuit was wired to an STD-bus card and placed on the STD-bus to receive computer commands. This circuit was virtually identical to the thruster motor control circuit discussed above in Subsection 3.1.7. One important difference, however, between the thruster motor control described above and the balancer motor control was the dynamic variable controlled by the LM629 control chips; specifically, the thruster motor control circuit was designed to provide closed-loop control of shaft angular velocity, whereas the balancer motor control circuit was designed to perform closed-loop control of shaft angular position. Fortunately, the LM629 was able to implement both proportional-integral-derivative (P-I-D) angular velocity control and P-I-D angular position control. The choice of velocity or position control mode in the LM629 was easily controlled in software.

The balancer motor control circuit is presented in Figure 3.4. This circuit is functionally identical to the previously-discussed thruster motor control

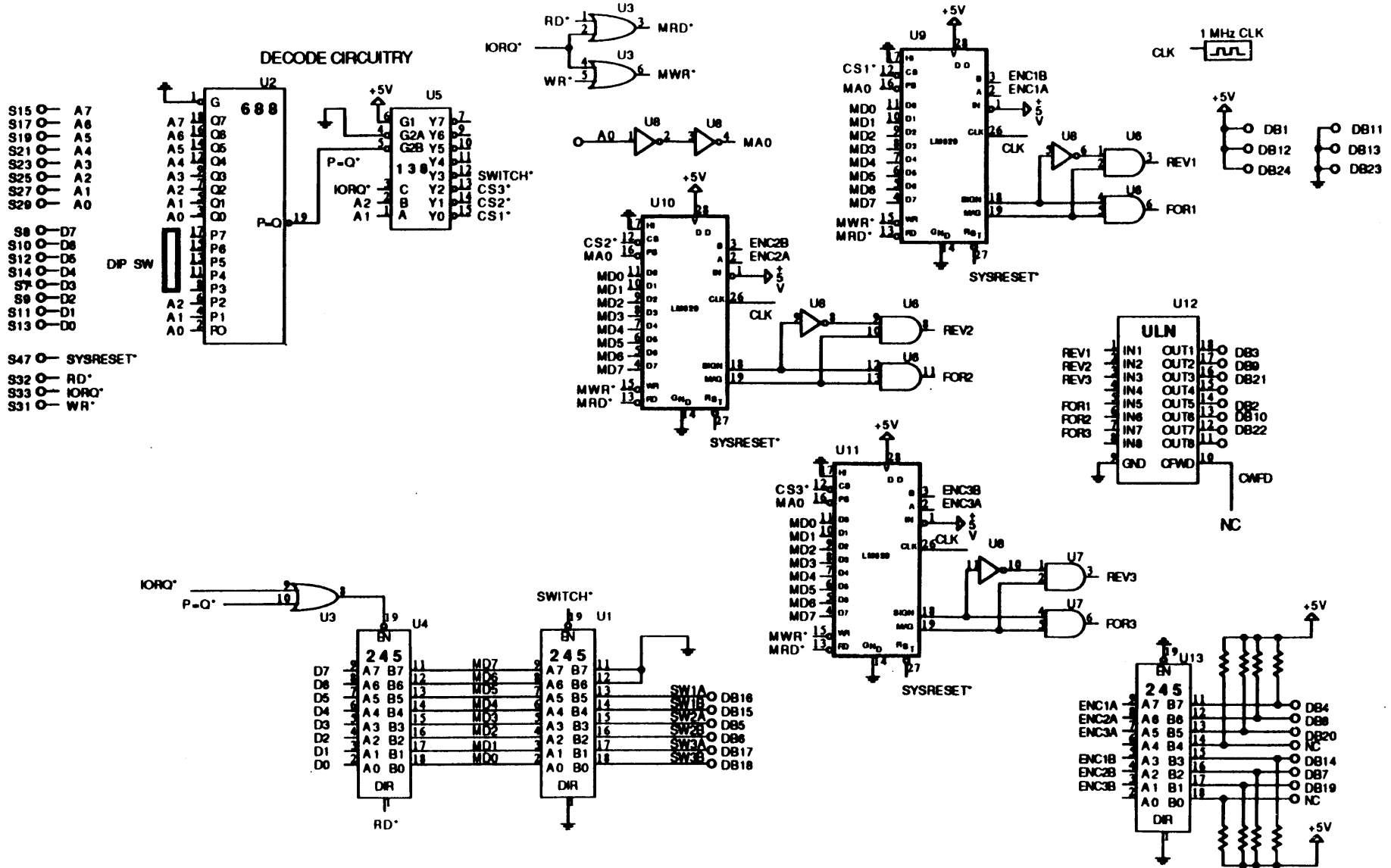


Figure 3.4 Balancer Motor Controller Circuit

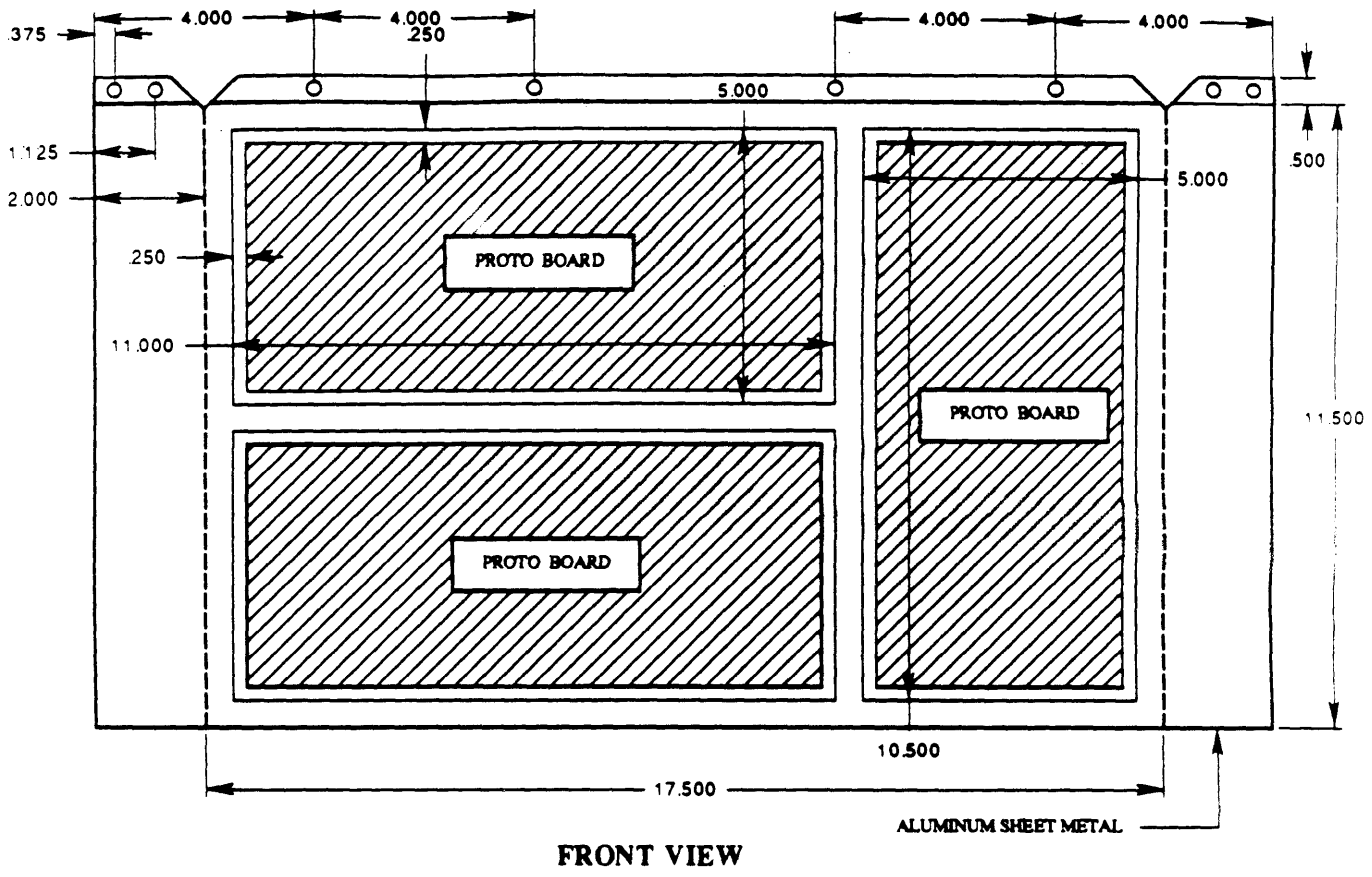
circuit. Here, however, an optical encoder was installed on each balancer lead screw. The A and B signals from the encoder's quadrature-encoded output were connected directly to pins 2 and 3, labeled ENCA and ENCB, of the LM629 chips. The software written to implement the balancer weight position control using this circuit is discussed in Chapter 4.

3.1.9 Network Hub Card

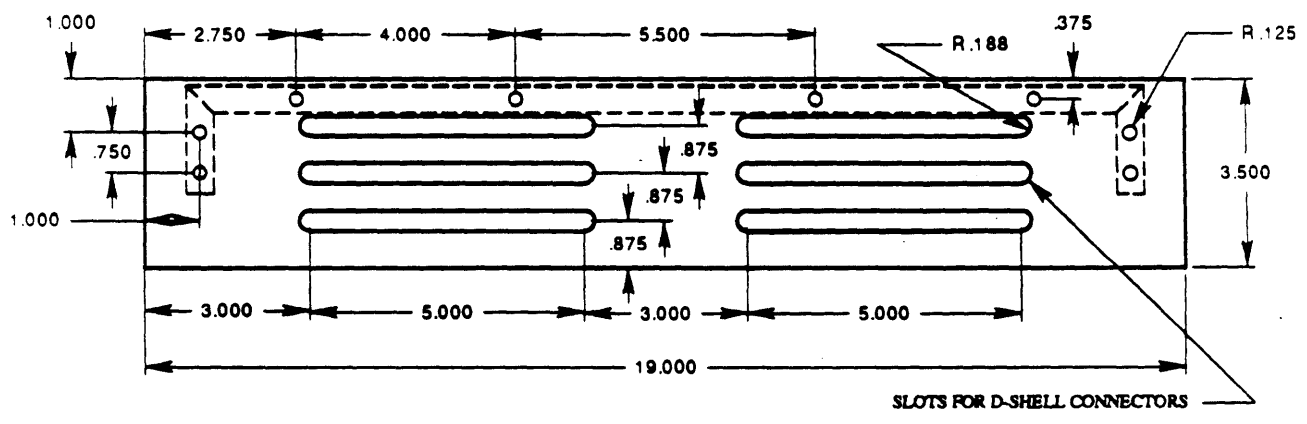
An Arcnet passive hub card was purchased and adapted to function on the STD-bus. While it was stated in Subsection 3.1.2 that all nodes of the QNX network were to be linked via coaxial cable, it was impractical to use more than one coaxial cable to link the control station computer with the onboard computers. For this reason, the Arcnet hub card was necessary to allow more than one onboard computer to be integrated into the QNX network. The hub card contained four BNC connectors for coaxial cable. One connector was used for the coaxial umbilical cable that was linked to the control station computer; one connector was used for the onboard Ampro computer; and the remaining two were reserved for network expansion.

3.1.10 Patch Board

To organize the multitude of signal connections in the electronics compartment, a patch board was designed. The patch board was placed to connect to all electronics compartment door connectors as well as to all computer I/O circuits, and to route the signals between the two groups of connections. Figure 3.5 shows the patch board assembly. All connections to the above-mentioned STD-bus circuit cards were soldered to D-type subminiature connectors. These connectors were mated with opposite gender D-type connectors mounted in the slots shown in the top plate of the patch board assembly. Signal lines from outside of the electronics compartment were also mated to connectors on the patch board. To reduce the radio-frequency (RF) noise present in digital signals from coupling to analog signals, the analog signals were separated from the digital signals. This separation was accomplished by using the left set of slots in the top of the patch board for analog signals, and the right set of slots for digital signals. Once all of the signals were routed to the patch board, the desired connections between the D-shell connectors were made using wire-



FRONT VIEW



TOP VIEW

Figure 3.5 Patch Board

wrapping techniques on the three proto boards shown in the front view. In addition to organizing the signal connections in the electronics compartment, use of the patch board allowed easy removal of various electronic components.

3.2 Propulsion

A survey of past SSL vehicles revealed that their propulsion subsystems, which consisted of electric motors with propellers, provided satisfactory actuation for underwater propulsion. Since STAR's total mass was comparable to these past vehicles, a similar propulsion subsystem was deemed sufficiently powerful for use on STAR. Thus, STAR's propulsion subsystem was designed to use the same electric motor/propeller combination found on ASTRO. This motor/propeller combination will hereafter be referred to as a thruster.

To satisfy the safety requirement presented in Subsection 2.1.3, the thruster propeller had to be shielded from possible contact with divers' hands. For this reason, a circular duct was designed to enclose the propeller. Grilles were used to seal the duct from hands while allowing water flow.

3.2.1 Motor Driver Circuit

The electric thruster motors draw large amounts of current when driving propellers through water. This current level was far too large for the motors to be interfaced directly with the onboard computer. Instead, the motors were supplied with power directly from dedicated power batteries (see Section 3.6 for discussion of the power subsystem). Motor commands, output from the computer and processed by the motor controller circuits, were used as input to a motor driver circuit, which switched the high-power supply lines to the motors.

The motor driver circuit was designed to take the low-power, PWM signal output from the motor controller board (see Section 3.1) and amplify the power of the signal so that it was sufficient to drive the electric thruster motors. To find out how much current was drawn by the motors during operation, a complete thruster was placed in the Water Immersion Facility

(WIF) of the LSTAR and attached directly to an ammeter-equipped power supply. Normal operating current was found to be approximately 4-5A, while stall torque was found to be approximately 15A. Thus, the motor driver circuit was designed to supply 5A continuously, and 15A for short periods. The motor driver circuit was designed by Professor Harold Alexander. Construction, de-bugging, and redesign were performed by Harald Weigl, a graduate student in the LSTAR.

Figure 3.6 shows the circuit diagram of the motor driver. Several of the salient features of the driver circuit will be discussed here. There were two inputs to the driver circuit that came from the motor controller circuit in the electronics compartment: a pulse-width-modulated forward signal, and a pulse-width-modulated reverse signal. These delicate TTL signals were then completely isolated from the noisy motor driver electronics by the use of opto-isolator diodes. The relatively weak output signals of the opto-isolators were insufficient to drive the power transistors; hence, TIP31 NPN transistors were used to boost signal power.

Power amplification of the input signal was accomplished with the use of high-gain Darlington-configuration power transistors. Two PNP and two NPN Darlington transistors were arranged in an H-bridge layout to provide bi-directional power to the motor. Each direction was driven by a diagonal pair of one PNP and one NPN Darlington. Each pair of transistors was controlled by the TIP31-boosted PWM signal dedicated to that direction. The H-bridge was supplied with +24VDC, labeled VBB, and GROUND directly from the batteries.

The motor driver circuit was carefully designed to ensure that, in the course of normal operation, all transistors would either be completely off, or saturated. This was important, since transistor efficiency and longevity are increased when operation in the linear region is minimized. To minimize the amount of time that saturated transistors spend in the linear region after they are switched off, resistors were added between the base and the emitter of each transistor. 100 Ω resistors were used for the TIP31 transistors, and 330 Ω resistors were used for the Darlington transistors.

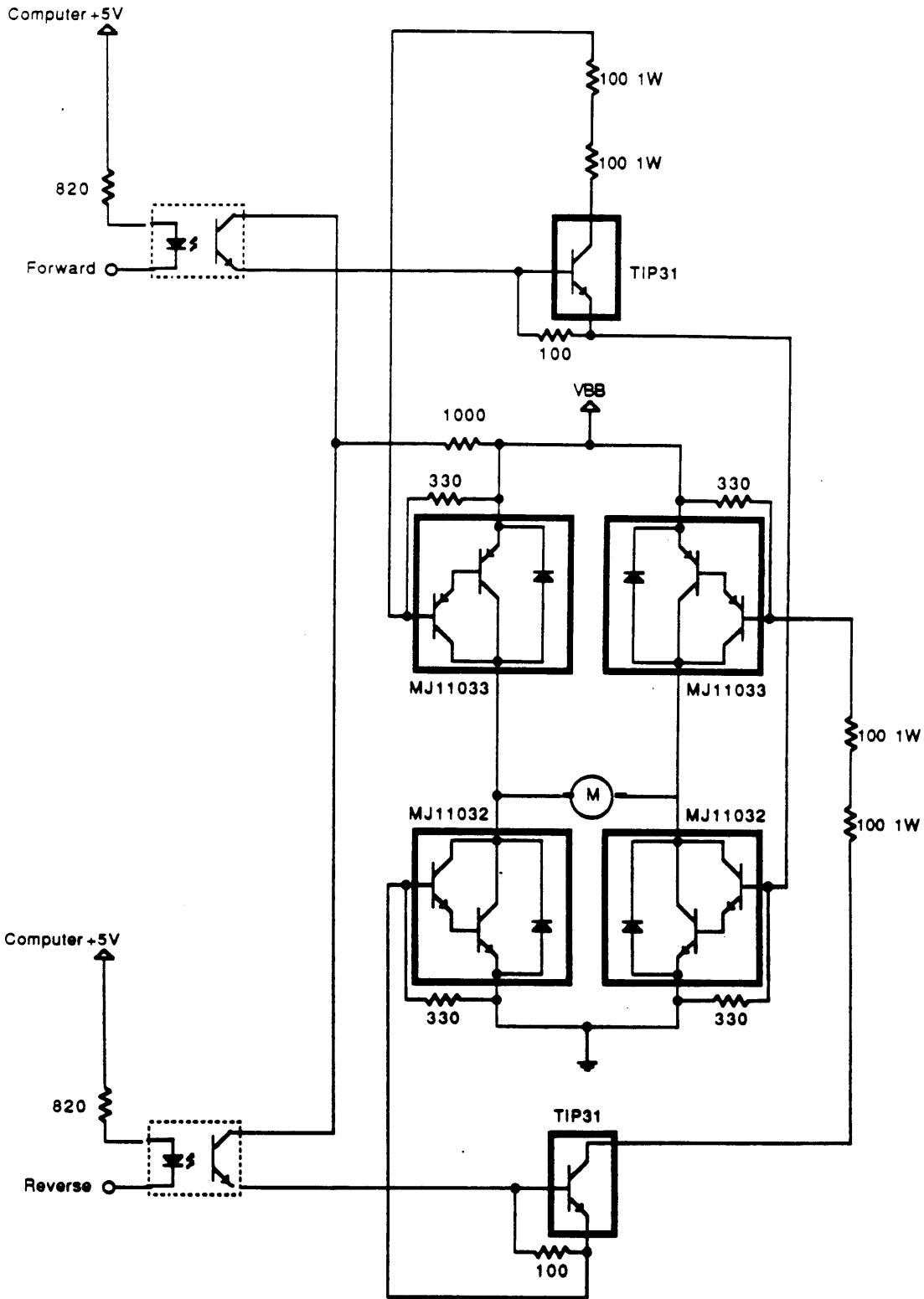


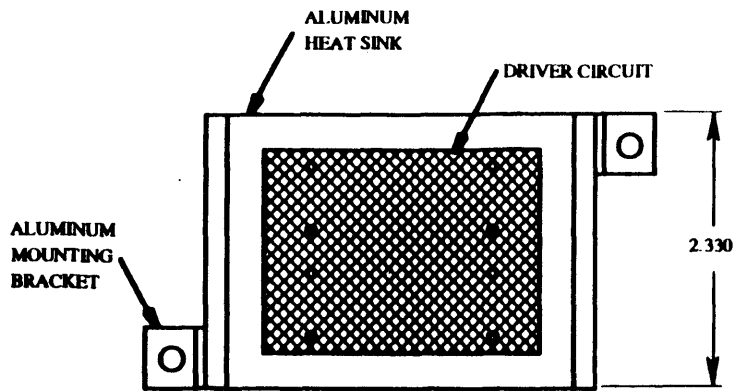
Figure 3.6 Thruster Motor Driver Circuit

While the driver circuit was designed to be as efficient as possible, there was still considerable heat dissipation by the high-gain Darlington power transistors. For this reason, it was decided to follow past SSL convention and mount the transistors to a heat sink, and in turn mount the circuit and heat sink at the thruster, where water could cool the heat sink. Aluminum was chosen as the material for the heat sink because of its high heat transfer rate. Naturally, for the driver circuit to operate in water, it needed to be waterproofed. This was accomplished with a non-conductive RTV potting compound, which was poured over the circuit to form a protective coating.

Figure 3.7 shows the motor driver circuit mounted on the piece of Aluminum I-beam used as a heat sink. The high-gain Darlington transistors, which produce great heat, were mounted flush against one side of the I-beam, shown in the bottom view of Figure 3.7. For connection with the rest of the driver circuit, the leads of the transistor were passed through the I-beam into sockets on the other side of the I-beam, shown in the top view of Figure 3.7. Both the Darlington side of the heat sink and the circuit side of the heat sink were potted with RTV potting compound, shown in section view A - A of Figure 3.7. The RTV compound used was manufactured by Castall, Inc., of Needham, Massachusetts. Three multi-conductor cables served to connect the driver circuit with other vehicle subsystems. These were also potted along with the electronics, and are shown in section view A - A. The three cables consisted of the following: one two-conductor power supply cable, which powered the H-bridge with +24VDC and ground from the batteries (see Section 3.6); one two-conductor cable that carried the PWM output to the motor; and one six-conductor cable, which connected the motor controller circuit in the electronics compartment with the driver circuit, supplying TTL +5VDC, TTL ground, PWM forward signal, and PWM reverse signal to the driver, and returning the encoder A and B signals to the motor controller circuit.

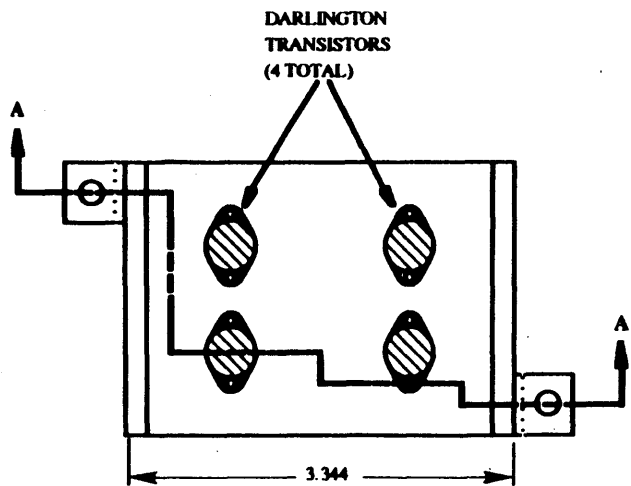
3.2.2 Thruster Duct

To determine a viable thruster duct design, the conclusions from previous duct efficiency experiments, performed by SSL researchers, were examined. In 1981, Susan Flint concluded that a duct constructed with a cross section in the shape of a Clark-Y airfoil was much more efficient

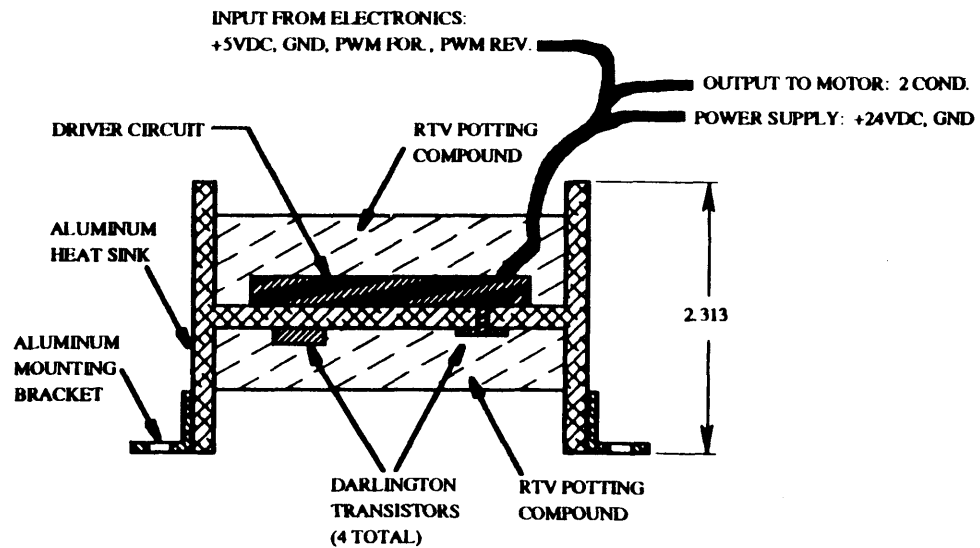


TOP VIEW

NOTE: ALL DIMENSIONS
IN INCHES



BOTTOM VIEW



SECTION A - A

Figure 3.7 Motor Driver and Heat Sink Assembly

than a cylindrical duct with a simple rectangular cross section [10]. In 1983, Michael Scardera tested the efficiencies of six different duct designs. Scardera concluded that ducts which had a rounded, symmetrical duct cross section produced the best results [11].

STAR's thruster duct design is shown in Figure 3.8. This drawing was produced by Paul Stach, an undergraduate researcher in the LSTAR. The design includes symmetric, rounded leading and trailing edges, giving similar efficiencies in both the forward and reverse directions. The cross section of the duct is composed of three arcs of different radii on the inside of the duct, and one straight line on the outside of the duct. Obviously, this complex geometry would be nearly impossible to machine by hand; hence, a computer-driven numerical-control lathe was used for duct machining. Duct machining was generously performed by the Laboratory for Manufacturing and Productivity. The ducts were machined from blocks of foam. This foam was then covered with an epoxy and fiberglass cloth layer to greatly increase duct strength.

3.2.3 Construction

The electric D.C. motors purchased for STAR's propulsion subsystem were originally intended for use as trolling motors for small boats. Manufactured by Minn Kota, of Mankato, MN, these motors' performance and reliability were proven in use with past SSL vehicles. Since these motors were designed for boat operation only, their shaft seals could not maintain watertight integrity to the depths at which STAR was designed to operate. As a result, the motors needed to be internally pressurized for underwater operation. For this reason, the pressure subsystem presented in Section 3.7 was necessary.

Figure 3.9 shows the electric thruster motor with propeller. Also shown are the modifications made to the thruster for operation on STAR. The motor was disassembled, and the various resistance coils which were used to produce different motor speeds were removed, leaving only direct power and ground to the motor. A through-hole was drilled in the motor fin to allow the fin to be rigidly attached to the duct. The cylindrical opening on the top of the motor was sealed by a PVC disk glued into the

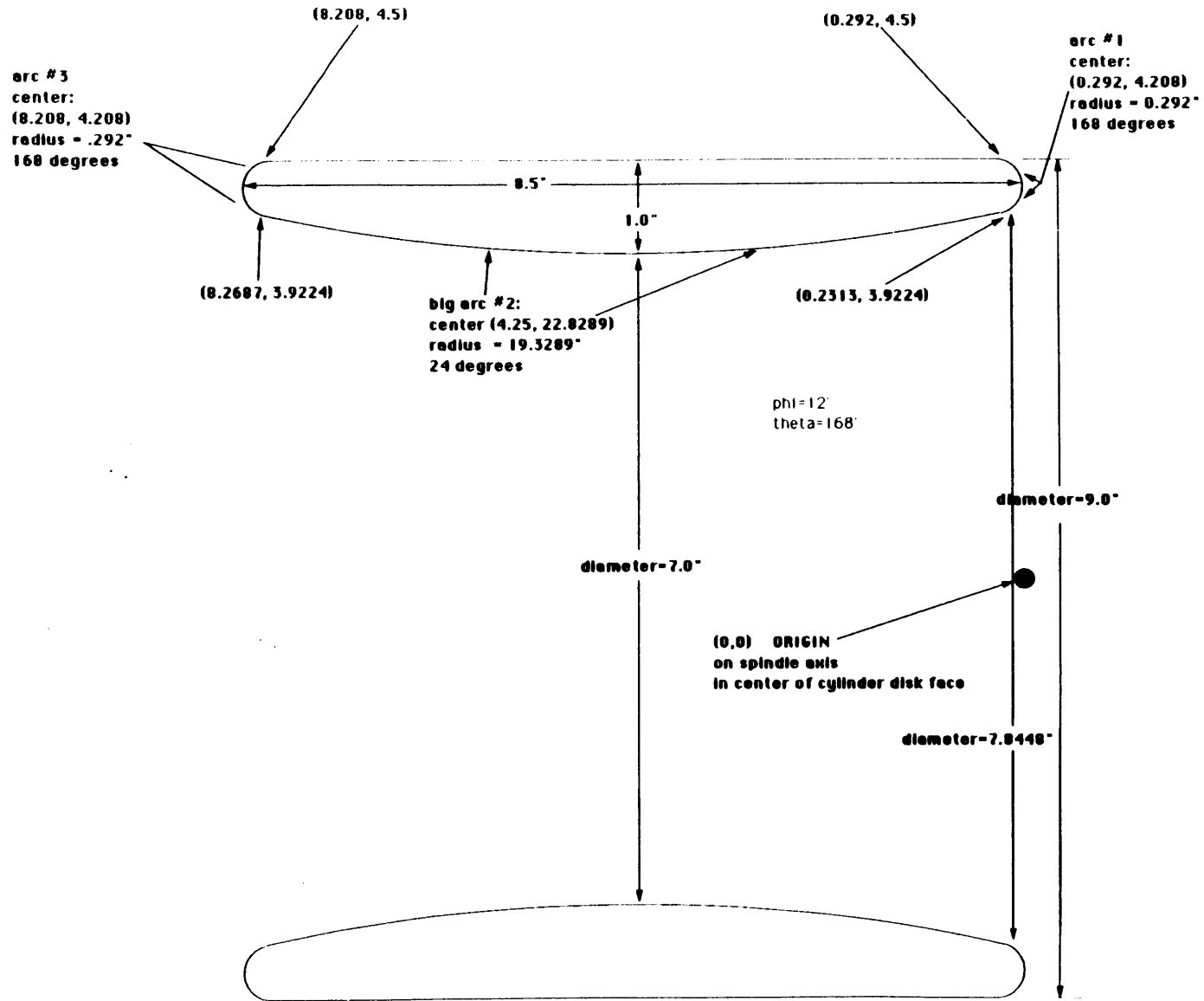


Figure 3.8 Thruster Duct Cross Section

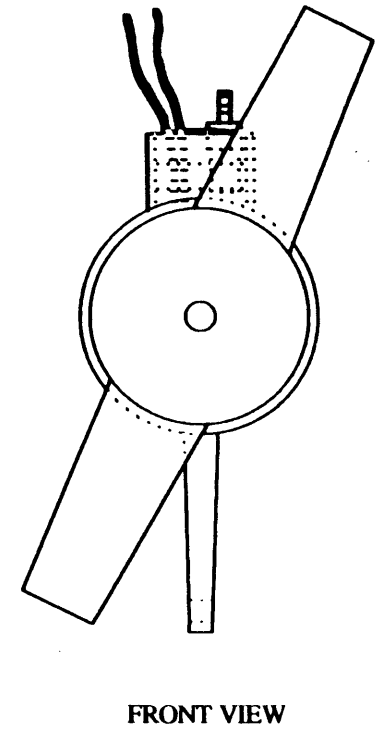
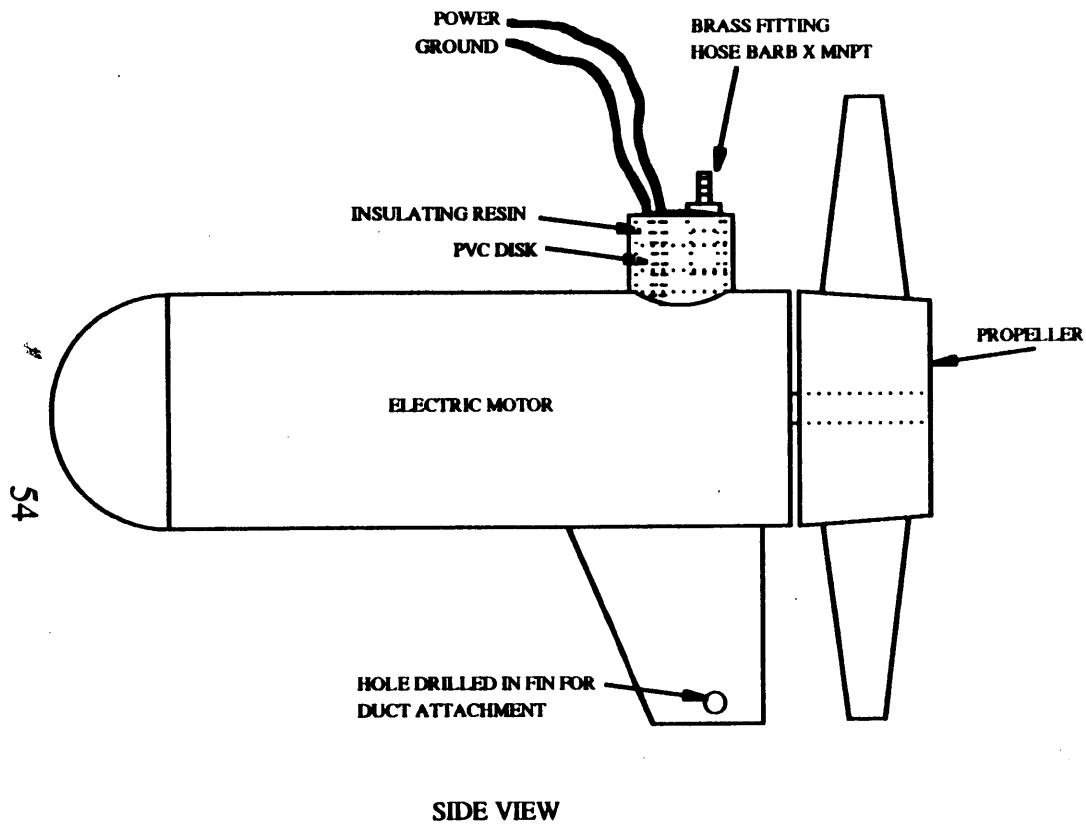


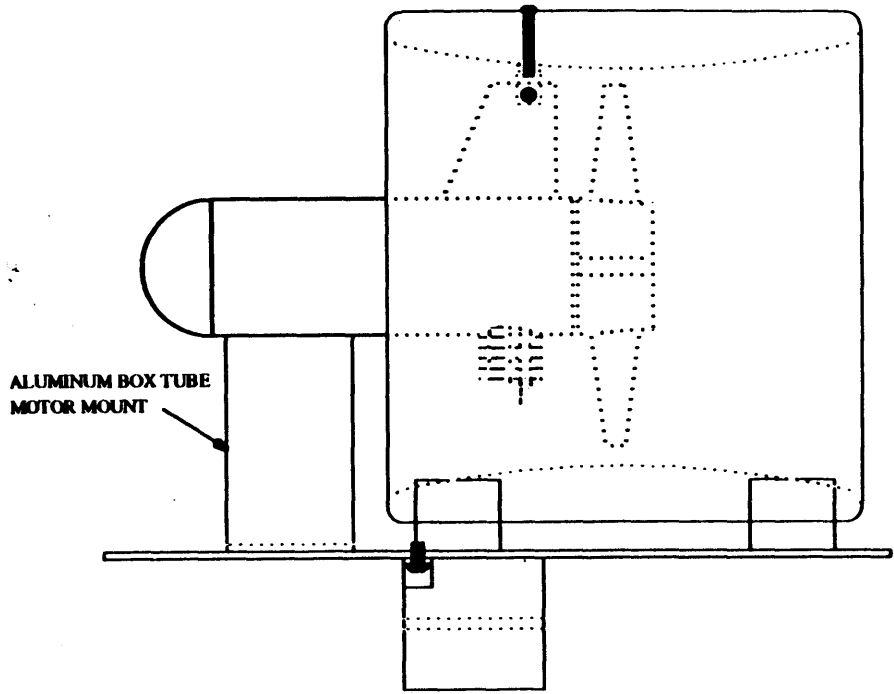
Figure 3.9 Electric Thruster Motor With Modifications

opening to the motor. Two small holes were drilled through this disk to allow the wires to pass out of the motor. To interface the motor with the pressure system, a threaded hole was machined into the PVC disk such that a brass hose barb x MNPT pipe fitting could be inserted. This fitting allowed the Tygon tubing of the pressure system to connect directly to the inside of the motor casing, where overpressurization was necessary. Once the PVC disk was in place, the rest of the cylinder above the disk was sealed using insulating resin. This insulating resin, manufactured by 3M, is designed for splicing high-power underground cables.

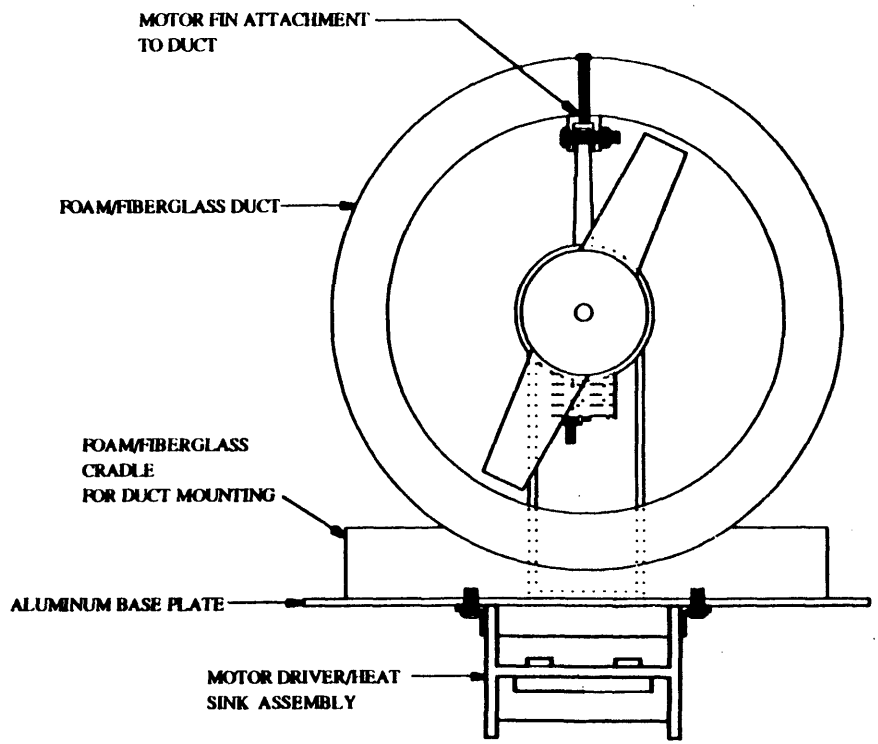
Figure 3.10 shows the entire thruster assembly, except for the plastic grilles which cover the ends of the duct; the grilles were left out of this drawing to provide a clearer understanding of the assembly. The thruster assembly consists of the following items: the electric motor and propeller, the duct with fiberglass mounting cradles, the motor driver circuit mounted on its heat sink, an Aluminum base plate, an Aluminum motor mount, and a piece of Aluminum U-channel that was used to rigidly attach the fin of the motor to the duct. This attachment was deemed necessary after an examination of ASTRO's thruster design. ASTRO's electric motors were cantilevered off of a motor mount into the duct; this arrangement proved too weak to withstand motor vibration, with the result that the propeller contacted the inside of the duct.

Figure 3.11 shows the entire thruster assembly with the plastic grilles in place. These grilles were cut from squares of 1/2" cell "egg crate" ceiling tile. The grilles were attached to the duct with two machine screws. This mechanical mounting was a departure from past designs, which used RTV adhesive to chemically attach the grilles to the ducts. The mechanical mounting was chosen over the adhesive bonding for two reasons: the mechanical mounting does not impede the flow of water through the grille as much as the RTV mounting; and the mechanical mounting is non-permanent, allowing easy removal of the grille to perform tasks such as motor or propeller replacement.

56

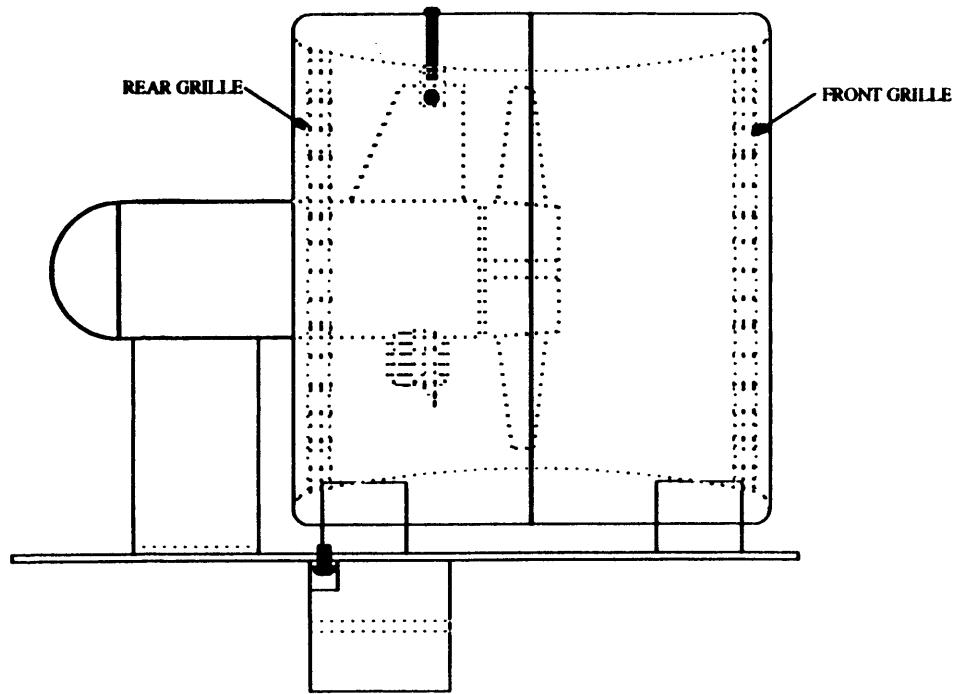


SIDE VIEW

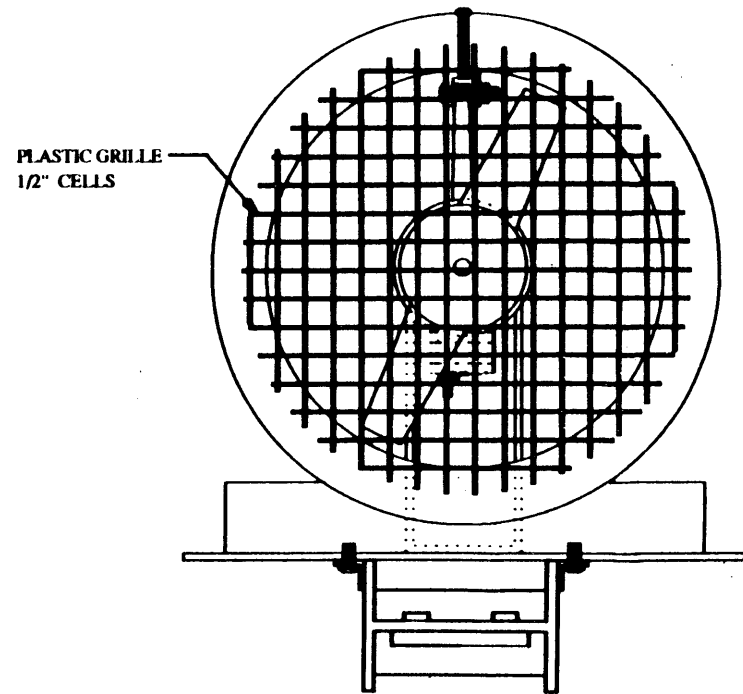


FRONT VIEW

Figure 3.10 Thruster Assembly Without Grilles



SIDE VIEW



FRONT VIEW

Figure 3.11 Thruster Assembly With Grille

3.3 Balancer

As stated in Subsection 2.2.3, the balancer subsystem had to have the capability to force STAR's center of mass and center of buoyancy to be coincident, since, despite design efforts to the contrary, slight rotational imbalances will inevitably be present. This result could be accomplished in one of two ways: the center of mass could be moved to the center of buoyancy, or the center of buoyancy could be moved to the center of mass. The first method involved moving onboard weights to new locations. Since it was obviously desirable to keep the volume of the moving weights as small as possible, a high-density material was typically used, such as lead. The second method of balancing, which was to move the center of buoyancy, involved relocating displaced volumes of water. A low-density material, such as foam, was needed for this task, in order to achieve the greatest buoyancy for a given volume. In order to choose which of the above methods to use, their efficiencies were examined. Lead has a density of 0.41 lb./in.³, and water has a density of 0.0361 lb./in.³, meaning that lead has an adjusted density of 0.3739 lb./in.³ in water. Foam, with a density of 0.00469 lb./in.³, produces a net buoyant force in water of 0.03141 lb./in.³. Thus, comparing the net downward force density of produced by lead to the net upward force density of produced by foam, it was evident that using lead to adjust the location of the center of mass was approximately 12 times more efficient, volumetrically speaking, than using foam to adjust the center of buoyancy. For example, if a moment of 100 in.-lb. was needed to make STAR rotationally balanced, and the balancing subsystem was limited to 10 in. of travel, 10 lb. of force would be needed to produce the required moment. Using foam, this requirement would necessitate a volume of 318 in.³. With lead, however, only 27 in.³ would be needed. Thus, the method of adjusting STAR's center of mass using the motion of lead weights was chosen for the balancer subsystem.

3.3.1 Sizing

The next balancer issue to be examined was sizing. Since space on STAR was limited, the balancer subsystem was designed to be as small as possible while still providing adequate vehicle balancing. To further define what is

meant by adequate, previous pool tests of the SSL were examined. In past pool tests of the SSL, when the neutrally-buoyant vehicles were balanced manually by divers, the greatest amount of time was spent on making small, final balance adjustments. It took little time to roughly balance each vehicle to the point where moving a 2 lb. lead weight from one side of the vehicle to the other completely changed the balance. For this reason, along with the desire to make the balancer subsystem as small as possible, it was decided to only use the balancer to make the small, final balance adjustments that are difficult and time-consuming for a diver to perform, leaving coarse balancing in the hands of divers. Thus, the balancer was required to be capable of producing a moment about each axis equivalent to that produced by moving a 3 lb. weight a distance of 50 in., or 150 in.-lb. From discussions with divers who had balanced SSL vehicles manually in the past, this figure of 150 in.-lb. along each axis was deemed sufficient to provide STAR with adequate balancing capability. To account for inaccuracies in estimation, this number was multiplied by a safety factor of 1.5, bringing the necessary balancing effort to 225 in.-lb. This use of past vehicles' data in STAR's design was made possible by the fact that STAR's gross vehicle weight was planned to be approximately equivalent to the weight of BAT and MPOD.

3.3.2 Actuation

Turning now to actuation, a method for linearly moving the balancer weights needed to be chosen. Direct linear motion actuators, such as cylinders, were expensive and wasteful of space. Also, linear actuators are difficult to use when implementing closed-loop position control, since linear position sensors are cumbersome and expensive. A better alternative was the use of standard D.C. rotary motors, which are inexpensive, compact, and readily-available. This choice required the conversion of rotary motion to linear motion. The most space-efficient way to perform this conversion is with the use of a lead screw and nut. Since the lead screw's pitch was known, the weight's position could be sensed by an inexpensive rotary position sensor attached to the lead screw, enabling closed-loop position control. Thus, to provide linear actuation of the lead weights, a D.C. motor/lead screw combination was chosen.

3.3.3 Electronics

To perform closed loop position control of the balancer weight, a digital circuit containing a specialized motion-controller chip was used. This chip was identical to the one used in the propulsion subsystem, and the supporting circuit is very similar. This circuit was located inside the electronics compartment. A detailed discussion of this circuit was presented in Subsection 3.1.8. Position control of the balancer weight is discussed in detail in Chapter 4.

The motion-controller chip was designed to accept rotary position feedback encoded in quadrature form. For this reason, an optical encoder was chosen over other types of rotary position encoders, such as resolvers and potentiometers.

Since the motors used in the balancer subsystem draw approximately 0.5 A at 24 VDC, which is a load of 12 W, the low-power pulse-width-modulated signal output of the motion-control circuit could not be used to directly drive the balancer motors. Instead, a motor driver circuit was used. This circuit basically functioned as a power relay, using the low-power control signal as input for the switching of a separate, high-power supply connected to the motor.

3.3.4 Balancer Motor Driver Circuit

The balancer motor driver circuit was very similar in design to the thruster motor driver circuit discussed in Subsection 3.2.1. There were three major differences in the two designs, however. The first was that the balancer motor required much less current than the thruster motors. Whereas the thruster motors' normal operation drew 4 - 5A, the balancer motors needed less than 0.5A. This difference resulted in the use of transistors with much smaller gains for the balancer motor driver circuit. With the use of smaller transistors, a heat sink was no longer necessary. The second major difference in driver designs was that the balancer driver was designed to incorporate the use of limit switches. These limit switches, when tripped, stopped motion in one direction; this kept the balancer motor from attempting to drive the motor past the end of the lead screw. The

third difference was that the balancer driver was to be mounted inside the balancer enclosure since its low-power transistors do not require a heat sink cooled by water. Hence, the balancer drivers did not require water-proofing.

Figure 3.12 is a circuit diagram of the balancer motor driver design. The H-bridge consisting of NPN and PNP transistors is reminiscent of the thruster driver design; however, instead of high-power Darlington pairs, TIP32 and TIP31 transistors were used. Once again, the PWM forward and PWM reverse signals were input to the circuit through opto-isolator diodes; however, in the balancer circuit, each of these two signals was input to the circuit in two places. This arrangement was necessary to allow the limit switches to stop motion in one direction while still allowing motion in the opposite direction. Again, 100Ω resistors were placed between the emitter and the base of each transistor to limit the amount of time that the transistors operated in the linear region. +24VDC (VBB) and ground were supplied independently to the circuit directly from the top battery drawer.

The balancer driver circuit was wired onto a piece of proto board. This board was bolted to a piece of angle bracket, and this assembly was in turn mounted to the motor mounting plate (see Figure 3.13, shown in the next Subsection) with screws threaded into holes in the plate. The driver circuit was mounted in this fashion to allow the circuit to be removed for repairs by simply removing the threaded PVC end cap.

3.3.5 Enclosure

The choice of electric motor for actuation required that each balancer assembly be enclosed in a waterproof container. PVC tubing was chosen for this function because of its light weight, low cost, and wide variety of available fittings.

Due to considerations of availability and cost, a lead screw/nut assembly with 20 in. of travel was chosen. This fact is mentioned here as it has direct bearing on the choice of pipe diameter. The choice of pipe inner diameter (I.D.) was narrowed to two choices, 3 in. or 4 in., since anything smaller would be inadequate to enclose the motor, and the next larger size

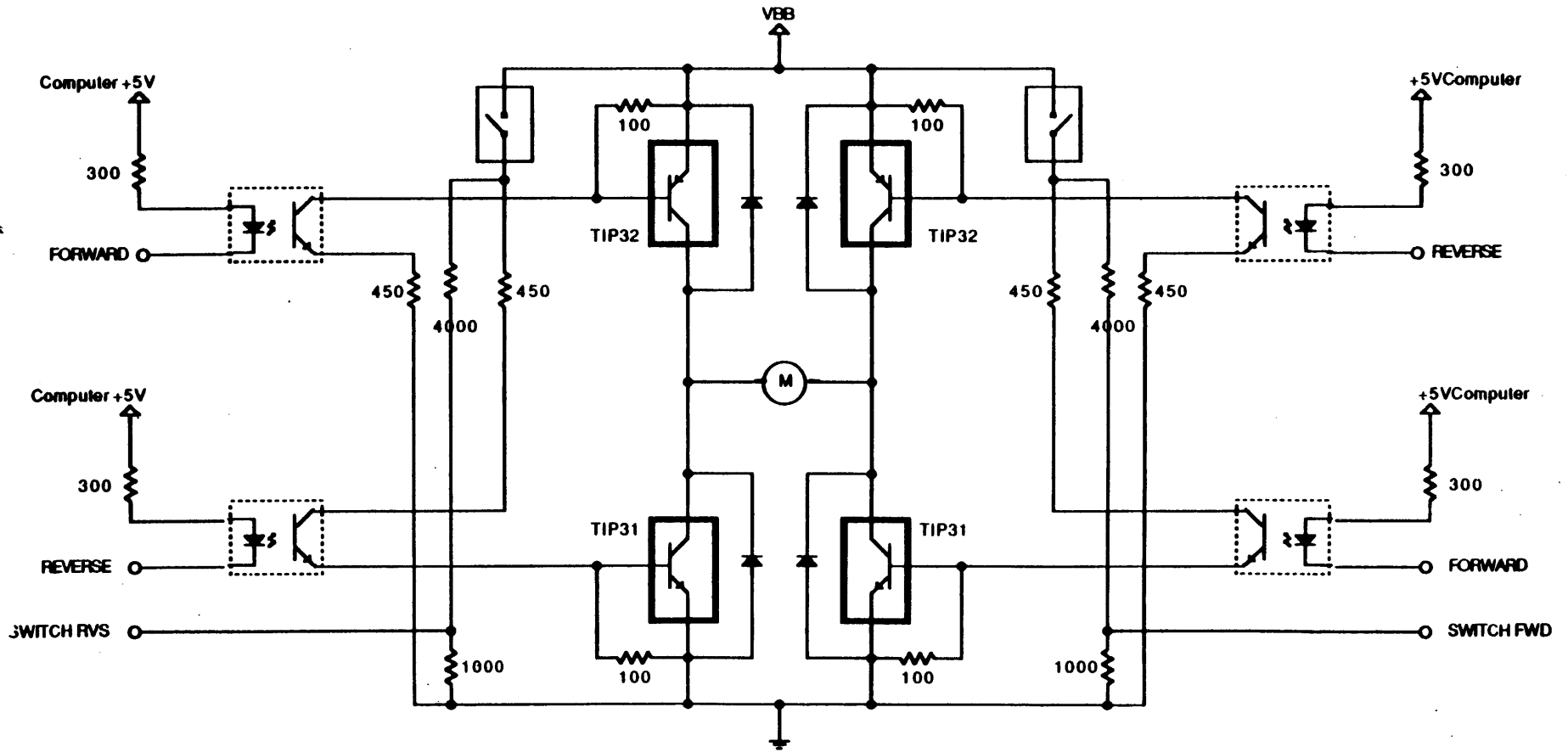


Figure 3.12 Balancer Motor Driver Circuit

of PVC, which is 6 in., was deemed too large for easy mounting on STAR's structure. Assuming that the balancer weights would be made in the shape of cylinders which would closely fit inside the PVC tube, the 3 in. I.D. pipe would require a cylindrical weight 6 in. in length to meet the requirement of 225 in.-lb. of controlled moment, since this weight length means that the original nut travel of 20 in. would be reduced to 14 in. The 4 in. I.D. pipe, however, would require a weight length of 3 in., meaning that the lead screw travel would only be reduced to 17 in. While both of these possible pipe diameters would provide the necessary control moment, the 4 in. I.D. pipe was chosen because its longer nut travel translates into more precise position control for a given optical encoder resolution.

3.3.6 Construction

Referring to Figure 3.13, the balancer was designed with circular support disks of Aluminum 6061-T6 on either side of the lead screw. The lead screw was held in place with two angular contact ball bearings, one mounted in each disk. Angular contact bearings were chosen over normal bearings to account for both radial loads, which occur when the balancer shaft is horizontal, and axial loads, which occur when the balancer shaft is vertical. To support the motor and optical encoder, which are positioned at either end of the lead screw, a motor mounting plate and an encoder mounting plate were attached with axial spacers to the lead screw support disks. The motor shaft was connected to the lead screw with a universal lateral coupling, which accommodated both simultaneous lateral and angular misalignment. The encoder shaft was connected to the lead screw with a simple slip coupling. For increased rotational strength, all four shaft ends were held in the couplings with set screws which impacted against flats machined on all shaft ends.

To prevent the weight from traveling past the end of the lead screw, limit switches were attached to both lead screw support disks. The normally-closed switch signals were integrated into the motor driver circuit discussed above in such a way as to prevent motion in the direction of the tripped switch, while still permitting motion in the opposite direction.

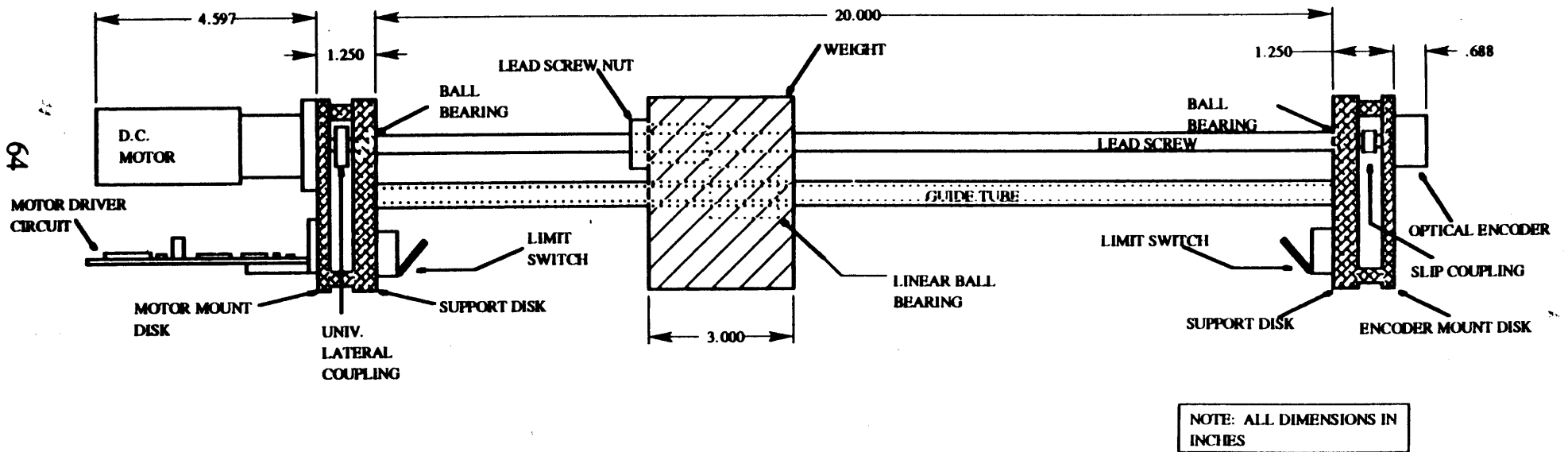


Figure 3.13 Balancer Assembly

The lead weight was attached to the lead screw nut with bolts which passed through the nut and which were turned into threads tapped into the weight. Since lead is a very soft metal, Heli-coil threaded inserts were used to strengthen the otherwise weak threads. A stainless steel guide tube was added for two reasons: to relieve the lead screw of most of the weight's load in the radial direction; and to prevent the weight from rotating with the lead screw when the screw was turned. Tubing was used as a guide rather than solid rod to allow the encoder and limit switch wiring to be passed through the tube to the motor end of the PVC tube. A linear ball bearing was imbedded in the weight to allow it to slide along the guide tube.

Figure 3.14 shows the balancer mechanical assembly enclosed in PVC tubing. One end of the tube was permanently closed with a slip fit end cap. The other end was closed with a combination of a slip fit x pipe thread coupling and a threaded end cap. The threaded cap allowed access to and removal of the motor driver circuit. Figure 3.15 is a photograph of a completed balancer. Figures 3.13, 3.14, and 3.15 are intended to give an overview of the balancer design; detailed engineering drawings of the various mechanical components are included in Appendix A.

3.4 Vision

Unfortunately, there was insufficient time for vision subsystem development at the time of this writing. Thus, neither the two pairs of stereoscopic cameras, which were deemed necessary for teleoperation experimentation, nor the monoscopic tilt-and-pan camera, which was necessary for machine-vision navigation, were developed.

3.4.1 Camera System Design

To aid in the preliminary pool testing of STAR, a simple, monoscopic belly-mounted camera system was developed. This camera enabled rudimentary teleoperated control of STAR by supplying the remote operator with motion feedback via screen display of STAR's environment. The camera used, a Pulnix TM-540RV, was designed for external clocking of its charge-coupled-device (CCD), making it readily synchronized with

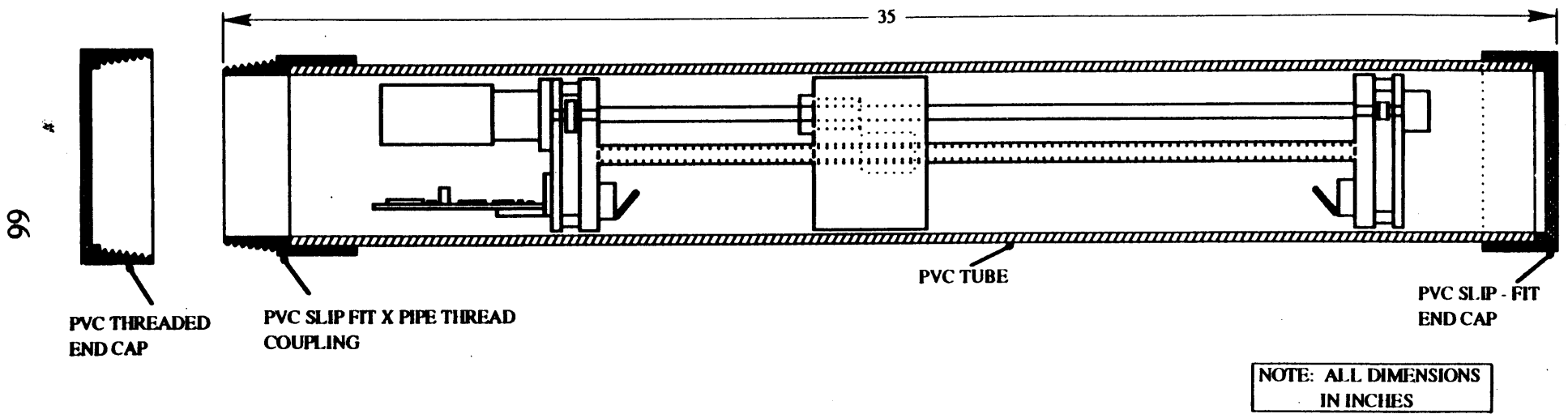


Figure 3.14 Balancer Assembly and PVC Tube

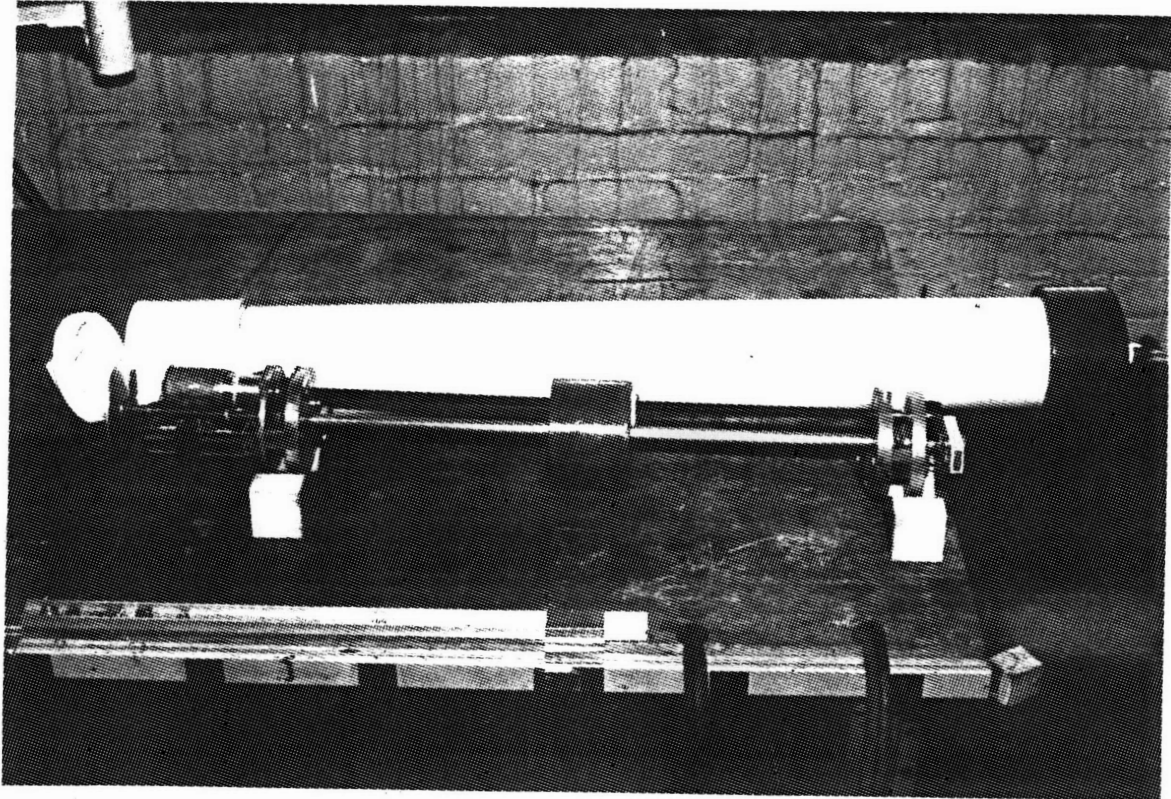


Figure 3.15 Photograph of Balancer Assembly and PVC Tube

machine-vision electronics. Thus, for the simple task of supplying a remote image to the operator, a timing circuit was designed and constructed. The timing circuit was included inside the waterproof camera enclosure to reduce the number of wiring inputs to the enclosure to two: +12 V and 12 V return. The only wiring output from the camera enclosure was a coaxial cable carrying the video signal to the remote operator.

3.4.2 Enclosure

The camera required a waterproof enclosure for underwater operation. To reduce the number of STAR enclosures requiring overpressurization, it was decided that the camera enclosure should be capable of operation with only 1 atm internal pressure. This requirement necessitated the use of O-ring seals on enclosure openings. To greatly reduce the amount of time needed to machine the O-ring glands, a round tube was chosen to enclose the camera rather than a rectangular tube. This enabled the O-ring glands to be easily machined using a lathe.

The camera and its enclosure are presented in Figure 3.16. The tube flanges were welded to the tube; since 6061-T6 is the best Aluminum alloy for welding, it was used for the flanges, the tube, and one of the end disks. The other end disk was made of Lexan to provide a clear window in front of the camera lens. O-ring glands were machined on both end disks, rather than on the flanges that mate with them, because the end disks are replaceable in the event of gland damage. The flanges were designed to have more width than structurally necessary (0.5 in.) in order to minimize the amount of disk deformation from thermal stresses encountered during welding.

The camera was attached to a bar cantilevered from the rear end disk. This allowed the camera to be easily removed from the tube. The timing circuit, which was soldered to a piece of circuit card, was simply taped to the top of the camera. For waterproof input and output connections, the +12 V and 12V return input wires, and the coaxial output cable, were potted into brass pipe fittings which were used as wire pass-throughs.

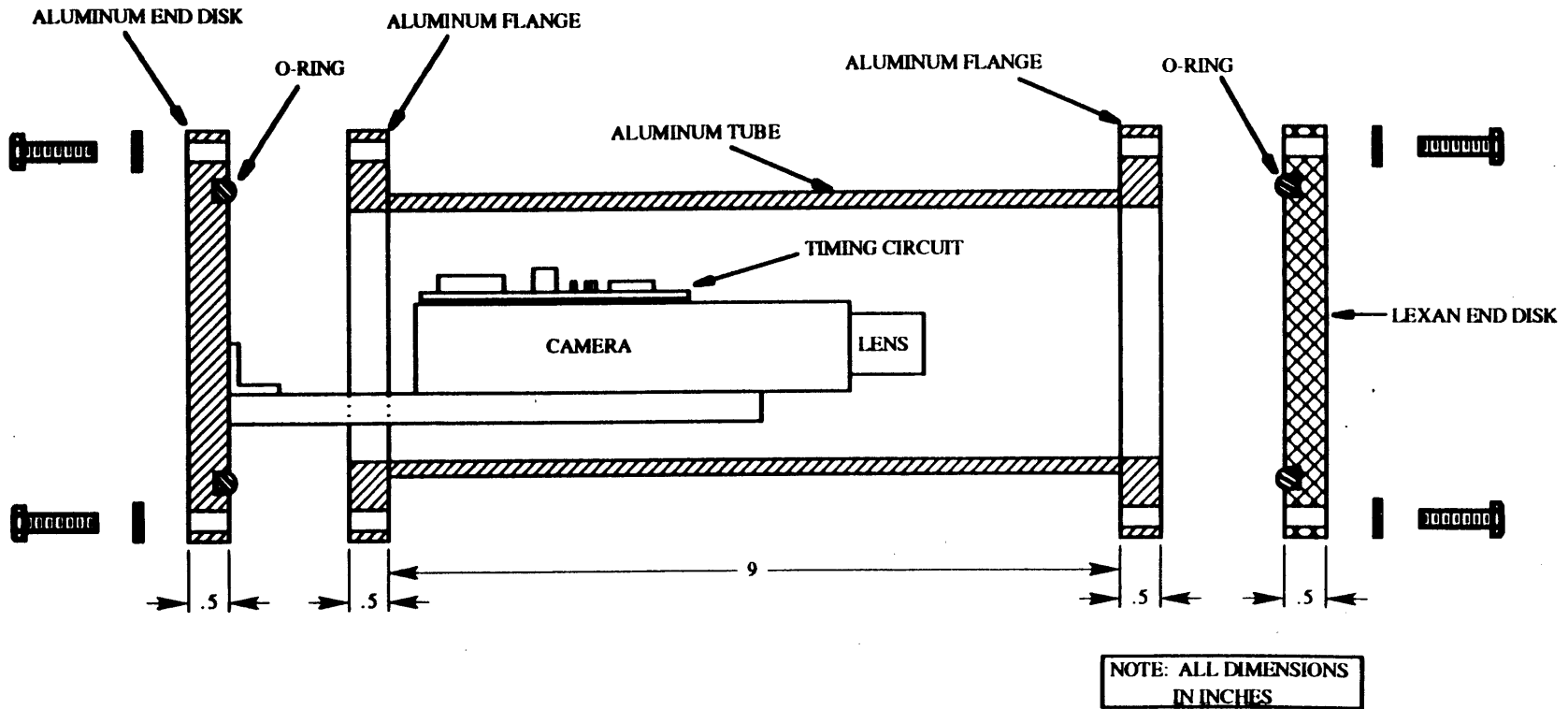


Figure 3.16 Sectional View of Camera and Housing

These brass fittings were then screwed into threaded holes in the Aluminum end disk behind the camera.

The Aluminum end disk was also used to mount the camera onto the vehicle. The camera was bolted to a simple Aluminum U-channel frame which was in turn bolted to the front plate of the pressure vessel (see Section 3.8). Figure 3.16 is intended only to give an overview of the camera and its enclosure; detailed engineering drawings of the enclosure flanges and end disks are included in Appendix A.

3.5 Sensors

As mandated in Subsection 2.2.5, the sensor subsystem was designed to include rate sensors to support vehicle control, accelerometers to support automatic vehicle balancing, and a pressure transducer to support control system debugging. These sensors were placed inside the electronics compartment of STAR since their measurements were to be utilized by the computer system. These sensors each return a voltage proportional to the magnitude of the quantity measured; hence, these voltages were interfaced directly to the analog-to-digital conversion card. The digitized sensor signals were then able to be directly read by the computer. The various power needs of the sensors were met by the power converters in the electronics compartment.

3.5.1 Angular Rate Sensors

On previous vehicles built by the SSL, fluid-based angular rate sensors were used. There was one major problem with these sensors, however: the measurement biases determined during calibration tended to drift during experimentation. For this reason, piezoelectric rate sensors, manufactured by Watson Industries, Inc., were chosen for STAR. The sensing mechanism in these sensors consists of piezoelectric bender elements mounted to a rigid base. These elements are resonantly driven in opposite directions; during angular motion, the sense elements vibrate 180° out of phase. When linear acceleration or vibration is present, however, the sense elements vibrate in phase. This allows the rejection of linear

motion from the output signal. The solid state electronics used in this sensor allow a signal drift specification of less than 0.1% full scale.

These rate sensors require $\pm 15\text{VDC} \pm 5\%$ with a 20 mA maximum. The output from these sensors is 0VDC at zero angular rate to $\pm 10\text{VDC}$ at full scale angular rate. A complete list of specifications is included in Appendix B.

3.5.2 Accelerometers

The types of accelerometers available can be divided into two categories: high-frequency accelerometers used for vibration measurement, and low-frequency accelerometers used for measurement of DC accelerations. Since the task of automatic balancing requires measurement of gravitational acceleration, the latter category of accelerometer was needed. The range of acceleration required to be measured was zero to one gravity (1g).

The accelerometer chosen was manufactured by NOVA Sensor, model NAS-002-C. A silicon cantilever sensor chip with integral air damping is used in this sensor to measure acceleration along one sensitive axis. The range of acceleration measured is $\pm 2g$. This accelerometer was chosen for its small size, high sensitivity, and good DC response.

The power requirements for these accelerometers were as follows: +12VDC with 5 mA maximum current. The output was a voltage range from 0 - 5VDC; hence, zero acceleration corresponded to an output voltage of 2.5VDC. A complete list of specifications are included in Appendix B.

3.5.3 Sensor Mount

Figure 3.17 shows the mounting arrangement used on each of the rate sensors. For protection from impacts that would tend to produce output errors, the sensor was packaged with foam inside a 3.25 in. long piece of 2 in. x 2 in. Aluminum box tube. Figure 3.18 is an assembly drawing showing the sensor subsystem base plate and the sensor mounting arrangement. The three rate sensor box tubes are mounted orthogonally to align with the vehicle axes. The three accelerometers are also mounted orthogonally to align with the axes shown. Since the accelerometers are

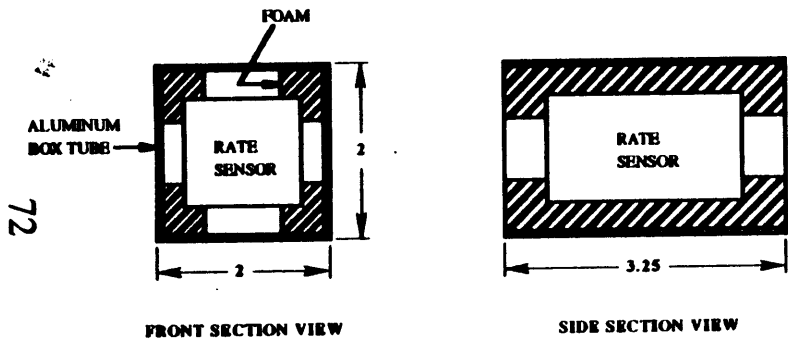


Figure 3.17 Detail of Rate Sensor Mounting

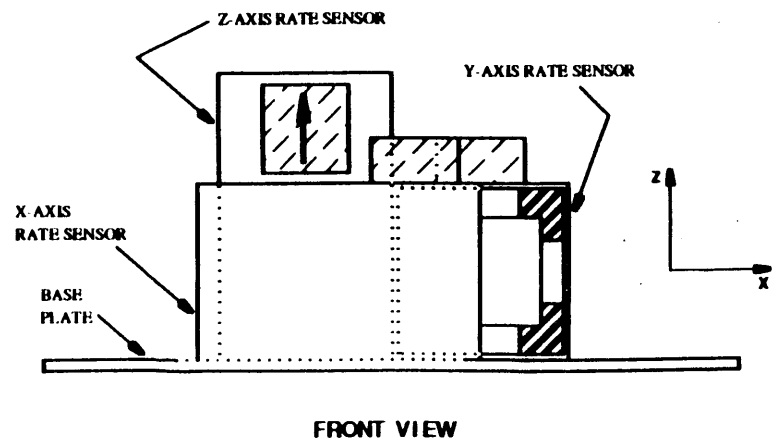
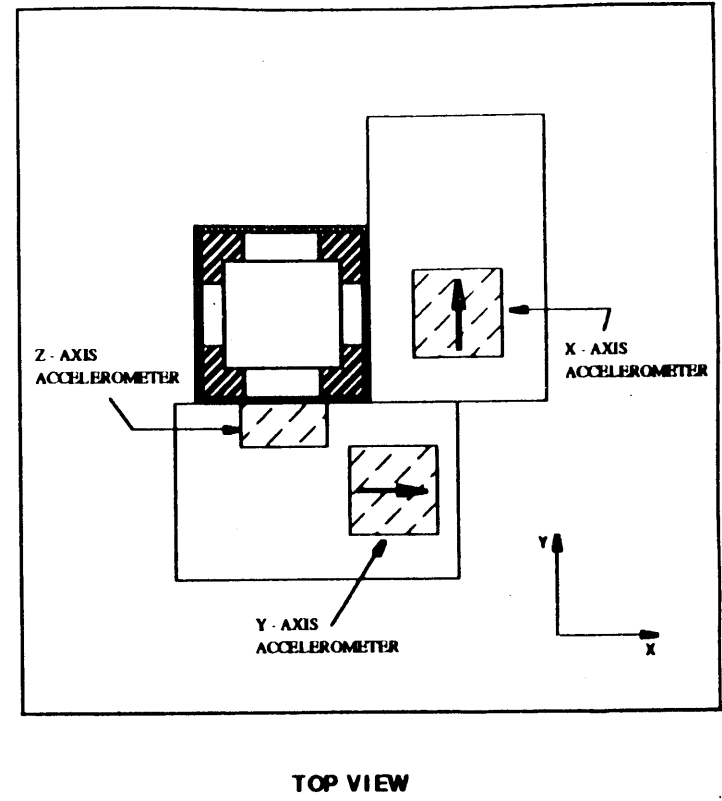


Figure 3.18 Sensor Subsystem Assembly

compact, measuring only 1 in. x 1 in. x 0.5 in., they are simply affixed to the rate sensor box tubes as shown. The arrow placed on each accelerometer indicates the sensitive axis of the accelerometer as well as the direction of positively-measured acceleration. The sensors were mounted on a base plate for several reasons. The primary reason was space-efficiency; however, having the sensor subsystem mounted on one plate allowed the subsystem to be removed from the electronics compartment as a whole. This was very useful for attitude control development, as the sensor subsystem could be removed and rotated by hand to evaluate control system response prior to pool testing.

3.6 Power

In Subsection 2.2.6, it was stated that rechargeable batteries were to be used to supply STAR with power. The power subsystems of the three SSL vehicles all used batteries, with much success. In choosing the type of batteries for use on STAR, two possibilities were considered: Lead-acid batteries, or Nickel-Cadmium batteries. Nickel-Cadmium batteries were capable of delivering higher performance, meaning that, for a given battery volume, Nickel-Cadmium batteries could supply more power than Lead-acid batteries. Also, Nickel-Cadmium batteries could be recharged more quickly than Lead-acid batteries. Finally, Nickel-Cadmium cells were capable of longer lifetimes, meaning they could undergo a greater number of discharge/recharge cycles before expiring than Lead-acid batteries.

There were several drawbacks to the use of Nickel-Cadmium batteries, however. Of primary importance was the fact that Nickel-Cadmium batteries were more likely to release Hydrogen gas during operation than Lead-acid batteries. The extreme volatility of Hydrogen gas made its presence in STAR very dangerous. Of lesser importance, Nickel-Cadmium batteries, unlike Lead-acid batteries, were required to be completely discharged on a regular basis to maintain longevity. Also, Nickel-Cadmium batteries were more expensive and more difficult to purchase in large sizes than Lead-acid batteries.

For the reasons outlined above, sealed Lead-acid batteries, manufactured by PowerSonic of Redwood City, CA, were chosen for STAR's power subsystem. Since the propulsion subsystem power requirements were much larger than those of any other subsystem, the needs of the propulsion subsystem were used to choose the voltage output of STAR's batteries. The electric thruster motors required 24VDC for operation; unfortunately, 24V batteries were not available, requiring the use of paired 12V batteries. Having determined the batteries' voltage output, the next issue was to size the current capacity of the batteries. To save space and increase simplicity, it was desirable to utilize a small number of large-capacity batteries rather than a large number of small-capacity batteries. The largest affordable current capacity was 20 A-hr.; hence, 12VDC sealed lead-acid batteries with 20A-hr. current capacity were chosen for use in STAR's power subsystem.

As mentioned earlier in Subsection 2.2.6, the power subsystem was divided into two separate parts due to the radically different power requirements of STAR's subsystems. The first partition was designed to satisfy the high-current requirements of the propulsion and balancer subsystems. The second partition of the power subsystem was designed to satisfy the stable, low-current, multi-voltage-level power requirements of the computer/electronics subsystem, the sensor subsystem, and the vision subsystem. Since these partitions were completely isolated from each other, each partition is presented separately in the following two subsections.

3.6.1 High-Current Power

The high-current power system was designed to supply the propulsion and balancer subsystems. To size the number of batteries needed to adequately supply the propulsion and balancer subsystems, the total amount of current needed, delivered at +24VDC, for six hours of normal operation was calculated as follows. Only the thruster motors are considered for this calculation because the current draw of the balancers is negligible compared to that of the thrusters. First, a very conservative estimate of 50% was used to quantify the percentage of total pool-test time that the thrusters are actually powered. Thus, 8 thruster motors, nominally

operating at 5A for 50% of 6 hr., require 120 A-hr. of current capacity. Since batteries of 20A-hr. capacity were chosen, 6 batteries were needed to power the thruster and balancer subsystems. To provide a margin of safety, 8 batteries were used.

Figure 3.19 is a diagram showing the layout of the thruster/balancer power system. All the components of the high-current power system shown in Figure 3.19 were mounted in the top battery compartment except for two of the eight batteries, which were mounted in the bottom battery drawer (see Subsection 3.8 for a detailed presentation of the structural placement of STAR's subsystems). The batteries were paired to provide +24VDC and GND to the thruster and balancer drivers. To prevent unequal discharge of the batteries, the battery-pairs were connected in parallel. To permit remote switching of the high-current power system, four relays were used in the +24V line. Each relay switches power to two thruster motors and one balancer motor. The thruster motor drivers were assigned to the relays such that drivers which actuated the same degree of freedom would be switched from separate relays. The balancer motor drivers were assigned to separate relays. This relay/driver configuration was implemented to minimize the current drawn through each relay. For safety, each battery was independently fused at its positive terminal; also, each positive supply line from the relays to the drivers was fused.

The lower left portion of Figure 3.19 shows the relay coils that control the relay switches. These coils were supplied with +24VDC from the power converters in the electronics compartment. The relay coils' connection to ground is switched by the driver circuit card located on the STD-bus. This arrangement permits remote switching of the high-power system relays via computer.

3.6.2 Low-Current Power

The delicate electronics contained in the computer/electronics subsystem, the sensor subsystem, and the vision subsystem require a variety of different voltage levels. Since these electronic components draw very little power, DC-DC power converters were used to generate the various voltages without danger of significant heat dissipation in the sealed, unventilated electronics compartment. The power converters also contain

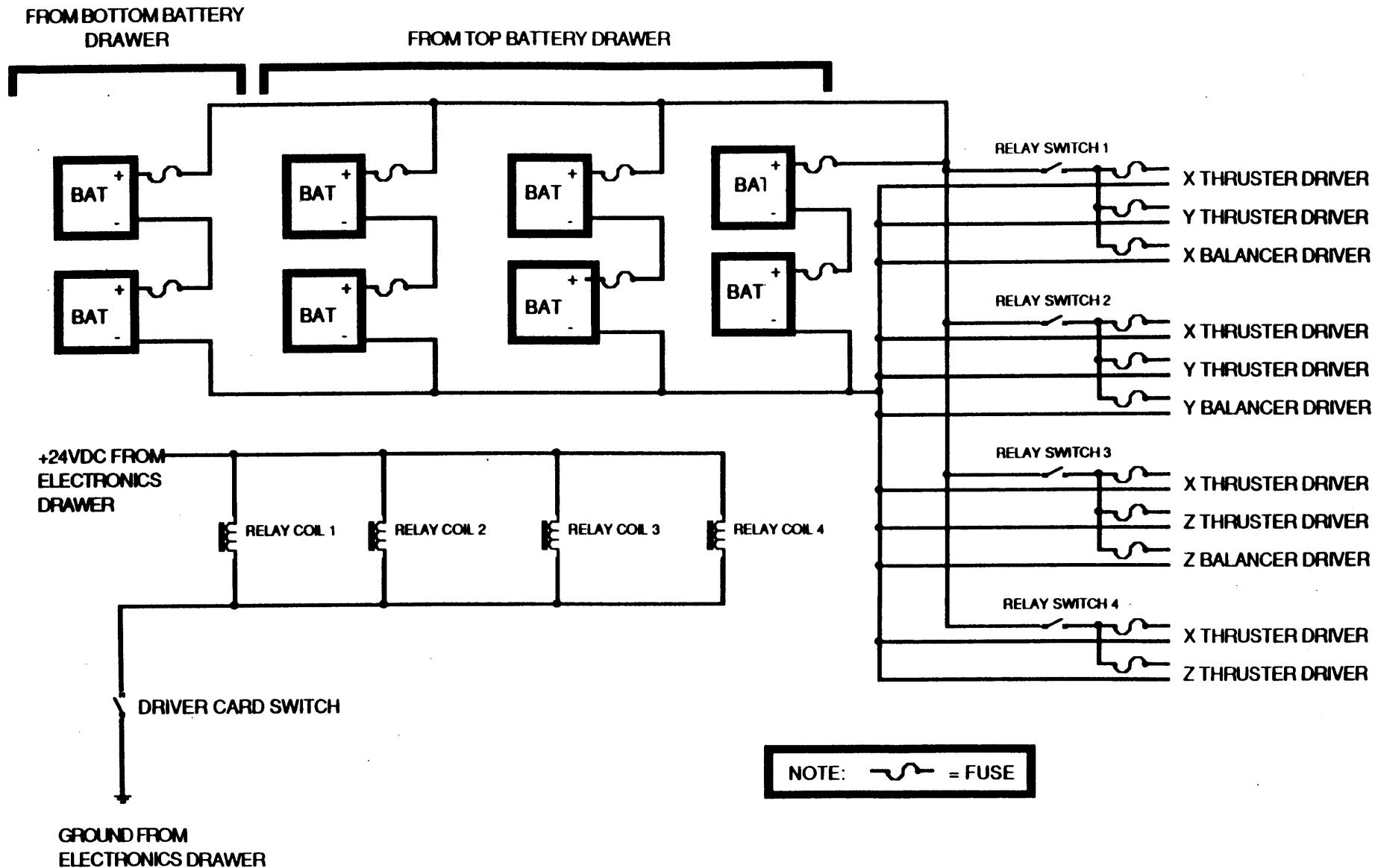


Figure 3.19 High-Current Power System Layout

the regulation circuitry necessary to supply the precise, steady voltages required by the above-mentioned delicate electronics. Figure 3.20 shows the low-current power configuration. The power converters were supplied with +24VDC and ground from two battery-pairs located in the bottom battery compartment. The power converters supplied the following power outputs, shown on the right side of the figure: +5VDC, -5VDC, 5V GND, +12VDC, -12VDC, 12V GND, +15VDC, -15VDC, and 15V GND. The +24VDC supply to the power converters was switched with a relay located in the bottom battery compartment. The relay switch was controlled by the relay coil, which was supplied with +24V from the right-most battery-pair in the figure. This coil was in turn controlled by the external ON/OFF switch shown in the figure. The ON/OFF switch was waterproofed and mounted on the exterior of the vehicle for access by divers. For safety, each of the batteries was independently fused.

Thus, the low-current power system is switched on and off by the exterior, waterproofed switch. Since this power system supplies the onboard computer with power, turning the exterior switch on boots the onboard computer. Once the onboard computer is booted, the DC driver circuit card can be accessed from the remote control station computer via the QNX network. In this way, the high-current power relays can be remotely switched. For safety, the DC driver circuit card shuts down the high-power relays when power to the STD-bus is shut down. This is important, as it permits divers to shut off the high-current power system from the exterior switch in the event that the computer network becomes unreliable.

3.6.3 Battery Chargers

To recharge the batteries after discharge, AC-supplied battery chargers, also manufactured by PowerSonic, were purchased. These chargers were mounted in two portable, waterproof cases to permit pool-side recharging. Each battery must be charged independently to eliminate preferential charging; hence, connectors were installed at the power and ground leads of each battery to permit easy, fast interfacing of the chargers to the batteries. Each recharger was outfitted with a voltmeter and rotary switch to permit easy measurement of the charge level in each battery. Figure 3.21 shows one of the recharger cases.

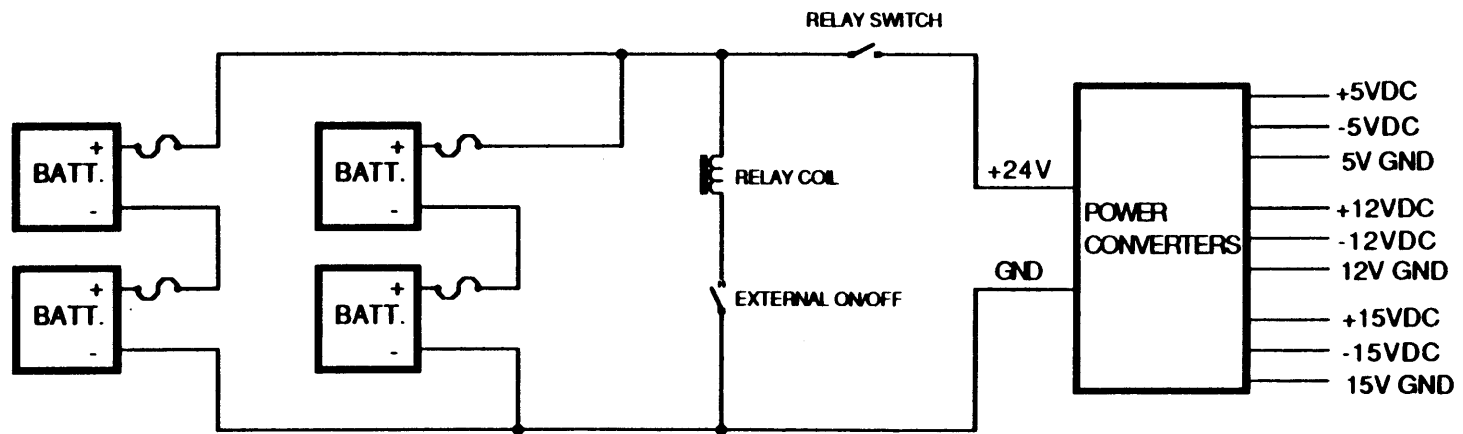


Figure 3.20 Low-Current Power System Layout



Figure 3.21 Photograph of Battery Recharger Case

3.7 Pressure

The pressure subsystem was designed to supply regulated, pressurized air to the thruster motor casings. A SCUBA pressure bottle and regulator were chosen for the pressure subsystem for two reasons: first, a compressor capable of filling SCUBA bottles was available at MIT's alumni pool, where experimentation would occur; and, second, SCUBA components are extremely durable and corrosion-resistant. Since SCUBA regulators are designed to supply air to divers at a pressure equal to that of the surrounding water pressure, the SCUBA regulator's second stage was modified to produce an over-pressure of 3 psi.

Figure 3.22 shows a side section view of the modified second stage. The diaphragm, which is exposed to the ambient water pressure, controls the needle supply valve via movement of the rocker arm. During unmodified operation, the internal pressure of the regulator is equal to the ambient water pressure. In this modified configuration, however, the spring-driven plunger shown at the top of the figure opens the needle valve until there is sufficient pressure in the regulator to push the diaphragm up and compress the spring. This pressure is easily adjusted to 3 psi. by rotating the threaded plug which holds the spring/plunger combination against the diaphragm. A linear ball bearing was used to guide the plunger.

Figure 3.23 shows a top and bottom view of the modified second stage. The bottom view shows the former exhaust and output openings. The exhaust vent was completely sealed using 3M insulating resin. A 1/4 in. hose barb x 1/8 in. MNPT pipe fitting was sealed, also using insulating resin, into the output opening to connect the output of the second stage to the rest of the pressure subsystem. The top view of the figure shows the vents in the second stage casing that expose the diaphragm to water.

An over-pressure of 3 psi. above ambient was chosen to maintain the waterproof integrity of the thruster motor shaft seals. The volume of air required to supply this over-pressure throughout STAR's six hour operational requirement was determined as follows. The internal volume of one thruster motor casing is approximately 18.85 in.³, or 0.0109 ft.³.

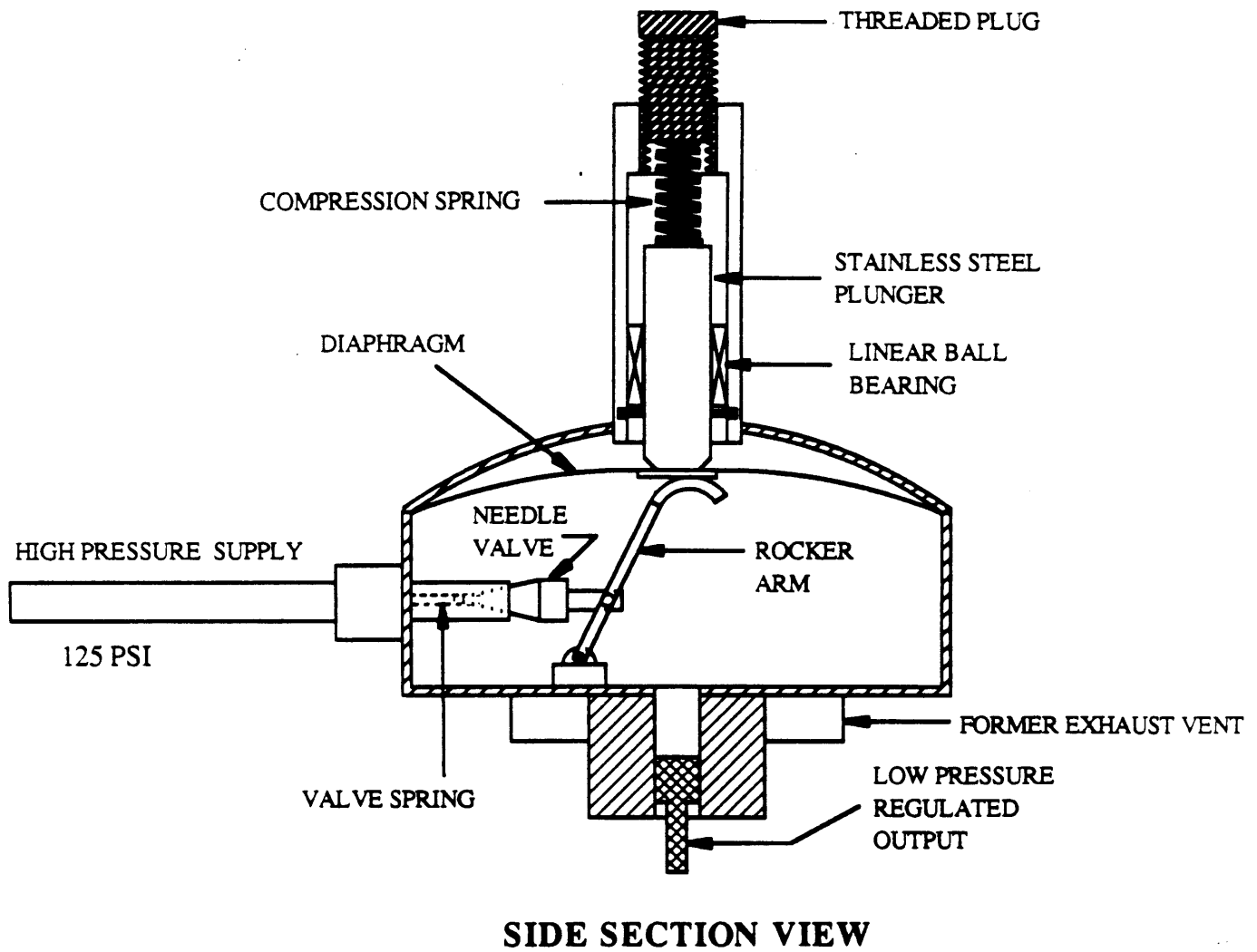
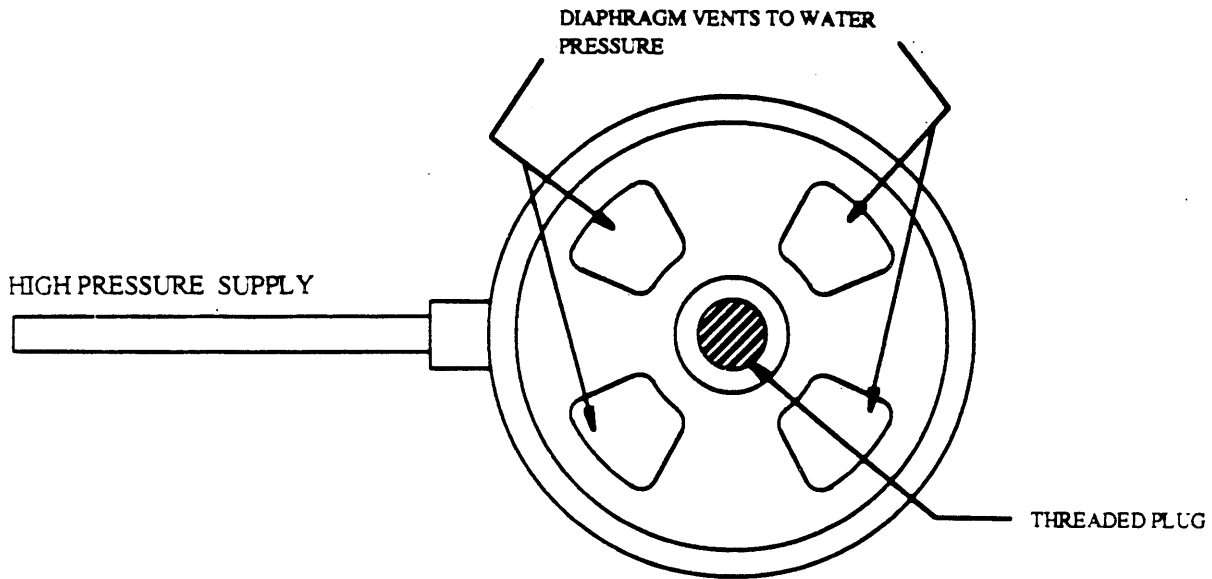
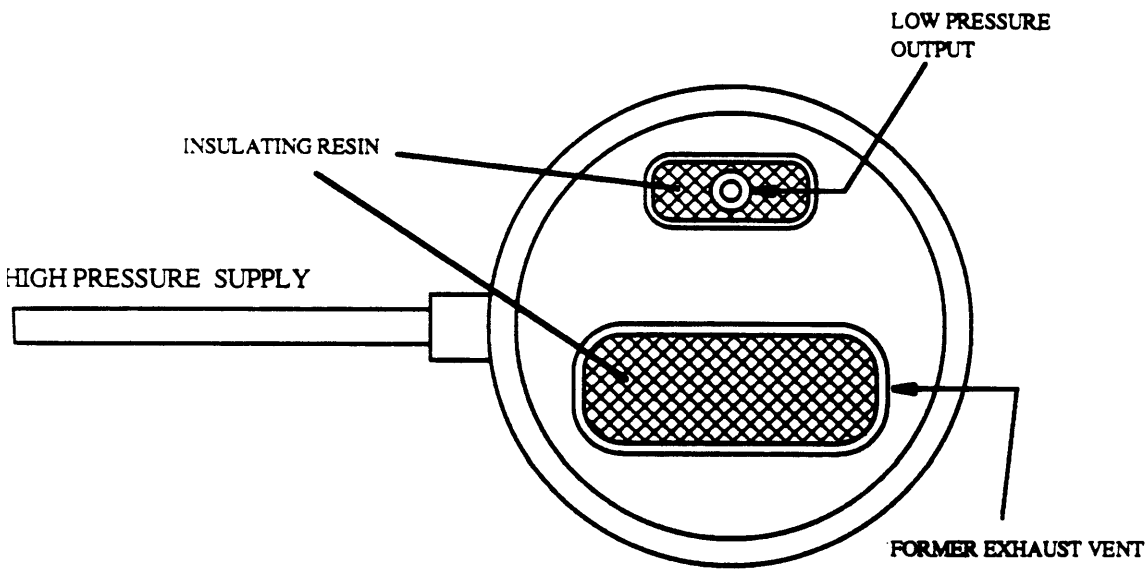


Figure 3.22 Side Section View of Regulator Second Stage



TOP VIEW



BOTTOM VIEW

Figure 3.23 Top and Bottom Views of Modified Second Stage

This amounts to a total volume of 0.0873 ft.³ for eight thrusters. At STAR's maximum design depth of 40 ft., the ambient water gauge pressure is 18 psi. To maintain an over-pressure of 3 psi. at the water's surface, 0.105 ft.³ of air is needed (to maintain a gauge pressure of 3 psi. in the casings); to maintain a 3 psi. over-pressure at a depth of 40 ft., 0.194 ft.³ is needed (to maintain a gauge pressure of 21 psi. in the casings). Thus, each time STAR descends from the surface to a bottom depth of 40 ft., an infusion of 0.0891 ft.³ of air is needed to maintain the over-pressure. When STAR resurfaces, this added volume of air is vented through the relief valves. Using a conservative estimate of 10 complete 40 ft. depth changes in one hour of pool testing, it was calculated that STAR's pressure subsystem would expend 5.34 ft.³ of air in a six hour period. To provide a margin of safety, a 15 ft.³ SCUBA bottle was purchased for use with STAR's pressure subsystem. This extra air volume also allowed for expansion of the pressure system to include manipulator joint motors and pressure-actuated end effectors.

Figure 3.24 presents the layout of the pressure subsystem. The SCUBA bottle, shown on the left side of the figure, contains air compressed to 2000 psi. The first stage of the regulator reduces the air pressure to 125 psi., which is used to supply the second stage. The modified second stage outputs a regulated 3 psi. gauge pressure. A manifold was machined from brass to connect the 3 psi. output from the second stage to the 2 relief valves and the 8 motors. The regulator used was a Dacor 460/XLT. The relief valves used were model 2902-PK-T, manufactured by Arrow Corp. All pressure line connections were made with quick-disconnect fittings, made of Delrin by the Colder Products Company of St. Paul, Minnesota.

3.8 Structure

Because STAR's computer/electronics and power subsystems are significantly larger and more massive than the other subsystems, the design of the waterproof enclosures containing these two subsystems drove the structural design of the entire vehicle. In past SSL vehicle designs, the containers used to house these subsystems were constructed of foam core overlaid with epoxy resin and fiberglass cloth. The fiberglass lids of these

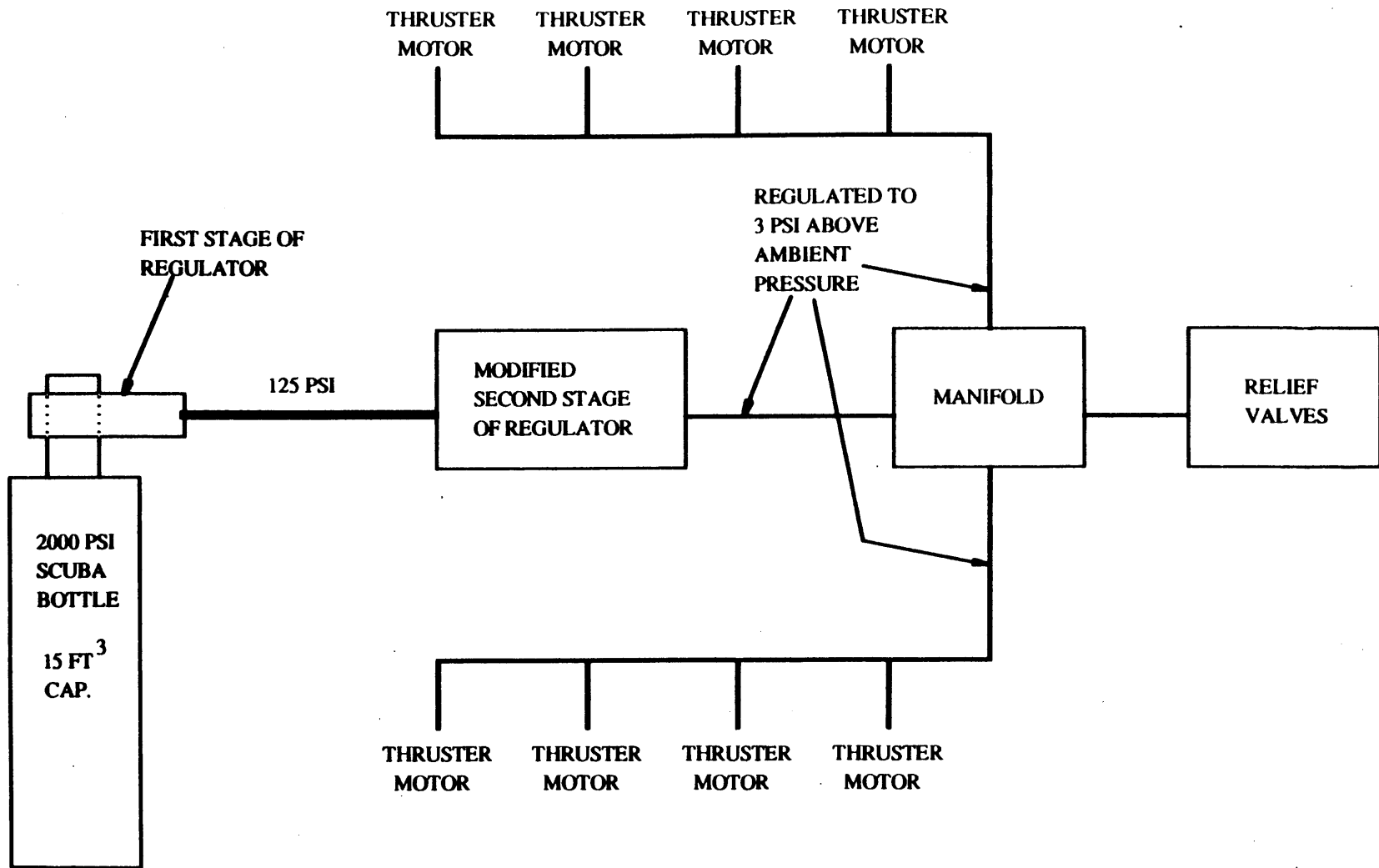


Figure 3.24 Pressure Subsystem Layout

cases were then sealed with a rubber gasket. This seal was not water-tight, however; as a result, each container was required to be pressurized above the surrounding water pressure.

There are several advantages to the foam-and-fiberglass construction method. First, since the foam's density is low, the boxes have very small mass, despite being strong and stiff. This results in easy handling of these containers outside of the pool. Second, the outer shell of epoxy and fiberglass provides excellent corrosion-resistance. There are several drawbacks to foam/fiberglass, however. First, since the construction method is imprecise, and the resulting material is not of consistent hardness, machining of the finished containers is impossible. This fact eliminates the possibility of using an O-ring to seal a foam container's lid, necessitating the use of a gasket, and, hence, over-pressurization. During past SSL experimentation, the use of pressurized containers was found to be undesirable for two reasons: first, the pressurization of large volumes necessitated the expenditure of large volumes of compressed air during pool testing, which adversely affected the buoyancy of the vehicle; second, air bubbles vented during upward vehicle movements became trapped under the vehicle, applying an external, buoyant force to the vehicle. Another drawback to foam construction of waterproof containers is that all bulkhead connectors and passthroughs must be permanently glued into the wall of the container, severely limiting the reconfigurability of the container's electrical and pressure connections to other subsystems.

As a result of the above-stated drawbacks with past SSL vehicle designs, STAR's computer/electronics and power subsystem enclosures were constructed of metal rather than a foam/fiberglass combination. The selection of metal was made primarily to enable the precise machining of O-ring glands to permit the use of non-pressurized containers. Several types of metal were considered for use, among them Titanium, stainless steel, and Aluminum. Titanium, while very light and very strong, is very difficult to machine, as well as very expensive. Stainless steel, an obvious choice for use in corrosive environments, is heavy and difficult to weld. Thus, the Aluminum alloy 6061-T6 was chosen for its light weight, machinability, low cost, and readiness for welding.

3.8.1 Pressure Vessel

As stated above, the computer/electronics and power subsystems enclosures drove the design of the entire structure. Safety considerations required that the power subsystem be placed in a separate container from all other subsystems. Since the power subsystem includes batteries, the power subsystem is significantly heavier than the computer/electronics subsystem. Having two containers of such disparate masses would present a problem for vehicle balancing, as the center of mass of the two containers would not be close to the center of buoyancy, located at the geometric center of the two containers. For this reason, the power subsystem was divided into two separate containers. This division allowed the two power containers to be placed on either side of the computer/electronics container.

To save space and weight, it was decided to use one container, partitioned into three compartments, to house the two parts of the power subsystem and the computer/electronics subsystem. Each of these subsystems was mounted in detachable drawers which slid out its compartment for access. For the remainder of this document, this container will be referred to as the pressure vessel. Since a pressure vessel large enough to enclose these three items would have to be very strong and massive to withstand the water pressure at a depth of 40 ft., it was decided to make this container the main structural element of the vehicle. This meant that all vehicle subsystems would either be mounted to the outside of the pressure vessel, or inside one of the container's compartments. For this reason, the front and the back of the pressure vessel were designed to be flanges, i.e., they extended beyond the rectangular shape of the container volume to provide external mounting surfaces for vehicle subsystems. A back view of the pressure vessel is presented in Figure 3.25, showing the layout of the battery and computer/electronics compartments. Figure 3.26, a side view of the pressure vessel, shows the front and back flanges. Figure 3.27 shows a section back view of the three drawers inside the compartments; note that, for clarity, the back plate of the pressure vessel is not shown. The pressure vessel was designed to be symmetric along all three axes to fulfill the requirement of rotational balancing.

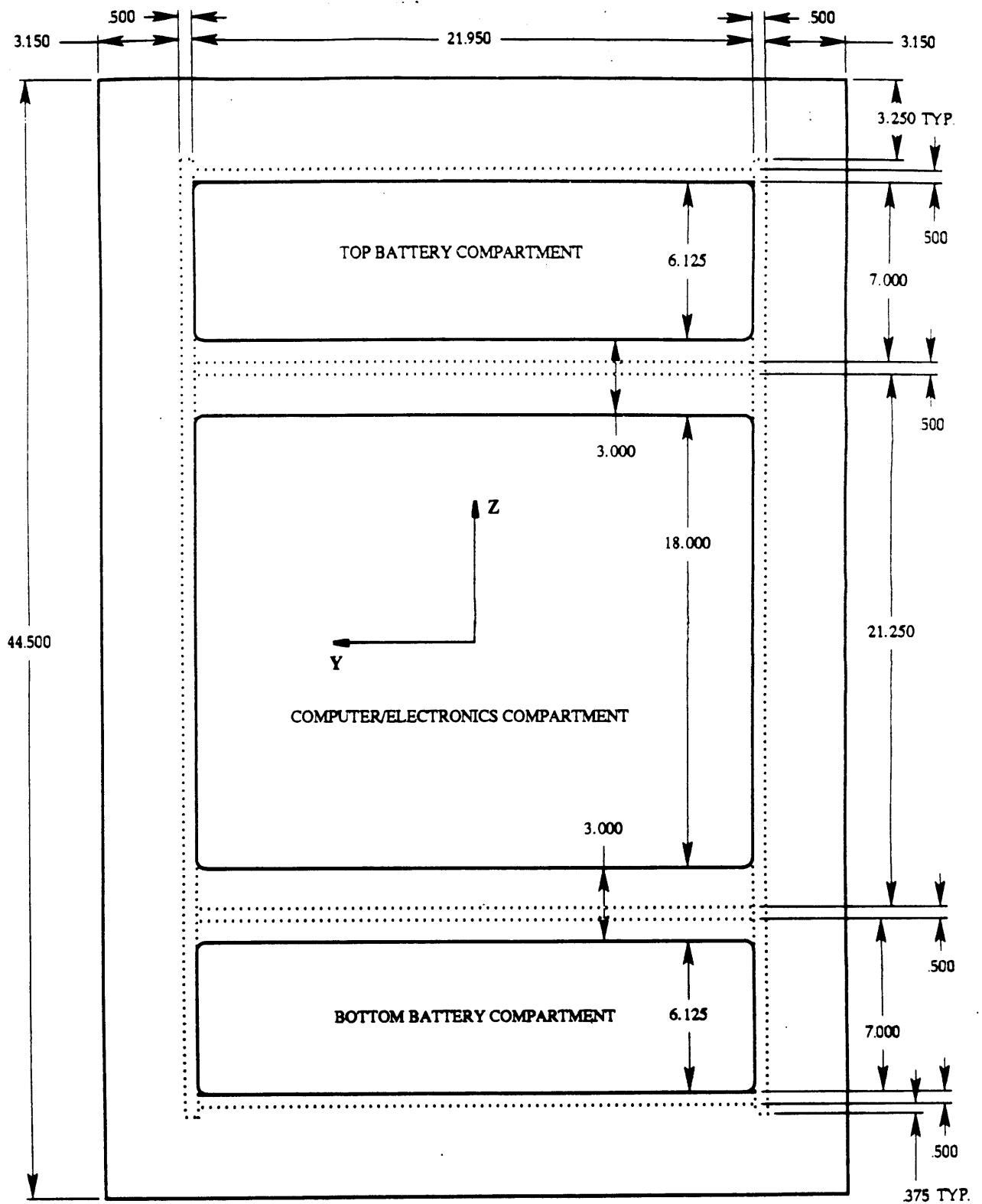


Figure 3.25 Rear View of Pressure Vessel

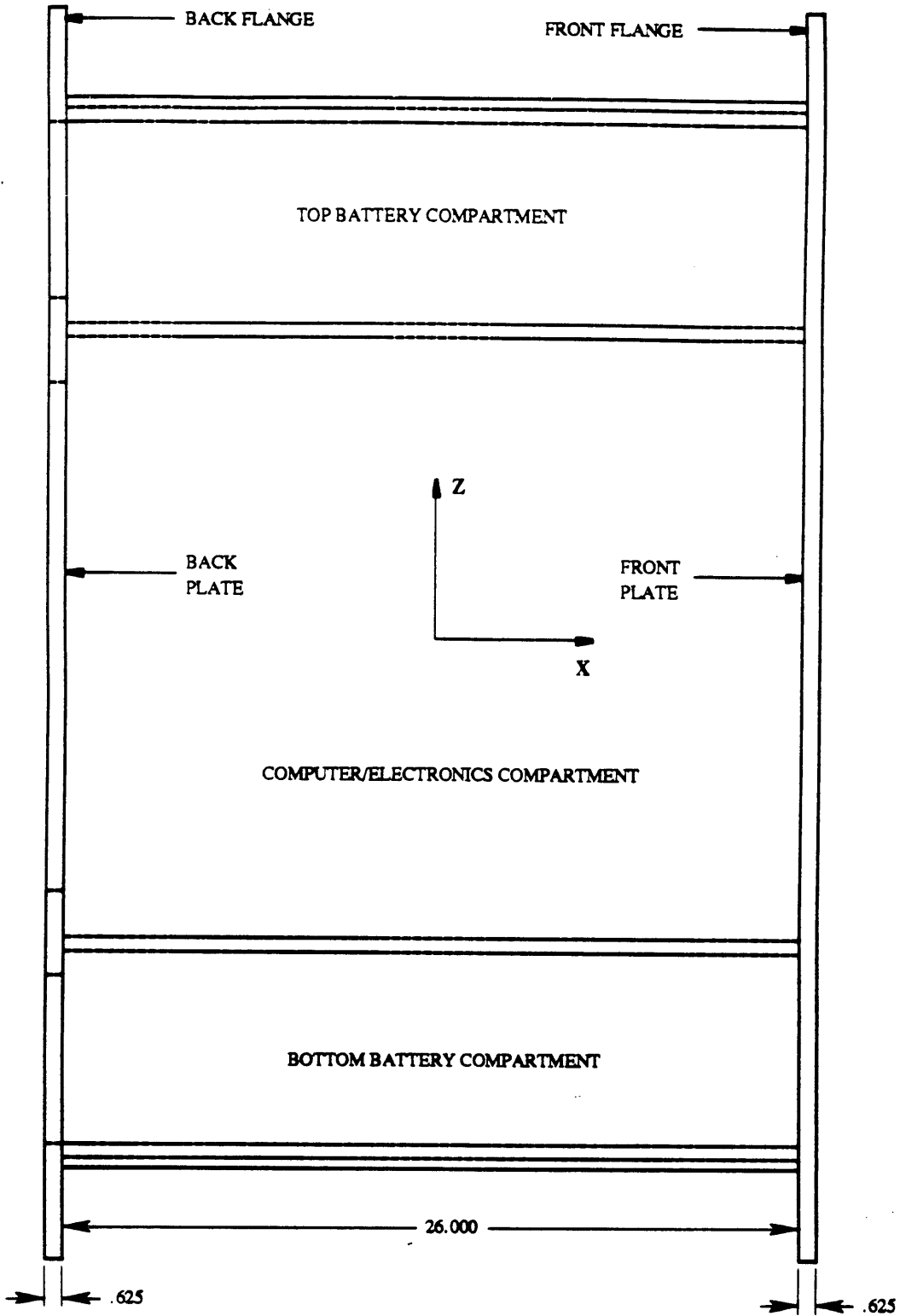


Figure 3.26 Side View of Pressure Vessel

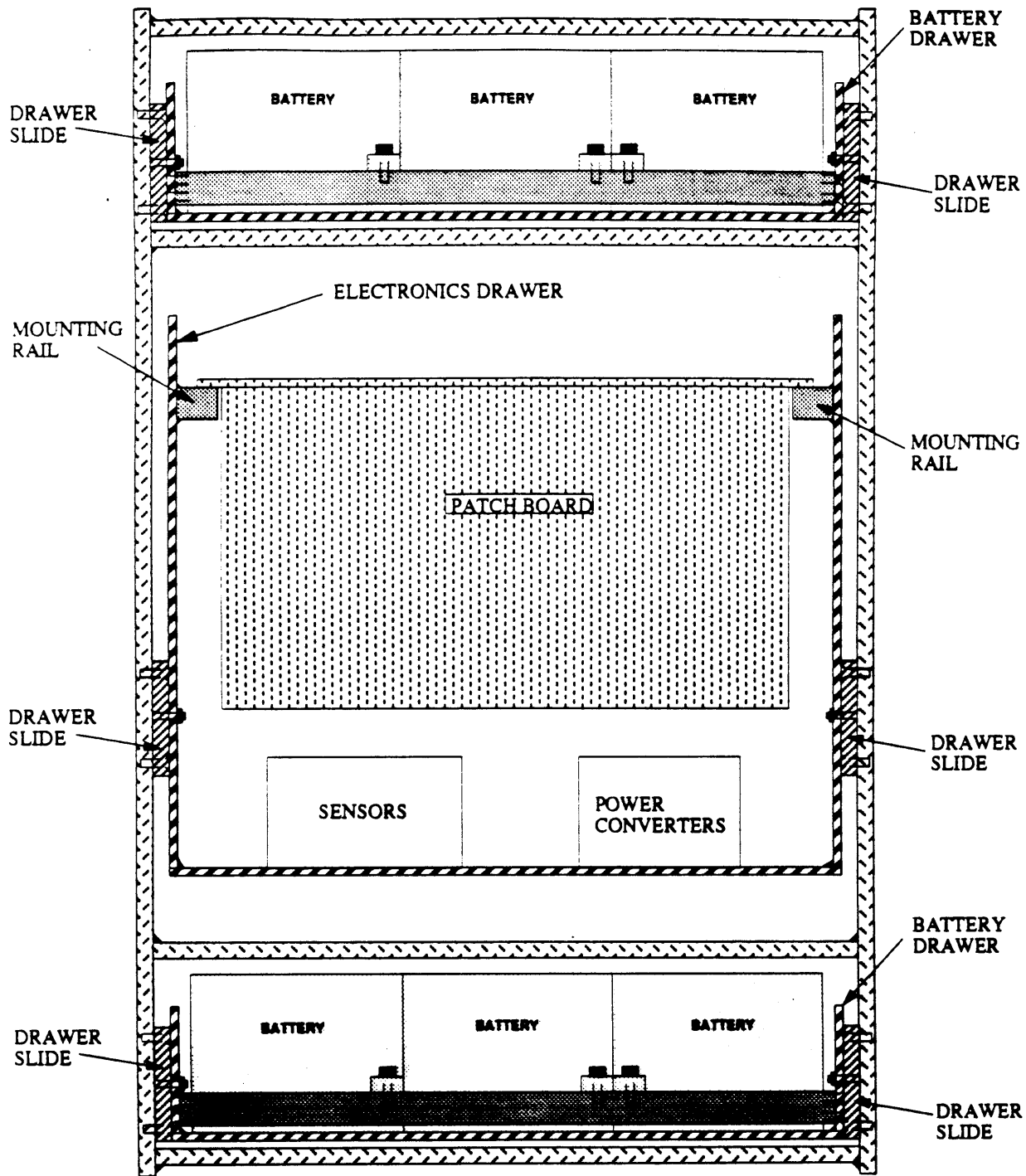


Figure 3.27 Rear Section View of Pressure Vessel Compartments

The dimensions of the pressure vessel were calculated as follows. In the vertical direction, the battery compartments were sized at 6.125 in. high in order to accommodate the height of the batteries mounted in their drawers. The computer/electronics compartment was sized at 18 in. high to contain the STD-bus mounted over the sensor subsystem in the computer/electronics drawer. The three compartment openings in the back plate were separated by 3 in. to allow space for the compartment doors' O-rings and rows of bolt holes. Thus, the pressure vessel was designed to be 37.25 in. from the bottom plate to the top plate. The back and front plates were extended past the edges of the internal volume in both the vertical and horizontal directions to form flanges. These flanges were used to mount the rest of STAR's structure. In the horizontal direction, the compartment width was designed to be 21.95 in to accommodate the 19 in. rack-mounted STD-bus, plus the width of the drawer and the width of the drawer slides mounted on either side of the drawer. The sides of the pressure vessel were designed to extend 0.375 in. past the top and bottom plates, shown in the lower right hand corner of Figure 3.26. This extension provided a lip to facilitate welding.

Thus, having determined the vertical and horizontal dimensions of the pressure vessel from interior space needs, the remaining depth dimension was calculated to make STAR neutrally-buoyant. Since the pressure vessel was to be used to mount all of STAR's external subsystems, the depth of the pressure vessel determined the dimensions of the external mounting structures. To perform this calculation, the masses and volumes of all of STAR's external components were calculated as a function of the depth of the pressure vessel. These formulas were placed into a computer spreadsheet, along with the masses of the internal components of the pressure vessel. Table 3.1 shows a two-page printout of this spreadsheet program. The creation of this spreadsheet permitted the depth of the pressure vessel, shown at the lower left of the second page of the table, to be varied such that the desired buoyancy was attained. A depth of 26 in. was chosen, which resulted in a net vehicle buoyancy of positive 36.02 lb. Since, during testing, it is much easier to increase the weight of the vehicle with lead weights than to make it more buoyant with foam, it was decided to design for a slight positive buoyancy.

Item	Quantity	X - Dim. (in)	Y - Dim. (in)	Z - Dim. (in)	Volume (in ³)	Density (lbs./in ³)	Weight (lbs.)
Sides	2	26	0.5	38	988.00	0.1	98.80
Horiz. Pieces	4	26	21.95	0.5	1141.40	0.1	114.14
Front	1	0.625	29.25	44.5	813.52	0.1	81.35
Back-Temp Hor end	2	0.625	21.95	4.125	113.18	0.1	11.32
Back-Temp Hor mid	2	0.625	21.95	3	82.31	0.1	8.23
Back-Templ. Vert.	2	0.625	3.65	44.5	203.03	0.1	20.30
Battery Doors	2	0.625	25.75	8.875	285.66	0.1	28.57
Electronics Door	1	0.625	25.75	20.75	333.95	0.1	33.39
Big Manipulator Plate	1	0.625	27.25	20	340.63	0	0.00
Measured	2	weight each =	30				60.00
Measured	1	weight each =	71.75				71.75
Measured	6	weight each =	7.5				45.00
Measured	16	weight each =	15				240.00
Measured	2	weight each =	25.5		510.00	0.1	51.00
Measured	1	weight each =	23		230.00	0.1	23.00
Measured	1	weight each =	4		40.00	0.1	4.00
Measured	6	weight each =	0.8125		48.75	0.1	4.88
Angle	4	length =	16		44.00	0.1	4.40
Channel	4	length =	25		28.13	0.1	2.81

Table 3.1 Buoyancy Calculation Spreadsheet - Page 1 of 2

Item	Quantity	X - Dim.	Y - Dim.	Z - Dim.	Volume	Density	Weight
				TOTAL	WEIGHT	----->	902.94
					Volume		
Box	1	26	22.95	37.25	22227.08	0.0361	802.40
tops of side plates	4	26	0.5	0.375	19.50	0.0361	0.70
Battery Doors	2	0.625	25.75	8.875	285.66	0.0361	10.31
Electronics Door	1	0.625	25.75	20.75	333.95	0.0361	12.06
End Flanges	2	0.625	29.25	44.5	1627.03	0.0361	58.74
Big Manipulator Plate	1	0.625	27.25	20	340.63	0	0.00
	2				510.00	0.0361	18.41
	1				230.00	0.0361	8.30
	1				40.00	0.0361	1.44
Angle	4				44.00	0.0361	1.59
Channel	4				28.13	0.0361	1.02
				TOTAL	WATER	WEIGHT=	914.97
	8	Positive by	3 lbs. each				24.00
Pressure Vessel Depth	=====	26	inches		TOTAL	BUOYANCY	36.02

Table 3.1 Buoyancy Calculation Spreadsheet - Page 2 of 2

All machining of the Aluminum 6061-T6 plates of the pressure vessel was performed prior to their being welded together with waterproof beads. The welded pressure vessel assembly was then black-anodized to protect the metal from corrosion. During anodizing, all threaded holes in the plates were plugged with rubber to prevent the threads from being coated.

3.8.2 Computer/Electronics Drawer

In addition to housing the computer/electronics subsystem, the middle compartment of the pressure vessel also contained the sensor subsystem and the power converters from the power subsystem. For the sake of brevity, however, the middle compartment will hereafter be referred to as the electronics compartment. Figure 3.28 is an engineering drawing of the electronics drawer. The computer rack, the STD-bus, and the patch board are all bolted to mounting rails on both sides of the electronics drawer. Figure 3.25 includes a back view of the layout of the components in the electronics drawer. Figure 3.29 presents a top view of the components of the electronics drawer. Again, although space for three computers is shown, only one onboard computer had been installed at the time of this writing.

A drawing of the electronics compartment door is included in Appendix A. This door was bolted to the electronics drawer. This enabled the entire drawer/door combination to slide out of the compartment without disconnecting any cables. The subsystems in the electronics drawer were interfaced to the other subsystems via bulkhead connectors placed in the electronics and battery doors. The bulkhead connectors were bolted into the compartment doors, using O-rings inserted into machined shelves to form a seal around the connector. Appendix A includes details of the connector holes and the O-ring shelves. Appendix A also contains the layout of connector holes in the electronics drawer. Due to the high cost of commercial bulkhead connectors for coaxial cable, a coaxial pass-through was designed to accommodate the QNX umbilical cable. This pass-through, shown in Appendix A, consists of an Aluminum disk with a circular O-ring gland and a pipe-threaded hole in its center. This disk was bolted over a through hole in the electronics door, allowing the coaxial cable, potted into a pipe-fitting, to be turned into the pipe threads. To

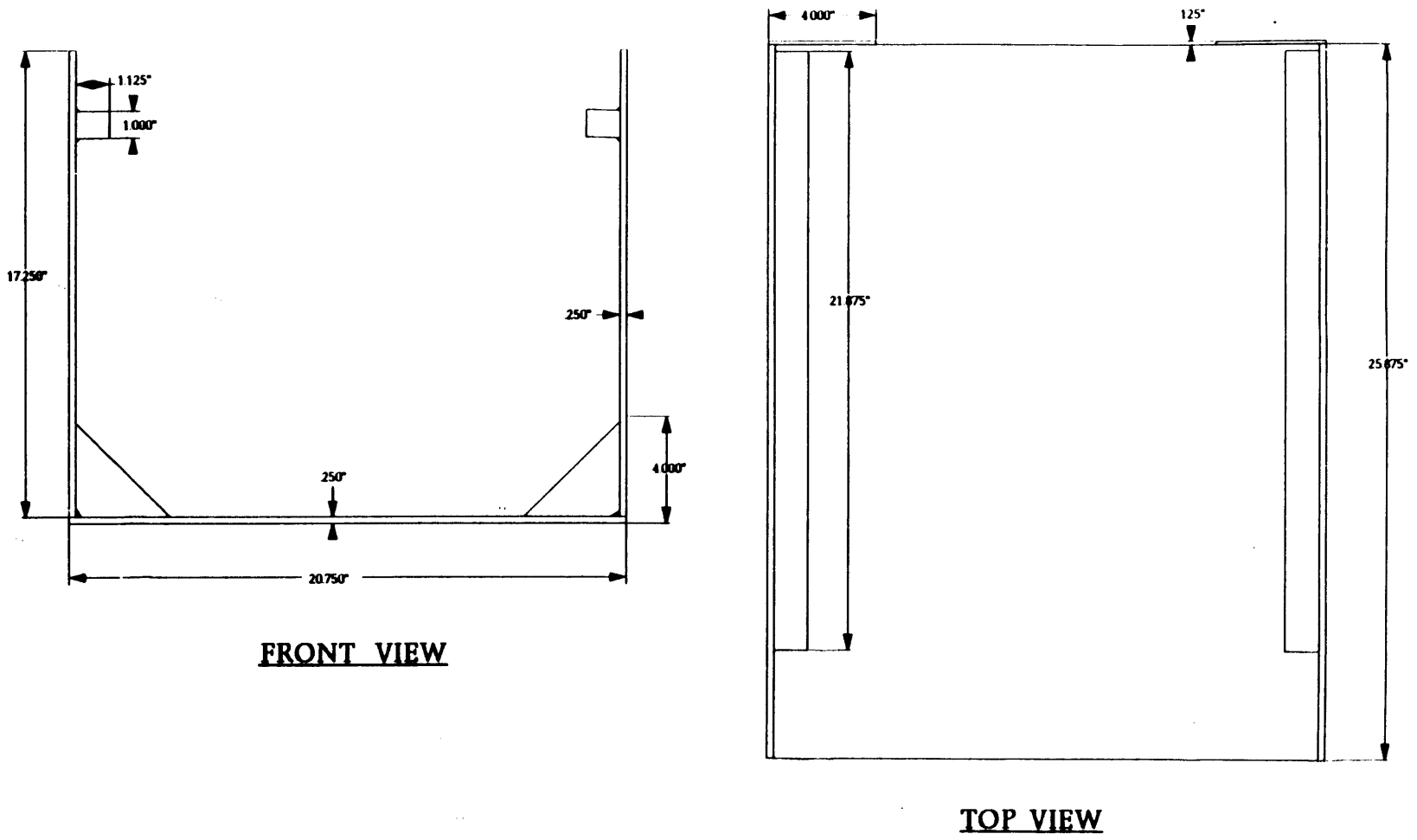


Figure 3.28 Electronics Drawer

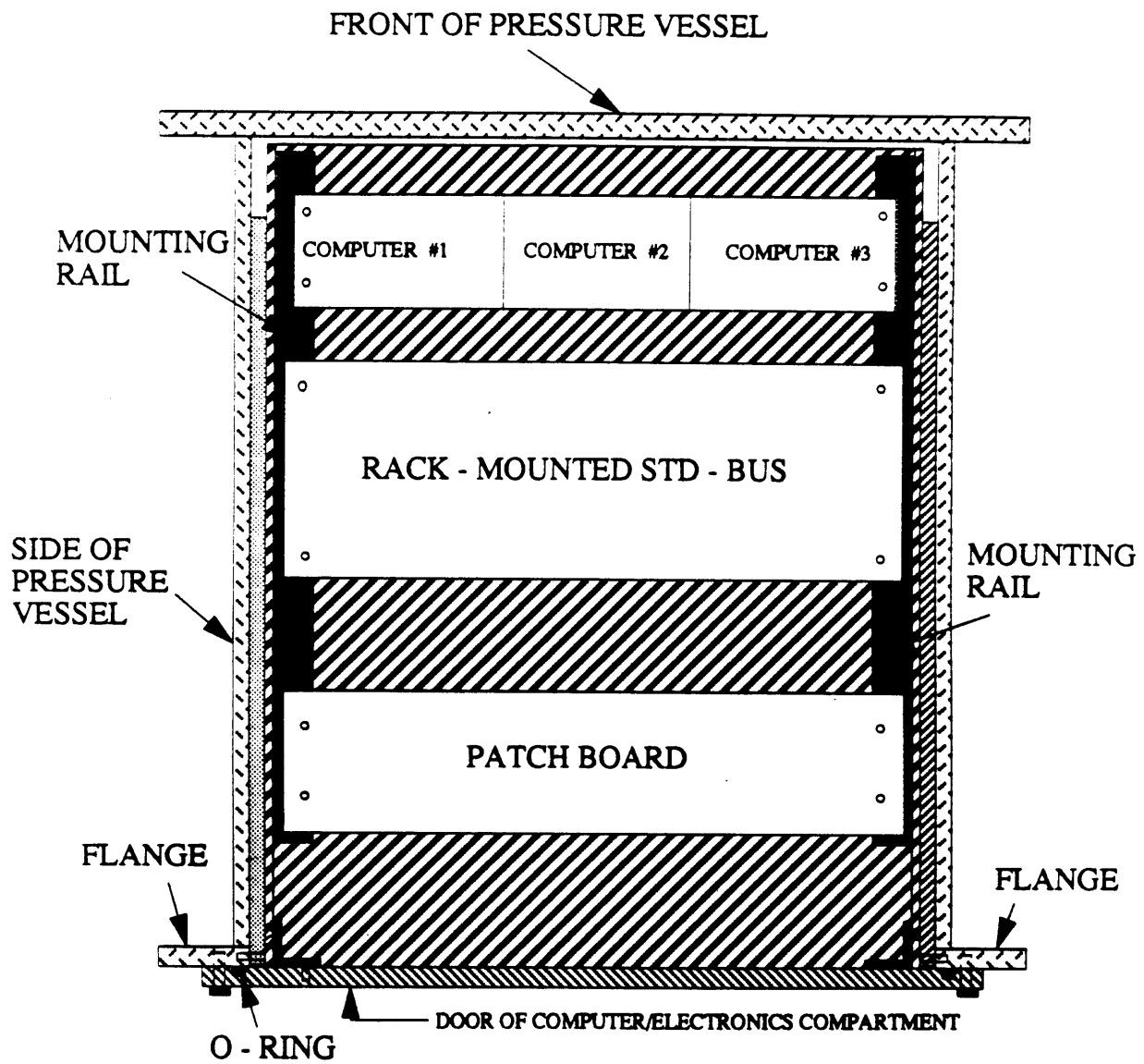


Figure 3.29 Top View of Electronics Drawer Layout

permit the electronics compartment to be flushed with Nitrogen prior to pool testing, a valved pressure tap was installed into the door of the electronics compartment. This safety precaution was necessary to reduce the risk of explosion, in the event of Hydrogen leaks from the battery drawers into the electronics drawer, by reducing the amount of Oxygen inside the compartment. Figure 3.30 shows the interior of the electronics drawer. The bulkhead connectors and the pressure tap are shown at the right side of the figure. Figure 3.31 shows a side view of the vehicle with the electronics drawer pulled out to the full extension of the drawer slides. The drawer slide is visible on the side of the electronics drawer. Note that the connectors attached to the door of the compartment were not required to be removed prior to opening the electronics drawer.

3.8.2 Battery Drawers

The two battery drawers house the components of the power subsystem, consisting of 12 batteries, 5 power relays, and 23 fuses. The layout of the components of the battery drawers is shown in Figure 3.32. Each battery is rigidly bolted on two of its corners to bars which span the drawer. The relays were mounted along with the fuses in the front of the drawer. The relays were wired and then sealed with potting compound before being mounted. The relays were sealed as a safety precaution to prevent possible ignition of Hydrogen gas in the event of discharge by the batteries.

Each battery drawer contains 6 batteries. The top battery drawer, which supports the high-current part of the power subsystem, contains 4 power relays and 17 fuses (6 battery fuses, 8 thruster motor fuses, and 3 balancer motor fuses). The bottom battery drawer, which mainly supports the low-current part of the power subsystem, contains 1 power relay and 6 fuses (6 battery fuses). Figure 3.33 shows an upper side view of an opened battery drawer. The bulkhead connectors and the valved pressure tap is shown at the right side of the figure. The need for a pressure tap in each compartment's door was discussed in Subsection 3.8.1. Figure 3.34 shows a side view of the back of STAR with the top battery drawer fully opened. Note that the connectors attached to the door of the compartment were not required to be removed prior to opening the battery drawer. A drawing of the door of the battery compartment door is included in Appendix A. A

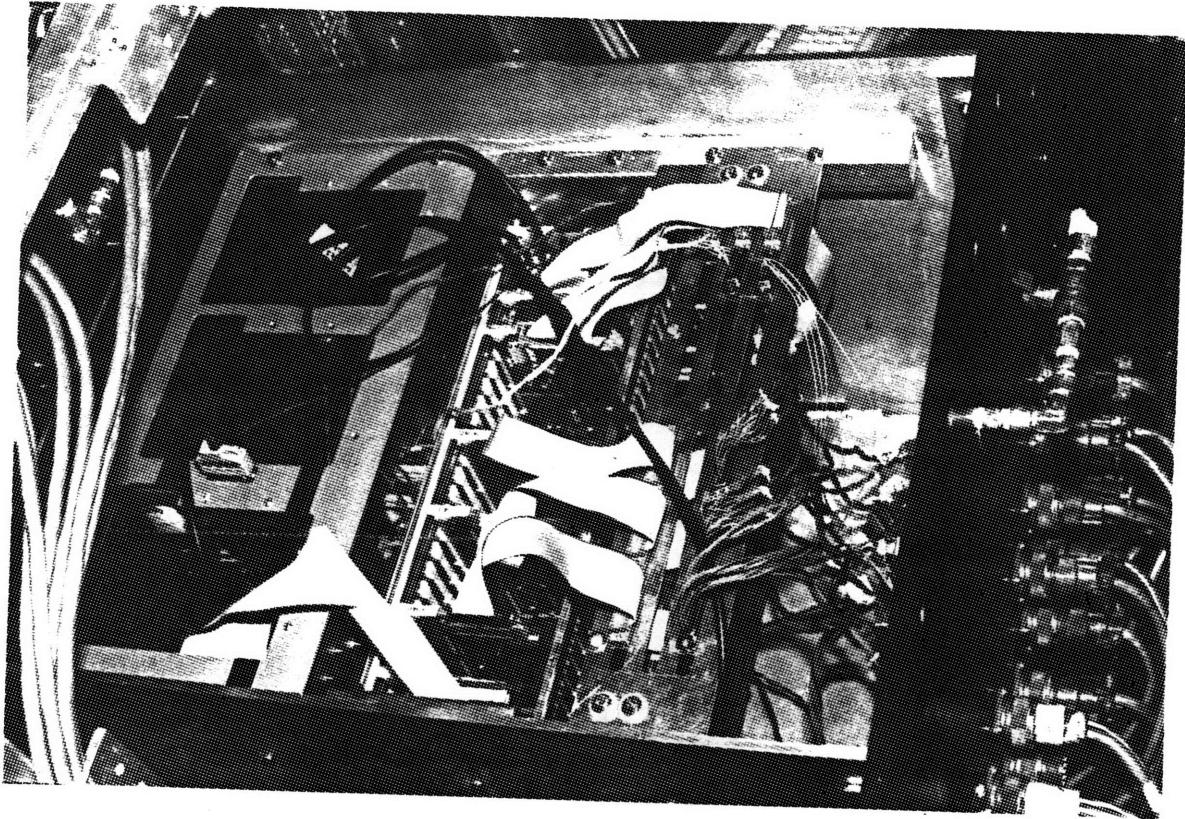


Figure 3.30 Photograph of Interior of Electronics Drawer

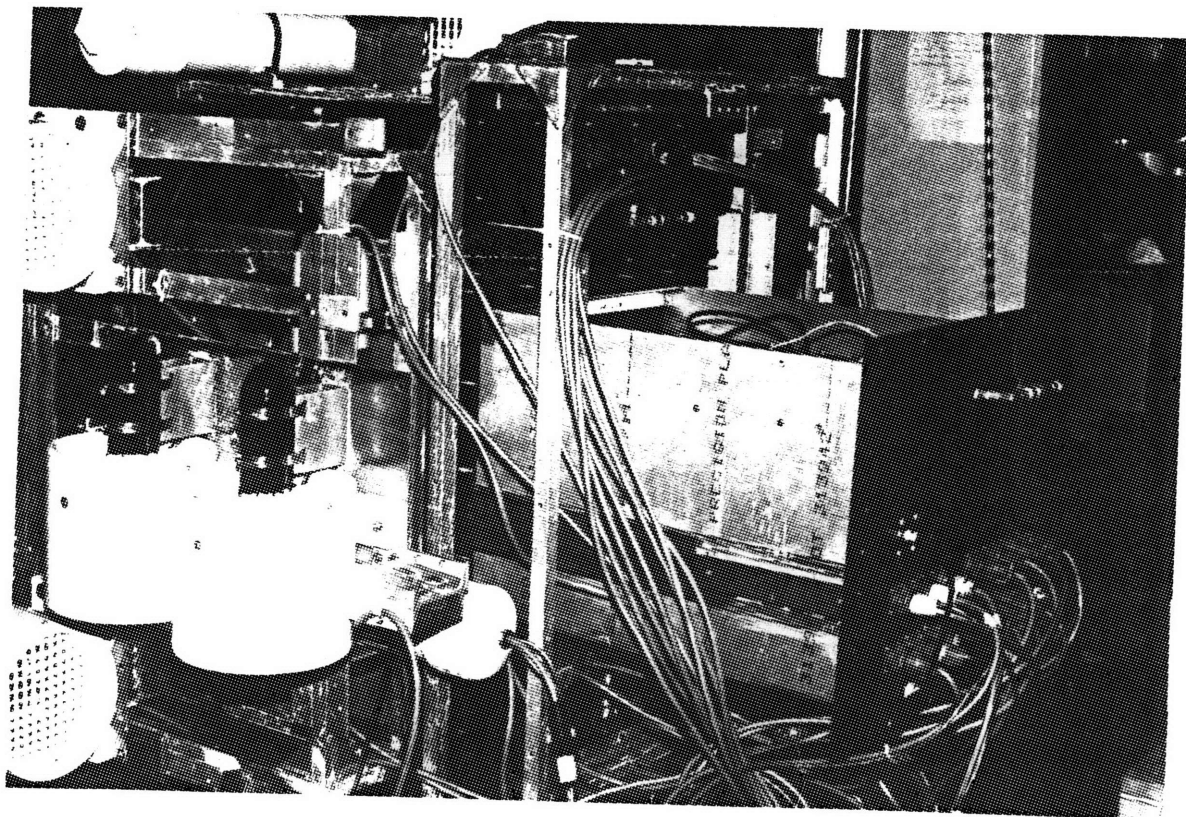
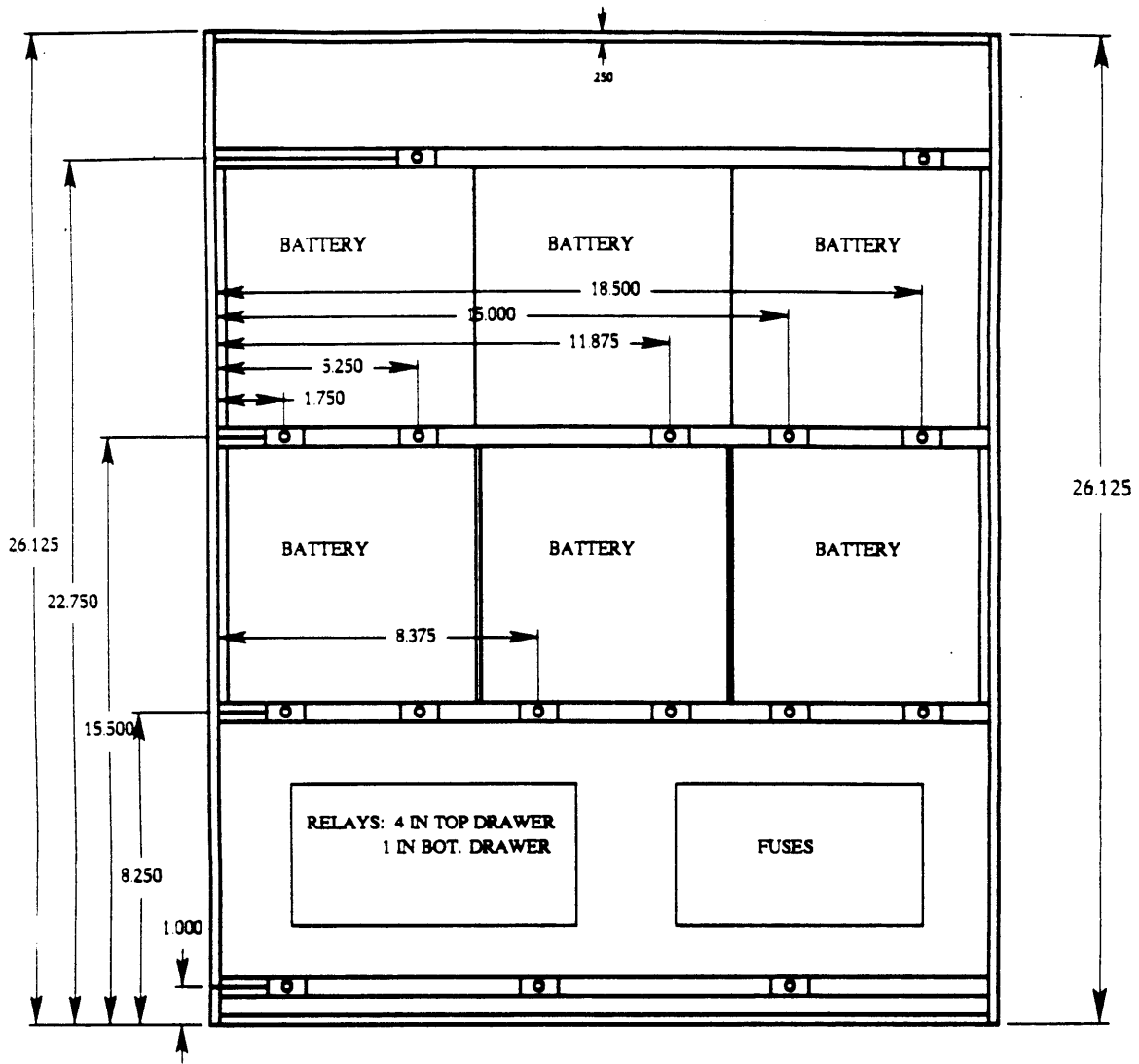
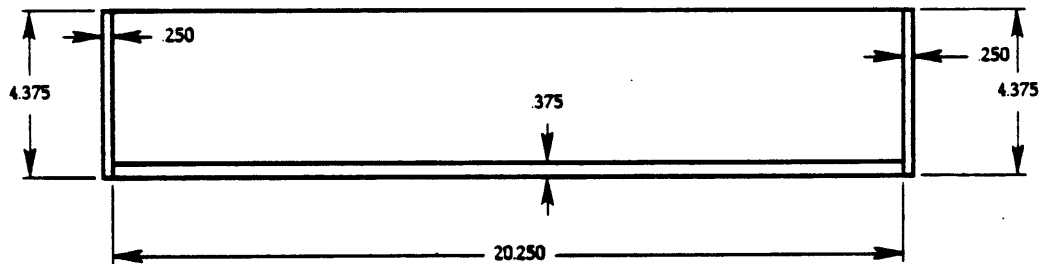


Figure 3.31 Photograph of STAR With Opened Electronics Drawer



TOP VIEW



FRONT VIEW

Figure 3.32 Battery Drawer Layout

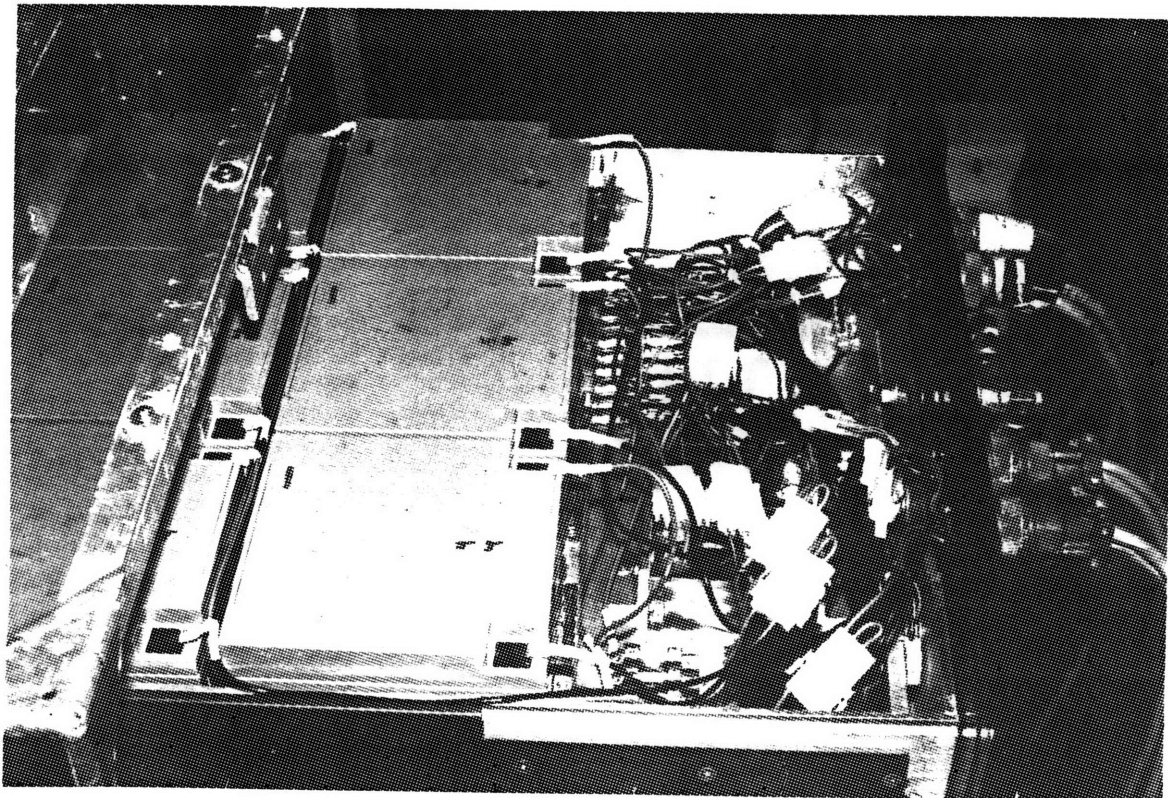


Figure 3.33 Photograph of Opened Battery Drawer

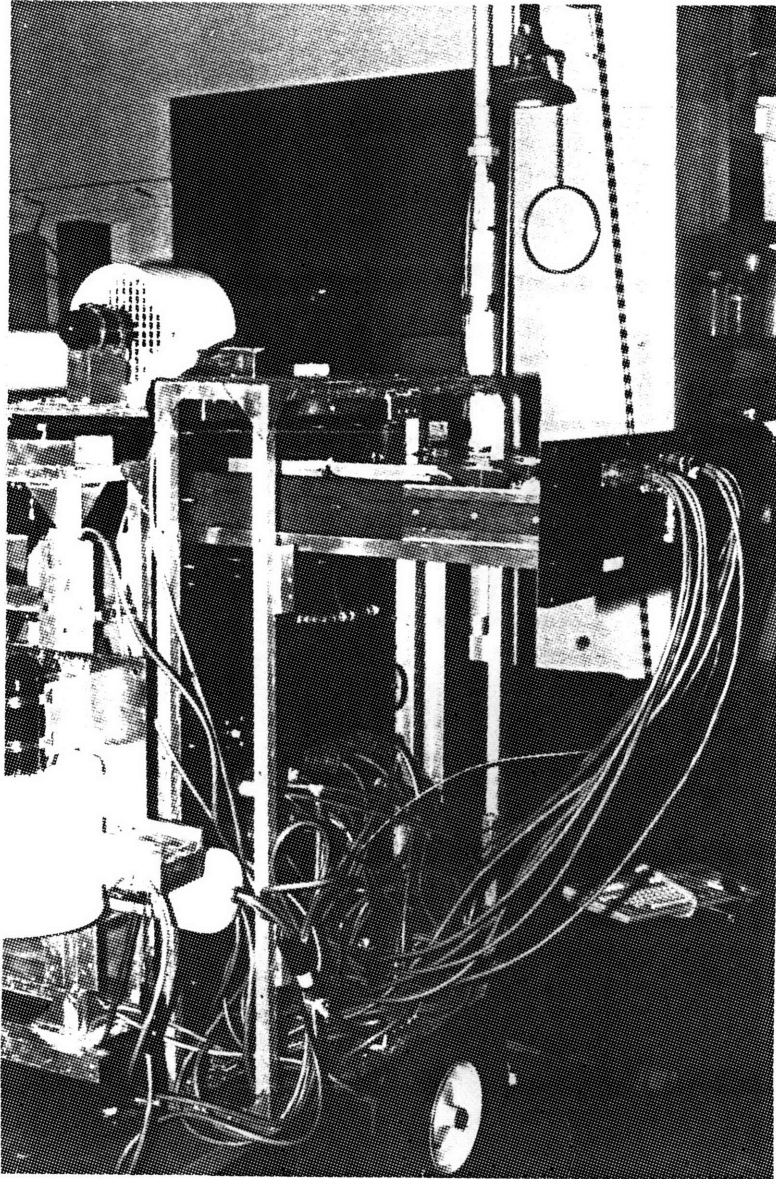


Figure 3.34 Photograph of STAR with Opened Battery Drawer

drawing of the door's connector hole layout is also included in Appendix A.

3.8.3 Rear Structure

During pool testing, there is a high risk that the vehicle will undergo impact with the pool walls or pool floor. The bulkhead connectors, cables, and pressure taps located on the compartment doors are too delicate to withstand such an impact. For this reason, a welded box-tube structure was designed to protect the rear of the vehicle. Box-tube aluminum was the main structural member, chosen for its light weight, high strength, and good weldability. Aluminum gusset plates were added in the corners to provide good welding surfaces. The structure, which mounted to the pressure vessel rear flange, was designed to enclose the compartment doors, preventing contact with the pool, while still permitting the doors to be opened for access the drawers. The design of the rear box-tube structure is presented in Figure 3.35. The structure is clearly shown mounted to the vehicle in Figure 3.34.

3.8.4 Side Mounting Structures

To mount the propulsion subsystem, the pressure subsystem, and the X- and Y-axis balancer tubes to the pressure vessel, side mounting structures were designed. Similar to the rear mounting structure, presented in Subsection 3.8.3, these structures were constructed of welded Aluminum box-tube, U-channel, and L-angle pieces. The design of the side mounting structures is presented in Figures 3.36, 3.37, 3.38. Each of the side structures was designed to mount along the side of the pressure vessel, between the front and rear flanges. The two pieces of L-angle, shown in a bottom view in Figure 3.38, were designed to fit precisely into the 26 in. span between the flanges, bolting to each flange through the bolt holes shown in a side view in Figure 3.37. The side structures were designed to have an internal width of 5 in. (see Figure 3.37) in order to permit mounting of the 3.5 in. diameter pressure bottle and the 4.5 in. diameter balancer tubes.

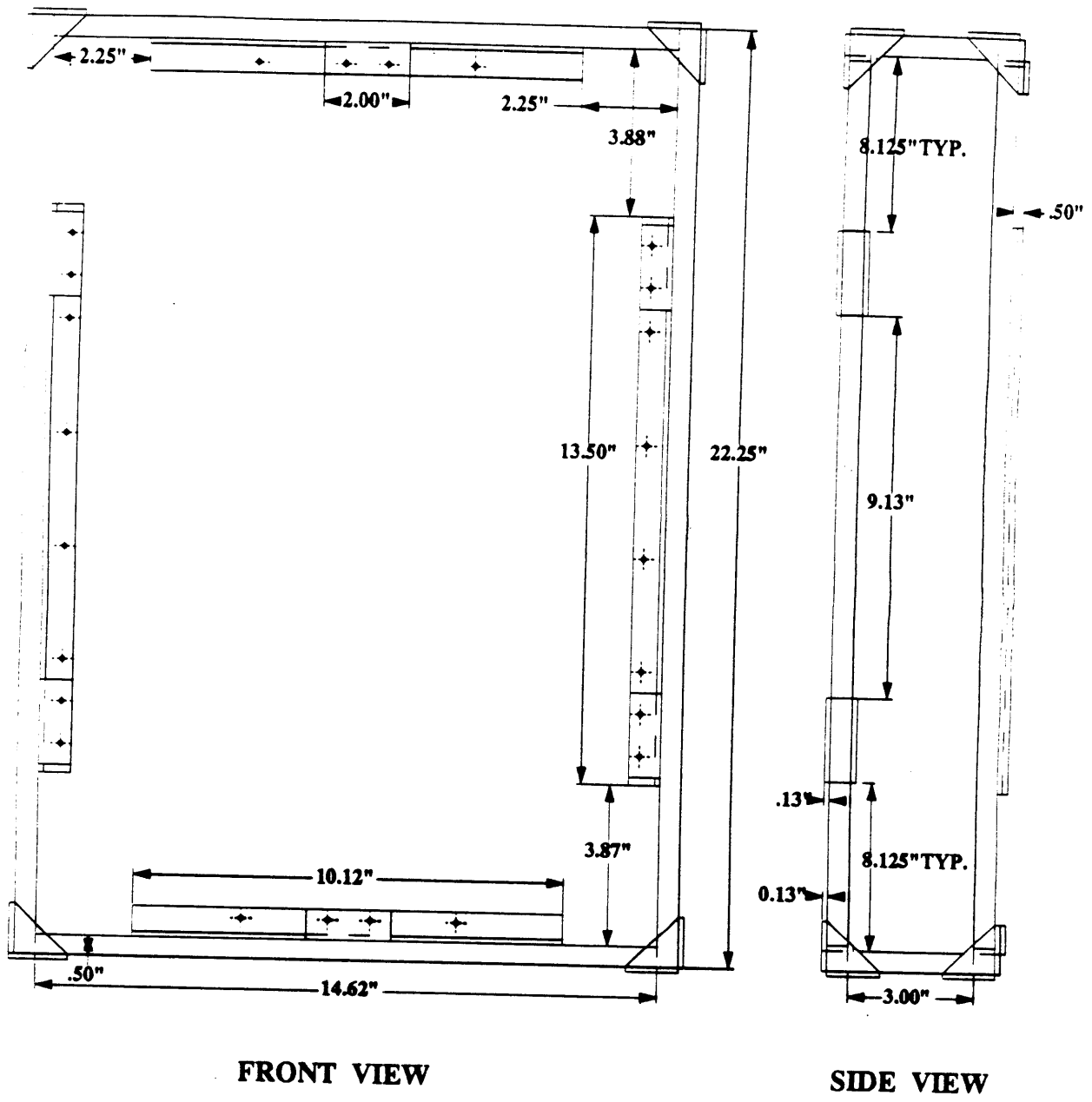


Figure 3.35 Rear Box Tube Structure

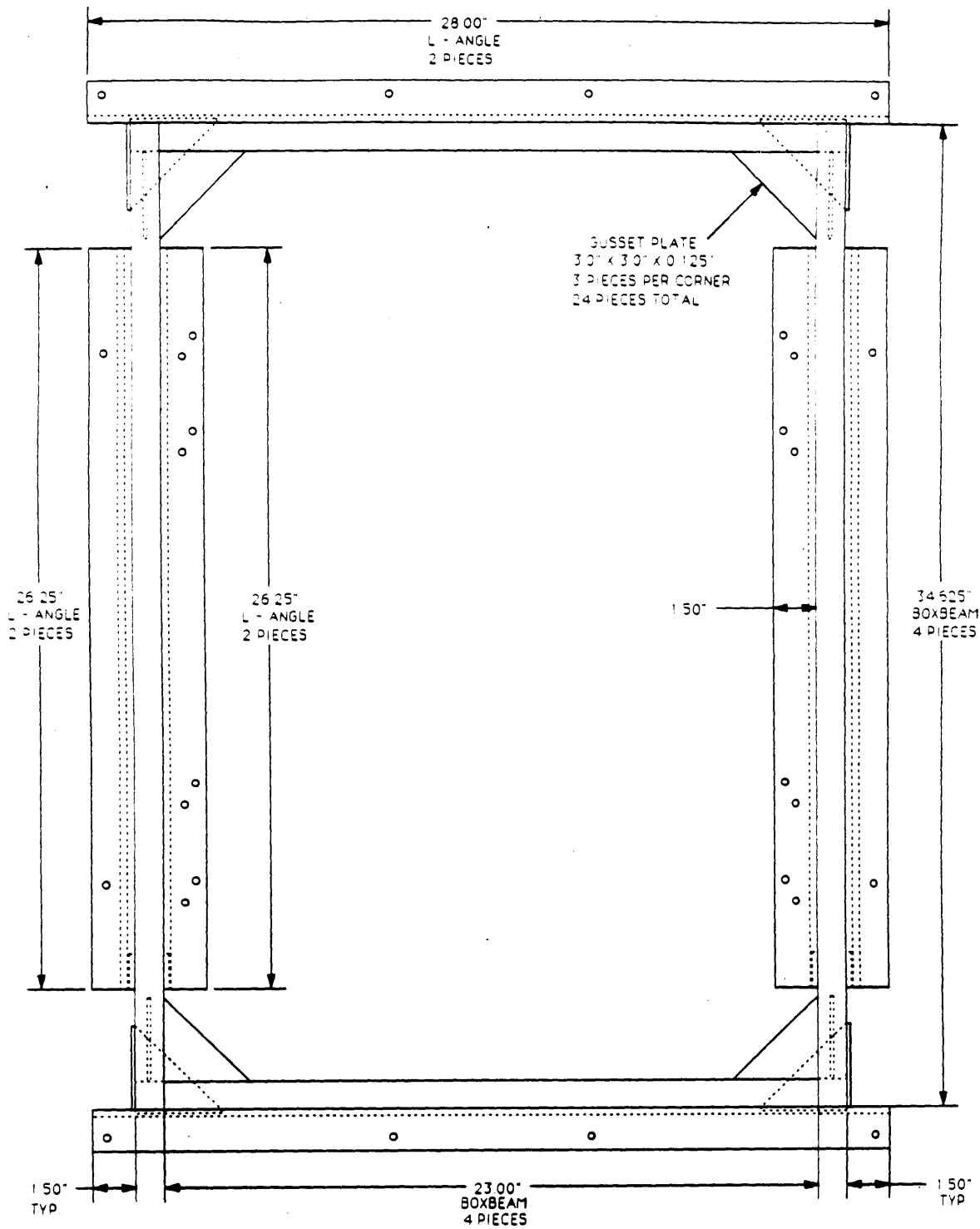


Figure 3.36 Front View of Side Mounting Structure

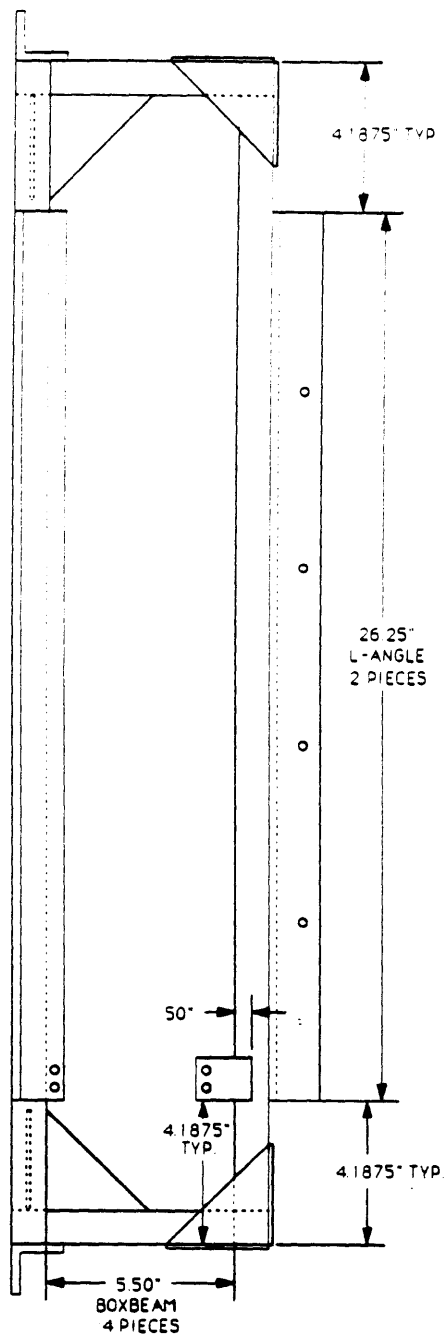


Figure 3.37 Side View of Side Mounting Structure

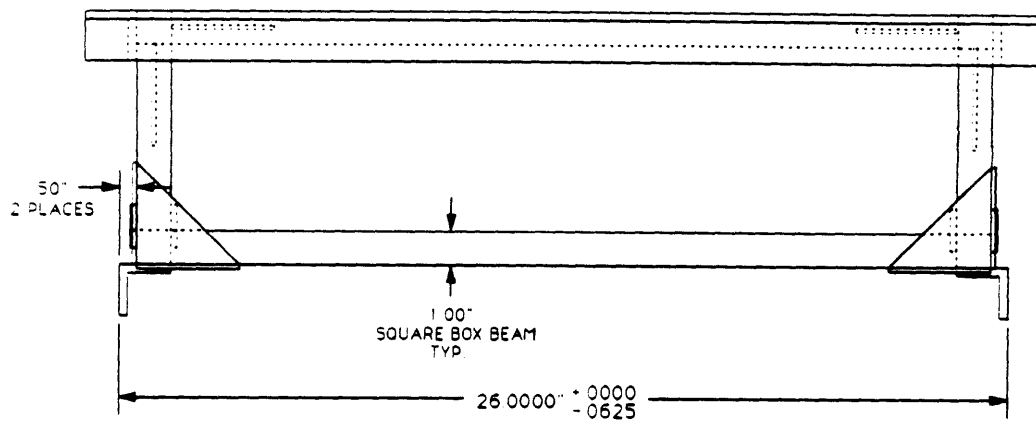


Figure 3.38 Bottom View of Side Mounting Structure

The four X-axis thrusters, the two Z-axis thrusters, the air bottle, and the X-axis and Y-axis balancers were mounted to the side structures as shown in Figures 3.39 and 3.40. Figure 3.39 shows a side view of the completed vehicle, and Figure 3.40 shows a rear view of the completed vehicle.

3.8.5 Top/Bottom Mounting Structures

The top mounting structure was designed to mount the top Y-thruster and the Y-balancer. Figure 3.41 shows a top view of the structure, which is composed of the following: two L-angle pieces mounted to the front and rear pressure vessel flanges; two U-channel lengths which, spanning the distance between the L-angle pieces, support the Y-thruster; and two additional U-channel lengths which support the Y-balancer.

Figure 3.42 shows the bottom mounting structure. This structure has only two lengths of U-channel which are needed to support the bottom Y-thruster. Since STAR must be mounted upon a cart, the bottom Y-thruster is removed during transportation between lab and pool. For its protection, the bottom Y-thruster is bolted to the right side structure, next to the Z-thruster, when the vehicle is being moved. This arrangement is shown in Figure 3.43.

3.9 Control Station

The control station used for teleoperated control of STAR was designed and built by Anna Cinniger while a graduate student in the LSTAR [8]. As a result, only the pertinent features of the control station will be briefly mentioned here.

The components of the control station include a computer, operator input devices, and visual feedback devices. The control station computer is a Gateway PC-type machine. The input devices available for use with a human operator consist of the following: two three-DOF joysticks; one two-DOF foot controller; and one head-tracking linkage. The visual feedback interfaces available to the operator include a 25 in. color cathode-ray-tube (CRT) monitor and a stereoscopic head-mounted display system incorporating two color liquid-crystal-displays (LCDs). The input devices

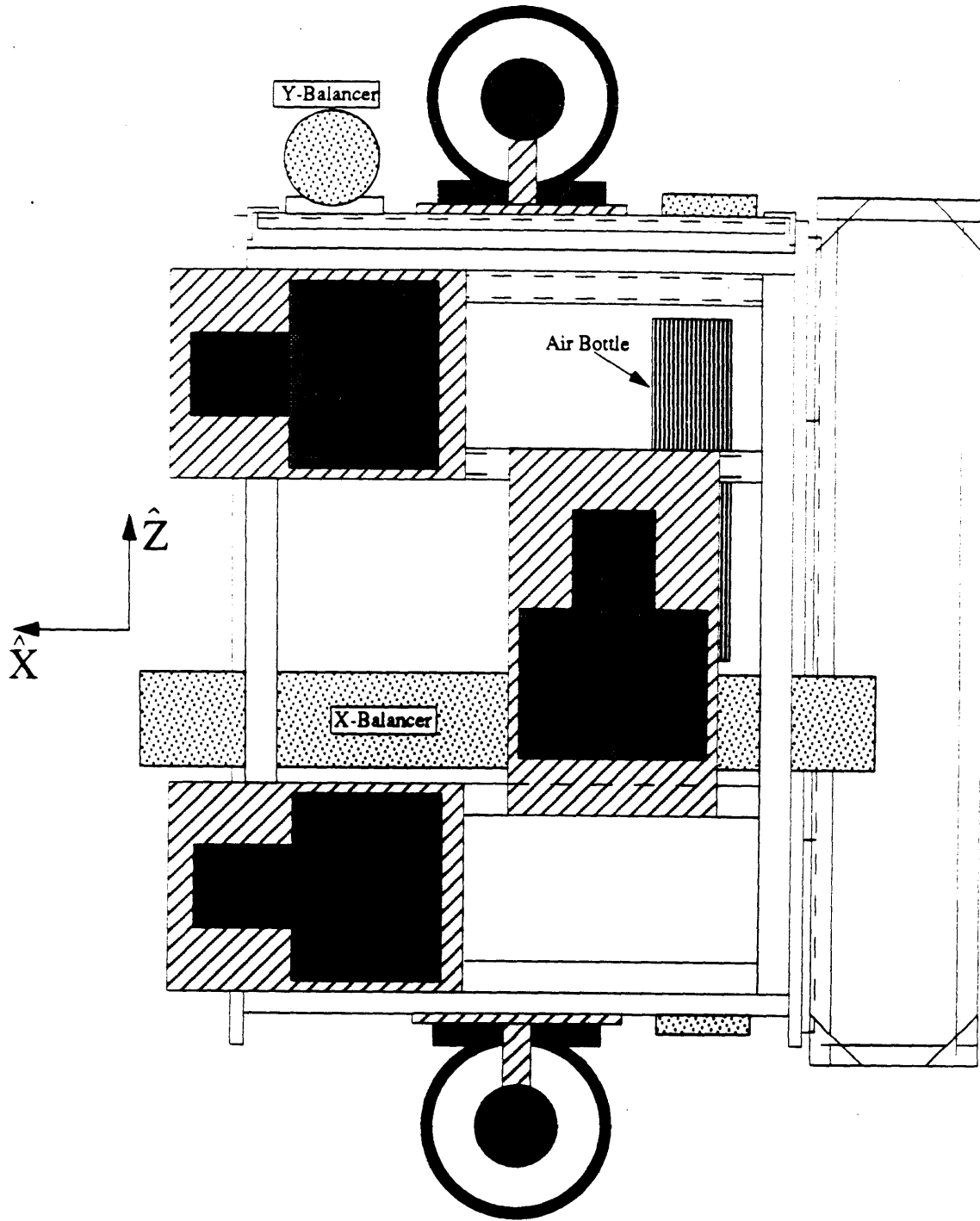


Figure 3.39 Side View of STAR Thruster and Balancer Layout

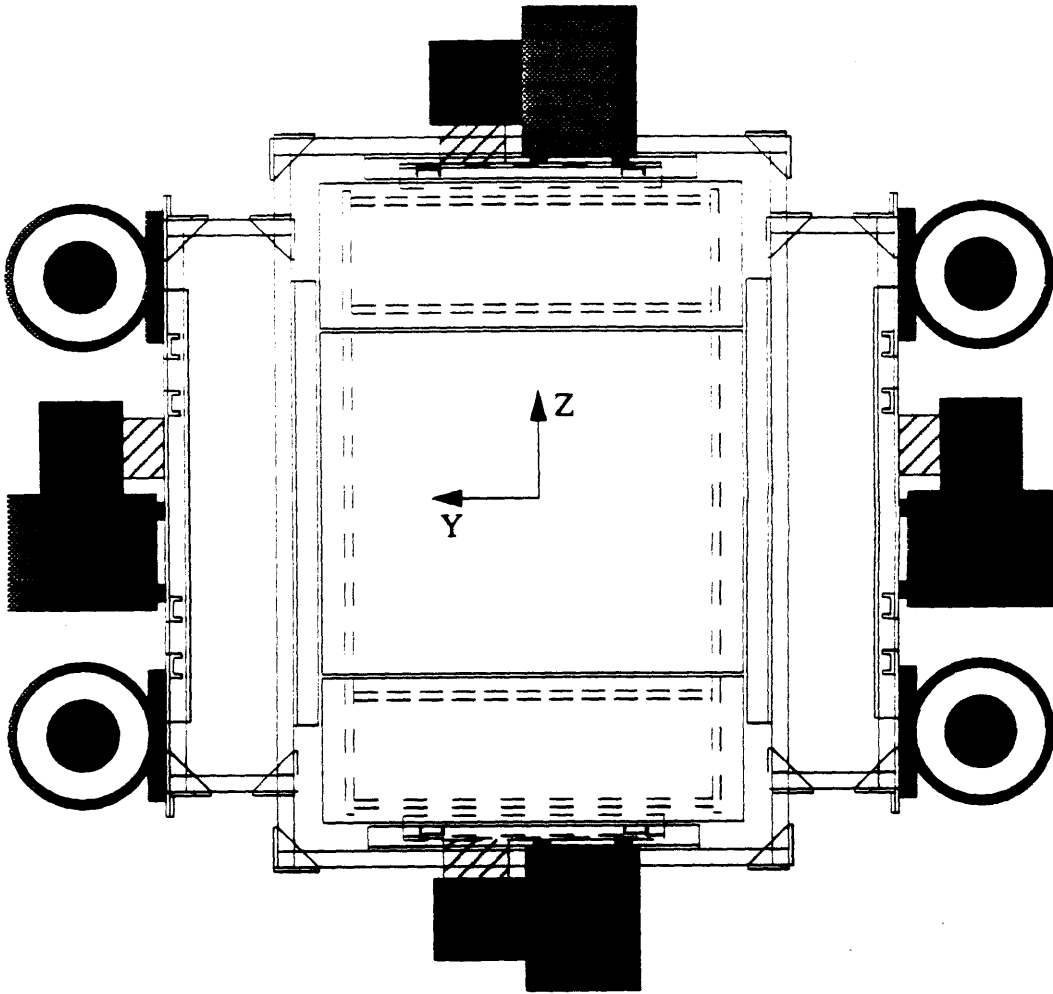


Figure 3.40 Rear View of STAR Thruster and Balancer Layout

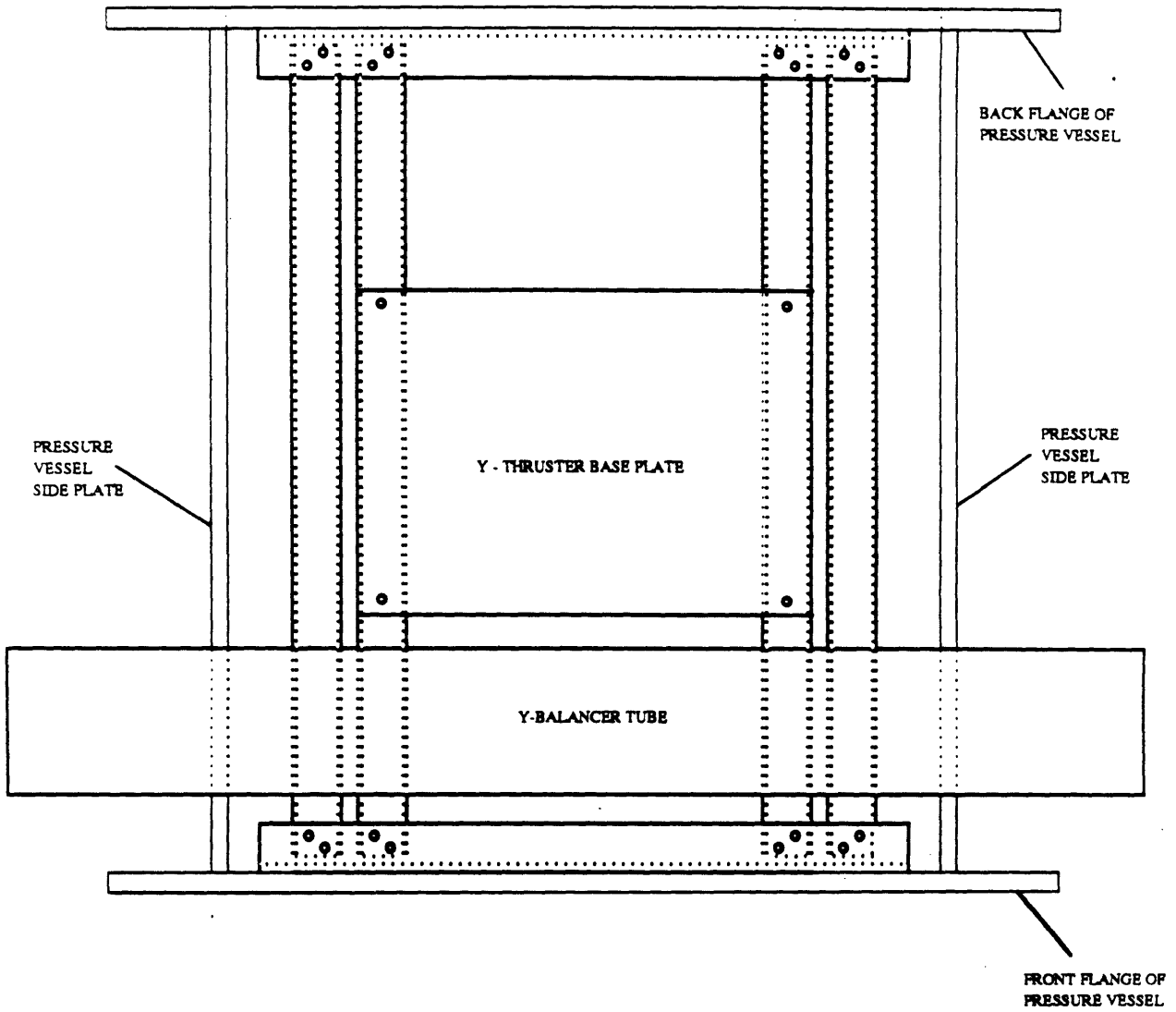


Figure 3.41 Top View of Top Mounting Structure

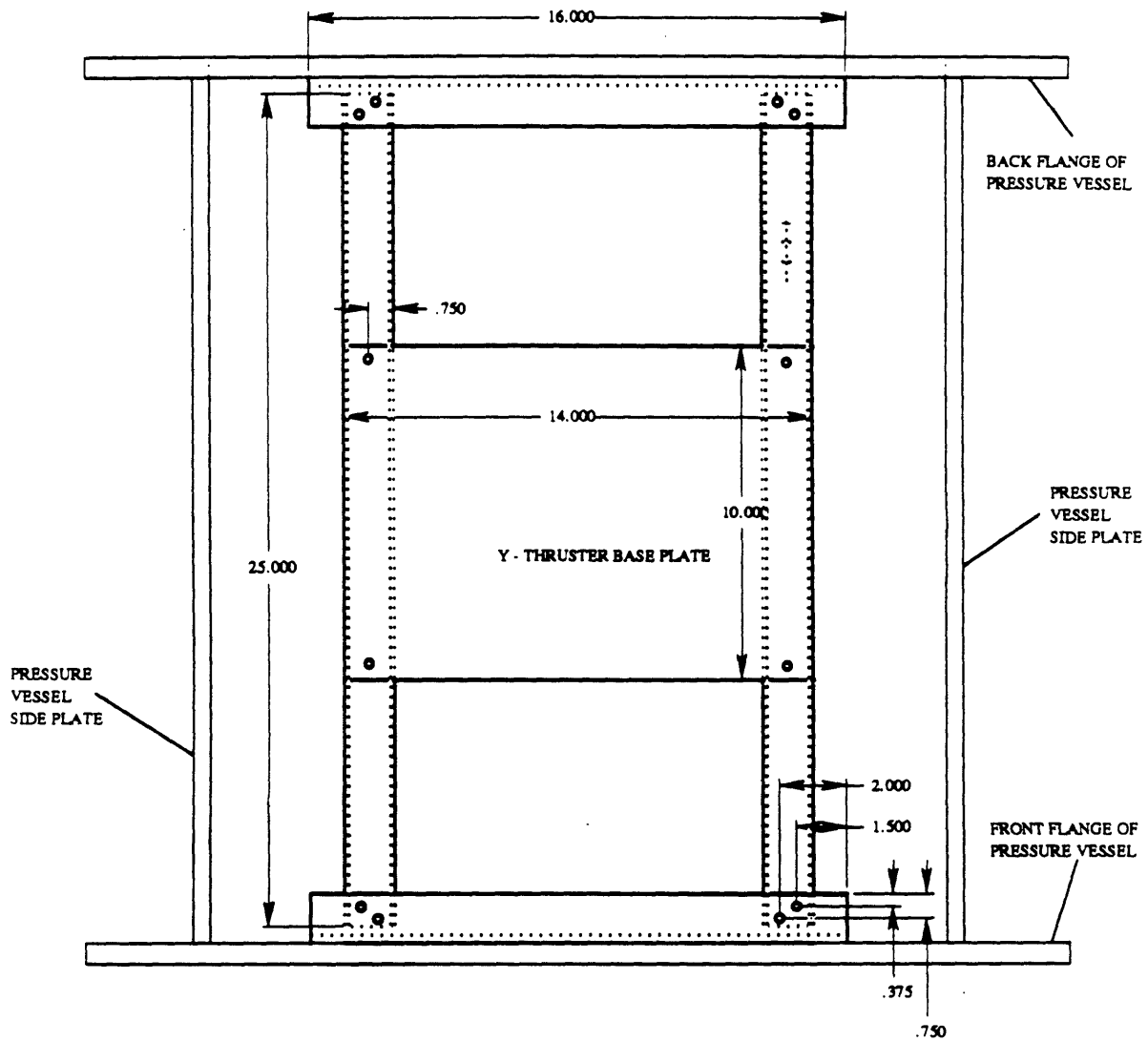


Figure 3.42 Bottom Mounting Structure

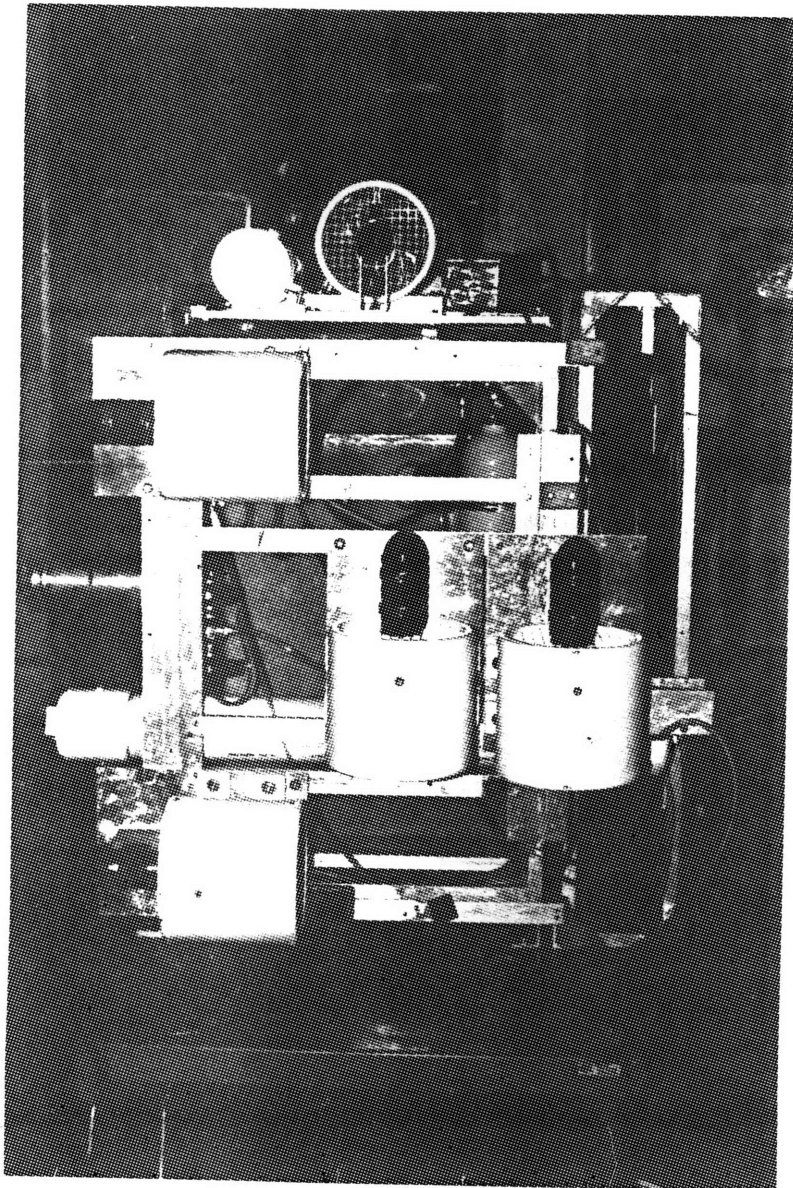


Figure 3.43 Photograph of Left Side of STAR

were interfaced to the control station computer via an A/D conversion circuit card placed on the internal PC-bus of the computer. The control station computer was linked, using the QNX operating system, to the onboard computer via a 93Ω coaxial umbilical cable.

Thus, in the teleoperated mode of vehicle control, the remote human operator utilizes visual feedback to formulate a command response. This human response is then input to the control station computer via one or more input devices. Software running on the control station computer then performs the task of reading the human commands from the input devices. This software also sends the commands to the onboard computer. Onboard software in turn converts the human commands into actuation signals sent to the appropriate motor controller circuits located on the STD-bus. These circuits then output the PWM signals to the thrusters.

In the autonomous control mode, the control station will likely be used start, stop, and modify onboard software during autonomous control system development. The QNX network also allows the control station computer to be used as a passive, data-gathering device during periods of autonomous control by the onboard computer.

Before each pool experimentation session, the control station is used to control the balancer subsystem. The human operator uses visual feedback from onboard cameras, or follows the directions of divers, to rotationally balance the vehicle by commanding balancer actuation.

STAR's design incorporates the use of several control systems. The balancer subsystem design includes linear position control of the three balancer weights. To provide consistent, accurate actuation, the propulsion subsystem was designed to include control of thruster motor angular velocity. For autonomous operation, a vehicle position and orientation control system based on vision-based navigation will be developed. At the time of this writing, however, only two control systems had been implemented on STAR: the balancer weight position control system, and a vehicle attitude control system. While it was hoped to achieve automatic balancing, two of the three accelerometers that were to be used for the calculation of the gravity vector failed, prohibiting the development of this system. The attitude control system was developed to demonstrate the computing, sensing, and actuation capabilities of STAR that are necessary for future implementation of an autonomous vehicle control system.

4.1 Balancer Control System

4.1.1 Hardware

The design of the three balancer assemblies is presented in Section 3.3. The balancer control system consists of a computer software implementation of the control algorithm, an optical encoder for angular position feedback, a motor controller circuit to perform control calculations and to produce a PWM command signal, and an electric motor for actuation of the balancer weights.

A Hewlett-Packard HEDS-7500 optical encoder is used to measure angular position of the balancer lead screw. This device, with a resolution of 256 counts-per-revolution (CPR), returns a quadrature-encoded signal directly to the motor controller chip described below. The HEDS-7500's power requirements are +5VDC and ground.

The National Semiconductor LM629 Precision Motor Controller chip is used to perform the intensive, real-time computational tasks required for closed loop position control of the balancer weights. The onboard computer communicates with the LM629 through an input/output (I/O) port to facilitate programming of a trapezoidal velocity profile and a digital compensation filter. The A and B encoder signals are interfaced directly to two pins of the LM629 to provide feedback for closing the position servo loop. The chip includes a trapezoidal velocity profile generator which calculates the required trajectory. In operation, the LM629 subtracts the actual position (from the encoder) from the desired position (from the calculated trajectory) to produce the servo error. This error is then processed by the digital filter to drive the motor to the desired position.

The LM629 outputs 8-bit sign and magnitude PWM signals. Thus, the minimum duty cycle possible is 1/128; 50% drive is 64/128; maximum positive drive is 127/128; and maximum negative drive is 128/128. As described in Section 3.1, the sign and magnitude signals are logically combined to produce separate PWM forward and reverse signals to the balancer motor drivers.

4.1.2 Implementation

The balancer control system algorithm is implemented in software using the C programming language. This computer code uses the LM629 to perform the real-time control law calculations. The LM629 uses a digital P-I-D filter to compensate the control loop. This means that the motor is held at the desired position by applying a restoring force to the motor that is proportional to the position error, plus the integral of the error, plus the derivative of the servo error. The following equation illustrates this control law:

$$U(n) = K_p * E(n) + K_i * \sum_{N=0}^n E(n) + K_d * [E(n') - E(n' - 1)]$$

where $U(n)$ is the motor control signal output at the discrete sample time n , $E(n)$ is the position error at sample time n , n' indicates sampling at the

derivative sampling rate, and K_p , K_i , and K_d are the discrete-time filter gains. The servo error, $E(n)$, is the difference between the desired position, obtained from the calculated trajectory, and the actual position, measured by the optical encoder. The sampling interval associated with the derivative sampling term is user-selectable from the control code; this capability enables the LM629 to control a wider range of inertial loads by providing a tailored approximation of the continuous derivative. There is also a user-selectable anti-reset windup which truncates the integral error term, eliminating the accumulation of huge amounts of error in the event of a stalled motor.

An overview of the control code will be presented here. A detailed listing of the program, entitled "BAL.C," is contained in Appendix C. The first ten functions of this program listing are utilities that are used to communicate with the LM629 by writing command bytes, reading and writing data bytes, and reading the status byte. The main of the program begins by querying the user to choose the balancer to be controlled. The filter parameters are then inputted along with the anti-reset windup. The chip is then initialized with this data. The program then enters into an options loop, which allows the user to select from seven options:

- 1) Change Filter Parameters
- 2) Read Current Real Position
- 3) Move Motor to New Position
- 4) Zero Encoder Position
- 5) Reset Motor and Quit Program
- 6) Read Switch status
- 7) Center Balancer Weight

The first five options are self-explanatory. Option six enables the user to check the status of the limit switches of the three balancers. The six limit switches are combined into a switch status byte (with two padded bits); this byte is hard-wired onto the same circuit card as the LM629's, allowing this status byte to be read in the same way as the status bytes of the three LM629's. This option is useful during balancing, as it alerts the user that the weight has traveled to the end of the lead screw.

Option seven was written as an aid to the balancing process. Centering all three balancers on their lead screws allows the divers to grossly adjust the vehicle balance with weights, while reserving the ability to make precise balance adjustments in all directions with the balancers. The program centers the weight as follows. A large negative position is commanded to the LM629 to move the weight to the end of the lead screw. The program enters a loop to wait for the limit switch status byte to reveal that the weight has reached the negative-end limit switch. Then, since the length of the lead screw is known in encoder-counts, a position corresponding to half the length of the lead screw is commanded to the LM629.

4.2 Attitude Control System

The attitude control system was designed to demonstrate the “controllability” of STAR. Controllability refers to the suitability of a dynamic system for closed-loop control. It was hoped that, by simultaneously controlling the vehicle’s three rotational DOF, the suitability of STAR’s computer/electronics, sensor, and propulsion subsystems for incorporation in closed-loop control schemes would be demonstrated.

4.2.1 Hardware

The attitude control system used the thrusters of the propulsion subsystem for actuation, the three rate sensors of the sensor subsystem for feedback, and the onboard computer for software implementation. Since all of these hardware platforms are detailed at length in Chapter 3, they will not be discussed here.

4.2.2 Implementation

The attitude control system is implemented in software using the C programming language. A detailed listing of the program, entitled ATTITUDE.C, is contained in Appendix C. The highlights of this program will be discussed here.

The main of the program starts by reading the D.C. biases of the rate sensors. The program prompts the user to have the divers hold the vehicle steady in the water before the biases are read. Once the divers have steadied the vehicle, a carriage return starts the bias-reading process. Ten rate sensor readings are taken and averaged to determine the angular rate bias of each sensor. The proportional and integral gains for the three axes (six gains total) are read from a file named "gain_file." The LM629 chips used to control the thruster motors are then reset using the function 'resetallmot();' initialized with appropriate filter values using the function 'loadfiltall();' and their position offsets set to zero with the function 'zerooffsetall().' The program now enters into the control loop. The attitude control system uses a proportional-integral (P-I) control law. The control law is calculated separately for each axis' rotational DOF. The loop is set to run at 30 Hz.

The program was originally written to force the angular rates to zero. To judge system response, however, the ability to apply a step input to the yaw control law (rotation about the Z-axis), while controlling the pitch and roll rates to be zero, was added to the code. This was accomplished by adding a user-selectable amount to the integral term in the control law. 'Yaw_cmd' is the variable name of this integral term modifier.

To facilitate data-gathering of the system response to the step input, the step input is not added until 15 control loops have passed ($i = 15$). Starting with loop number one, the yaw rate, yaw command, and yaw integral term are written into a two-dimensional data array named 'dt[][].' The control loop and data-gathering processes end when the user types 'e.' The final portion of ATTITUDE.C is devoted to writing the data array to a data file.

This chapter documents the program of check-out and testing that was undertaken upon STAR's construction. Section 5.1 describes the results of the pool test sessions. Section 5.2 presents attitude control data acquired during the August 17, 1991 testing session.

5.1 Testing

Each subsection of this section describes one testing session. All testing sessions took place on separate days at MIT's Alumni Swimming Pool.

5.1.1 February 9, 1991

The pressure vessel plates were completed by December, 1990. The plates were welded together and the entire vessel anodized by the end of January, 1991. On February 9, 1991, the pressure vessel and its compartment doors were transported to the swimming pool for leak-testing of the pressure vessel's welds and the compartment doors' O-ring seals. The testing procedure consisted of simply weighting down the empty box with weights, such that it was negatively buoyant, and leaving it underwater in the deepest part of the pool for several hours.

Unfortunately, upon subsequent removal of the pressure vessel from the pool, it was discovered that the pressure vessel was not leak-proof. The pressure taps in the doors were used in conjunction with an air pump to over-pressure the interior of the box, allowing the use of soap bubbles for leak detection. It was found that there were numerous leaks in the pressure vessel welds.

To remedy this problem, it was necessary to remove the layer of anodizing surrounding the leaks to permit re-welding. This was a difficult and time-consuming process, since the anodizing had to be ground down using Cobalt grinding disks. In hindsight, it is clear that the pressure vessel

should have been leak-tested immediately after it was welded, rather than waiting until after it was anodized, to permit easy re-welding of leaky joints.

5.1.2 June 8, 1991

This pool test saw the first integration testing of all but two of STAR's subsystems. The goals of this test were to leak-test the pressure vessel and to test subsystem integration. The balancer and vision subsystems were not yet ready for testing on this date. The control station computer was networked to the onboard computer, and the propulsion subsystem was sent actuation commands from the control station.

Two of the eight thruster motors failed to respond during the pool test. During subsequent debugging, it was found that, in each thruster, one of the motor driver power transistors had been shorted to the heat sink. The pressure system appeared to have water droplets on the inside of the pressure lines. No leaks in the system could be found, however. The pressure vessel was found to be completely waterproof.

5.1.3 July 6, 1991

The balancer subsystem, without closed-loop control, was integrated into the vehicle for this pool test. While the balancers were effective in helping the balancing process, the PVC balancer tubes leaked badly. One of the thruster motors failed completely, and another failed in one direction only, pointing to a deep-seated bug in the motor driver design. After a short period of teleoperated control utilizing the remaining six thrusters, the high-current power abruptly failed.

The failure of the power subsystem was found to be the result of blown fuses. One of the 15A fuses in each battery pair was blown. These fuses were replaced with 20A fuses. The problem with the motor drivers was determined to be incorrectly-sized resistors used to turn on the optoisolators. This problem was fixed, and the motor drivers were re-sealed with potting compound. The threaded caps of the balancer tubes were found to be the source of the balancer tube leaks. To remedy this leak, the

Teflon tape previously used to seal the threaded caps was replaced by Swak thread sealant.

5.1.4 July 20, 1991

This pool test was fairly successful as the vehicle was flown around the pool for approximately 45 minutes. At this point, however, the balancers began to leak, which caused the vehicle to become negatively buoyant. The vehicle was pulled from the water, and the balancers were removed to allow further testing. After a short period of teleoperated control, however, the high-current power failed again. Also, several water droplets were again noticed in one of the air lines of the pressure system.

The balancers were severely corroded by the water, forcing a major overhaul. The problem with the high-current power was again caused by blown fuses. As a result, 35A fuses were used to replace the 20A fuses. It was hypothesized that the water droplets found in the pressure system were the result of insufficient pressure in the system to expel water from small leaks around pressure connectors. To remedy this, a stronger spring was placed in the modification to the SCUBA regulator, producing an over-pressure of approximately 5 psi. above ambient.

5.1.5 August 3, 1991

The overhaul of the balancers was not yet completed in time for this pool test. The monocular camera housing was added to the vehicle, providing vision feedback to the remote operator. This pool test was very successful, as 7 hours of vehicle teleoperation were performed without interruption, surpassing STAR's design goal of six hours of continuous operation. None of the fuses of the power system blew during this test. The camera worked well, providing good resolution of the underwater environment. The increased pressure in the pressure system was sufficient to keep the pressure lines clear of any water.

This pool test was well documented. Videotape recordings were made of the output of the vehicle camera during flight. Views of the vehicle from a separate, stationary camera at the pool surface were also recorded. The

vehicle was also photographed extensively using an underwater 35 mm camera.

5.1.6 August 17, 1991

The August 17th pool test was extremely successful in every way. The vehicle was operated continuously for approximately six hours. The balancer tubes, recently overhauled and re-sealed using copious quantities of Teflon tape, were found to be water-tight. The balancers were used to successfully balance the vehicle using closed-loop control of the balancer weights. The attitude control system was implemented for the first time. The gains of the attitude control system were adjusted and a viable combination obtained. The ability of the attitude control system to force the vehicle's three angular rotation rates to zero was clearly demonstrated by the fast, powerful response to diver-induced disturbance torques. Also, the system response to two different-sized step inputs to the integral term of the yaw-axis control law was observed. Data was recorded in computer files to document this system response. This data is discussed at length in Section 5.2 below. The pressure lines of the pressure system were observed to be free of water droplets.

5.2 Attitude Control Data

Data was recorded during the August 17, 1991 pool test to document the system response of the attitude control system. The three-axis vehicle control system was started as described in Section 4.2. A step input was then applied to the yaw axis of the control law. The data gathered was yaw rate, integrated yaw rate, and yaw command.

Data was taken for step inputs of 1 and 2. Figure 5.1 shows the integrated rate term of the yaw control law for both step inputs. Note that the step was applied to the integral term after 30 control loops, which corresponds to approximately 1 s. Figure 5.2 shows the yaw command calculated by the control law. Figure 5.3 presents the resulting yaw angular rate.

It is evident from Figure 5.3 that the yaw angular rate sensor had saturated at approximately -35° , meaning that the vehicle yaw rate had exceeded the

maximum sensitivity of the rate sensor. This sensor saturation resulted in an inaccurate integrated rate term, producing the inaccurate constant downward slope of the integrated rate plot shown in Figure 5.1. These inaccuracies in the control law calculation, resulting from sensor saturation, are potentially de-stabilizing. This is evident in the angular rate overshoot, which was approximately 12%. Referring to Figure 5.1, if the sensor had not saturated, the plot of the integrated rate would not be a straight line. The slope of the integrated rate plot would likely decrease in magnitude as the integral approached zero, resulting in less angular rate overshoot.

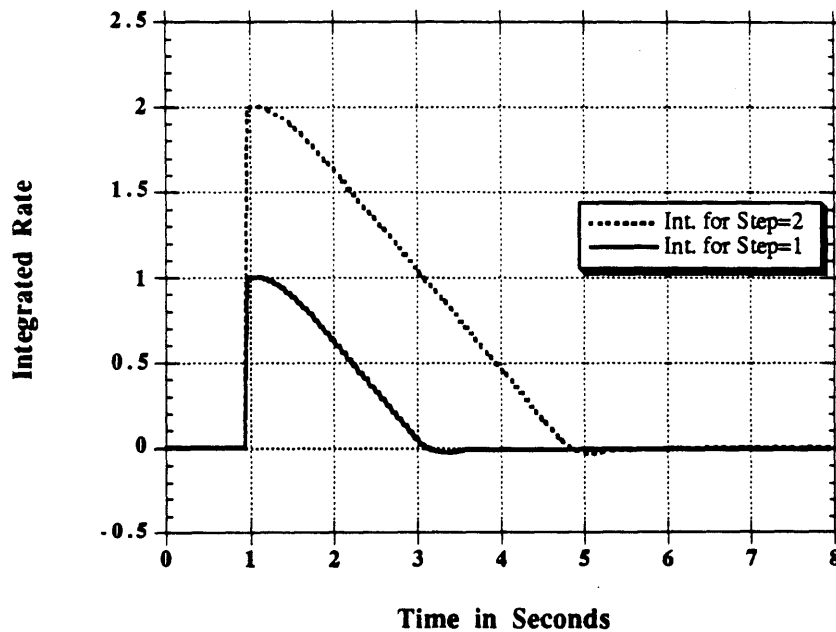


Figure 5.1 Integrated Rate vs. Time

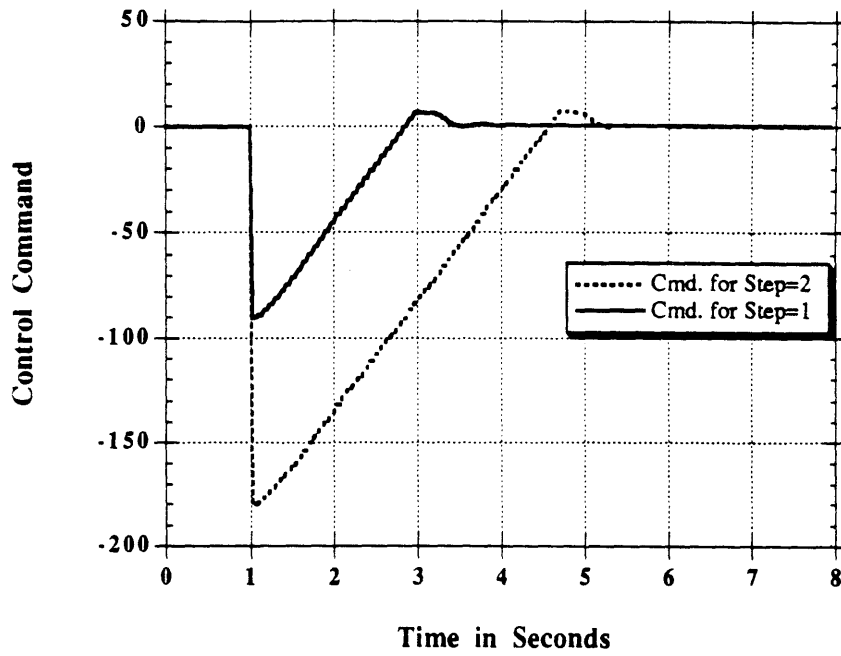


Figure 5.2 Control Command vs. Time

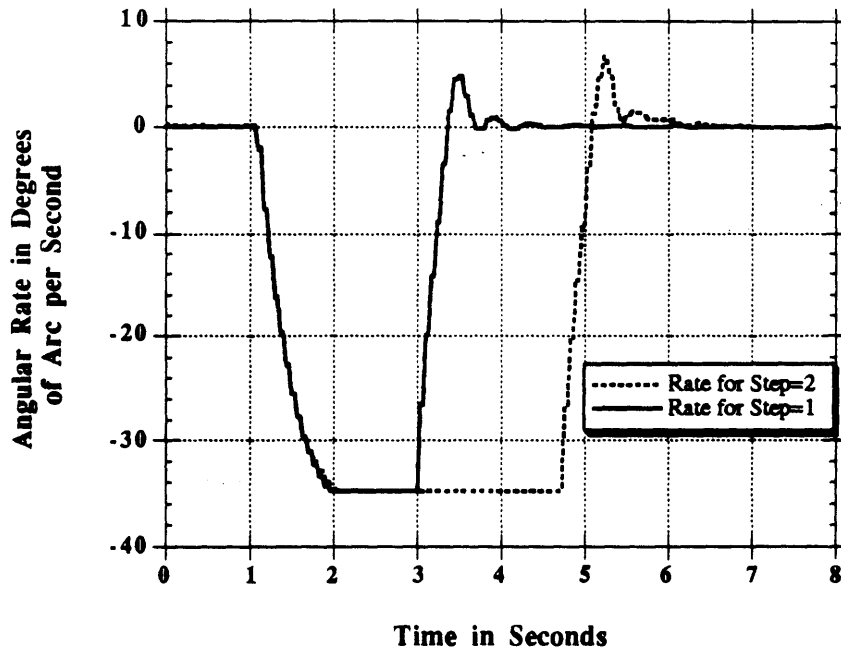


Figure 5.3 Angular Rate vs. Time

Despite the above-mentioned problems resulting from sensor saturation, the data presented above clearly documents STAR's well-behaved response to vehicle control. The yaw rate actuation is shown to be fast and powerful, accelerating the vehicle from 0 °/s to greater than 35 °/s in approximately 1 s. The computer/electronics subsystem is shown to be fast enough to allow this stable implementation of closed-loop vehicle attitude control.

STAR's design, formulated in Chapters 2 and 3, was validated by the program of testing and check-out described in Section 5.1. After the sixth pool test, on August 17, 1991, all vehicle subsystems were proved to be operational.

Several of the key departures of STAR's design from past SSL vehicle designs were shown to provide improvements in efficiency and/or performance. The choice of non-pressurized, Aluminum enclosures for the computer/electronics and power subsystems instead of pressurized, foam/fiberglass enclosures was shown to eliminate past problems with buoyancy and reconfigurability. The use of the QNX operating system to construct a computer network containing the onboard computer and the control station computer was found to be very successful. The QNX network was found to provide improved communications over the PiVeCS communications link used in past SSL vehicles. Specifically, the use of QNX resulted in more accessible message-passing, the ability to link more than one computer, remote control of computer node tasks, and the ability to download software from one node to another. These improvements resulted in faster software development for STAR than had been seen for past SSL vehicles. This increase in development speed was demonstrated by the fact that STAR's attitude control system was developed in three months, whereas a similar system developed for ASTRO required one year [5]. The use of the STD-bus to interface the digital electronics circuit cards to the computer network was successful. The choice of an STD-bus over a PC-bus resulted in a more space-efficient electronics compartment than those found in past SSL vehicles. STAR's balancer subsystem was successful in fulfilling its goal of facilitating vehicle balancing. This subsystem was found to reduce the amount of pool test time required for vehicle balancing.

Thus, STAR's design was successful in producing a neutral-buoyancy simulation testbed for space robotics research that improved upon past SSL vehicle designs.

Recommendations for future work include the following improvements to the vehicle. Optical encoders should be added to the thruster motors to enable closed-loop angular velocity control of each thruster. This would improve the precision and reliability of the thruster actuation. The vision subsystem should be expanded to include a stereoscopic camera pair. A tilt-and-pan (T&P) platform should also be constructed for these cameras. The Y-balancer can be moved aft from its present position on the top mounting structure to a position behind the Y-thruster. This would permit the T&P unit to be mounted on the front of the top mounting structure. Interference with the end of the Z-balancer may be encountered as a result of this move. Additional computer(s) should be added to facilitate vision-based navigation. RAM cards should be placed on the STD-bus to facilitate the gathering of data during real-time control operations.

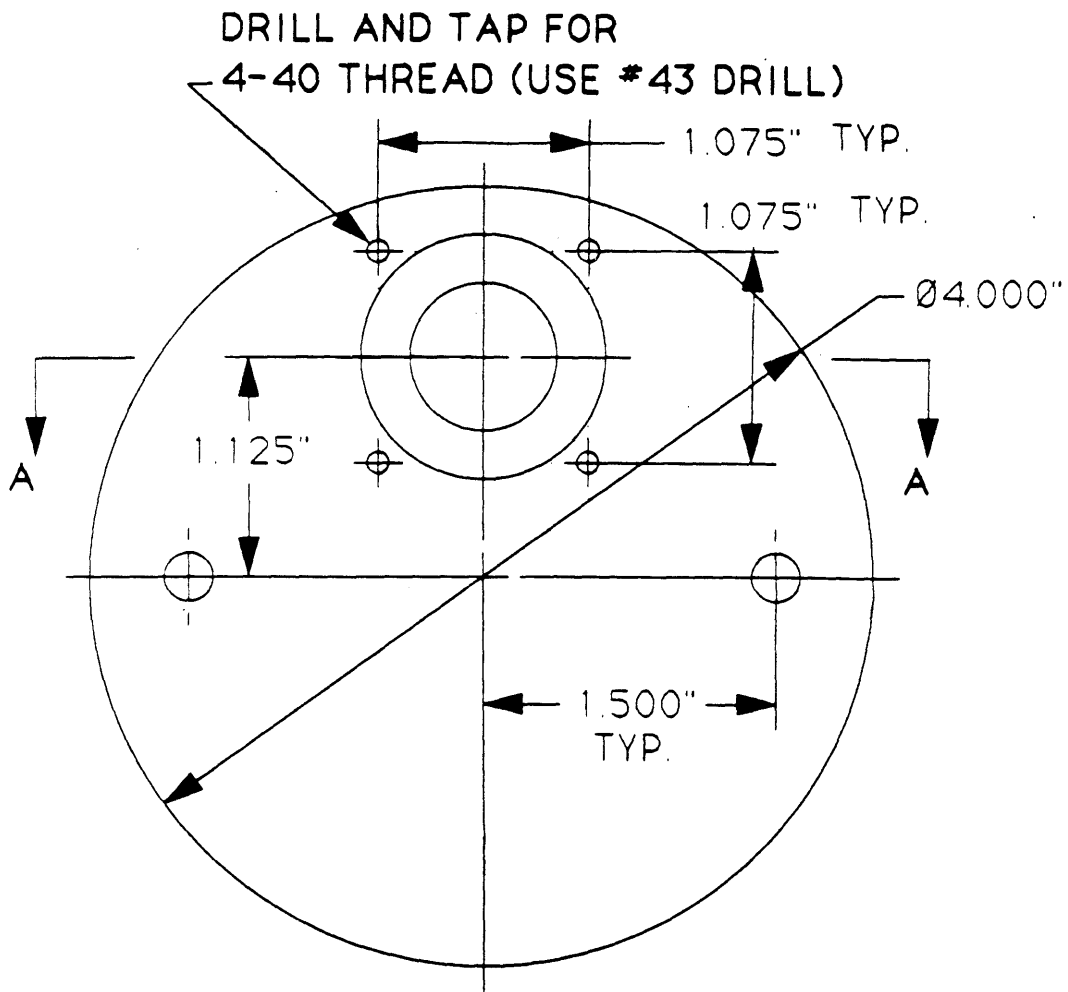
References

- [1] Shain, Eric B., "Design and Control of a Beam Assembly Teleoperator," S.M. Thesis, Department of Aeronautics and Astronautics, Massachusetts Institute of Technology, 1983.
- [2] Spofford, John R., "Coordinated Control of a Free-Flying Teleoperator," Sc.D. Thesis, Department of Aeronautics and Astronautics, Massachusetts Institute of Technology, 1988.
- [3] Tarrant, Janice M., "Attitude Control and Human Factors Issues in the Maneuvering of an Underwater Space Simulation Vehicle," S.M. Thesis, Department of Aeronautics and Astronautics, Massachusetts Institute of Technology, 1987.
- [4] Kowalski, Karl Gerald, "Applications of a Three-Dimensional Position and Attitude Sensing System for Neutral Buoyancy Space Simulation," S.M. thesis, Department of Aeronautics and Astronautics, Massachusetts Institute of Technology, 1989.
- [5] Power, Wendy Marie, "Closed-Loop Depth and Attitude Control of an Underwater Telerobotic Vehicle," S.M. thesis, Department of Aeronautics and Astronautics, Massachusetts Institute of Technology, 1990.
- [6] Alexander, Harold L., "Experiments in Teleoperator and Autonomous Control of Space Robotic Vehicles," Proceedings of the American Control Conference, Vol. 2, p. 1474, July 28, 1991.
- [7] Machlis, Matthew A., "Investigation of Visual Interface Issues in Teleoperation Using a Virtual Teleoperator," S.M. thesis, Department of Aeronautics and Astronautics, Massachusetts Institute of Technology, 1991.

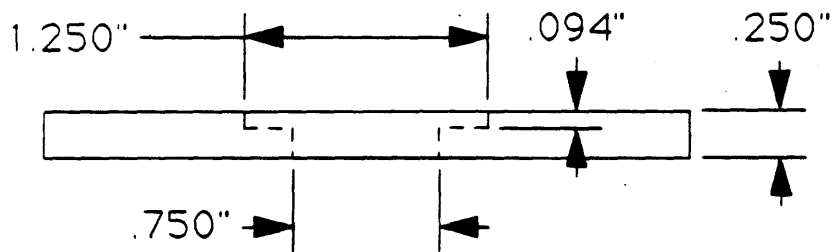
- [8] Cinniger, Anna G., "Control Interfaces and Handling Qualities for Space Telerobotic Vehicles," S.M. thesis, Department of Aeronautics and Astronautics, Massachusetts Institute of Technology, 1991.
- [9] Sanner, Robert M., "The Pilot-Vehicle Communications System (PiVeCS)," SSL Report, June, 1990.
- [10] Flint, Susan Elizabeth, "Investigation of the Effect of Duct Configuration on Shrouded Propellers," SSL Report #41-81, June, 1981.
- [11] Scardera, Michael P., "Duct Testing: Search for an Improved Neutral Buoyancy Propulsion System," SSL Report #38-83, May, 1983.

Appendix A

Drawings

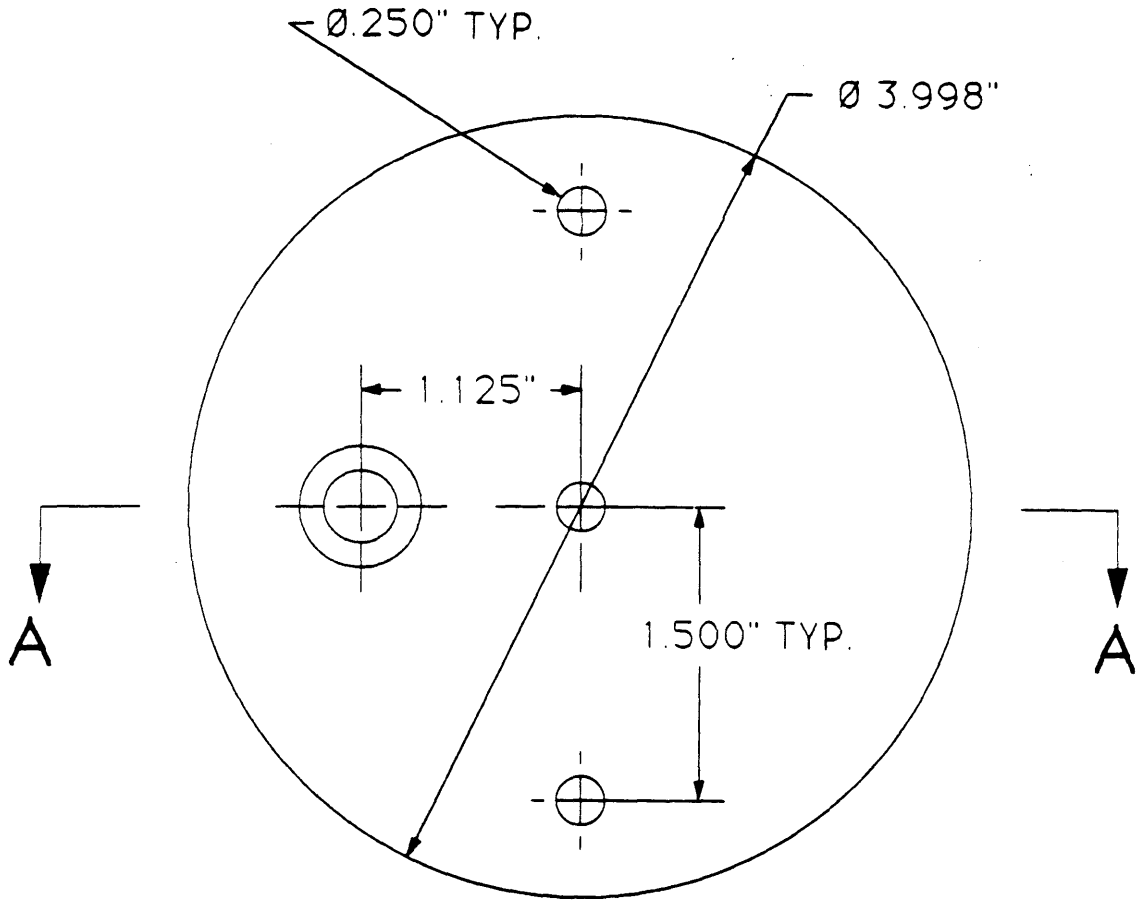


FRONT VIEW

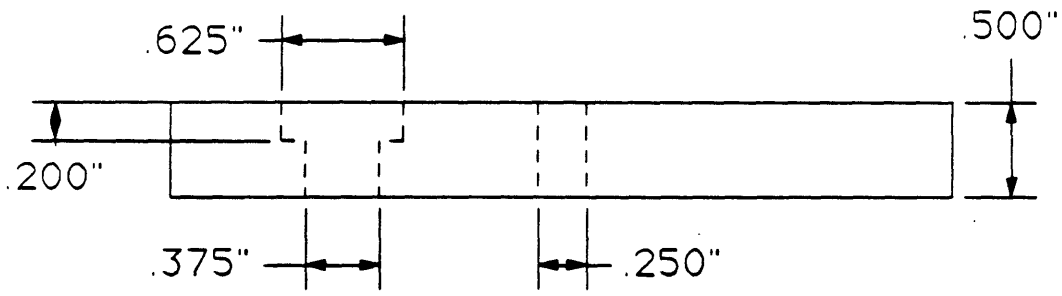


SECTION A-A

Figure A.1 Balancer Motor Disk



FRONT VIEW



SECTION A-A

Figure A.2 Balancer Lead Screw Mounting Disk

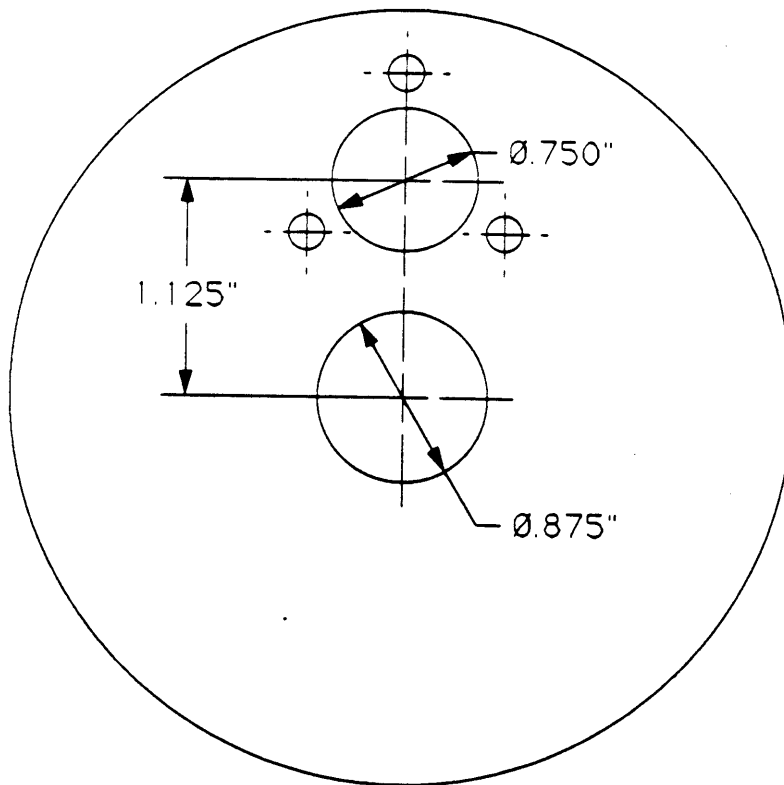
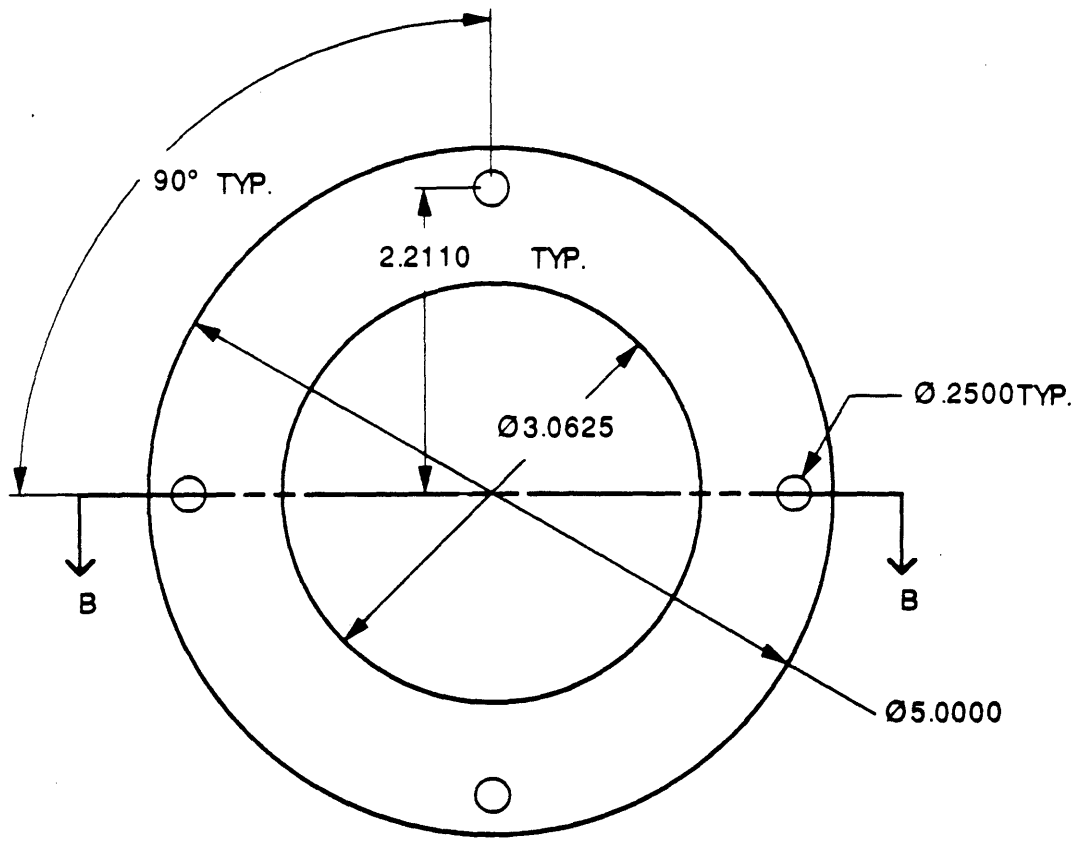


Figure A.3 Balancer Weight



**TUBE FLANGE - Make two
of Aluminum**

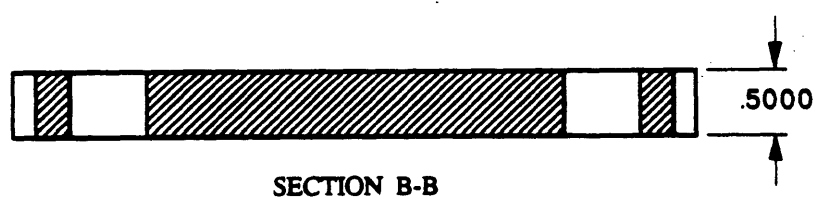
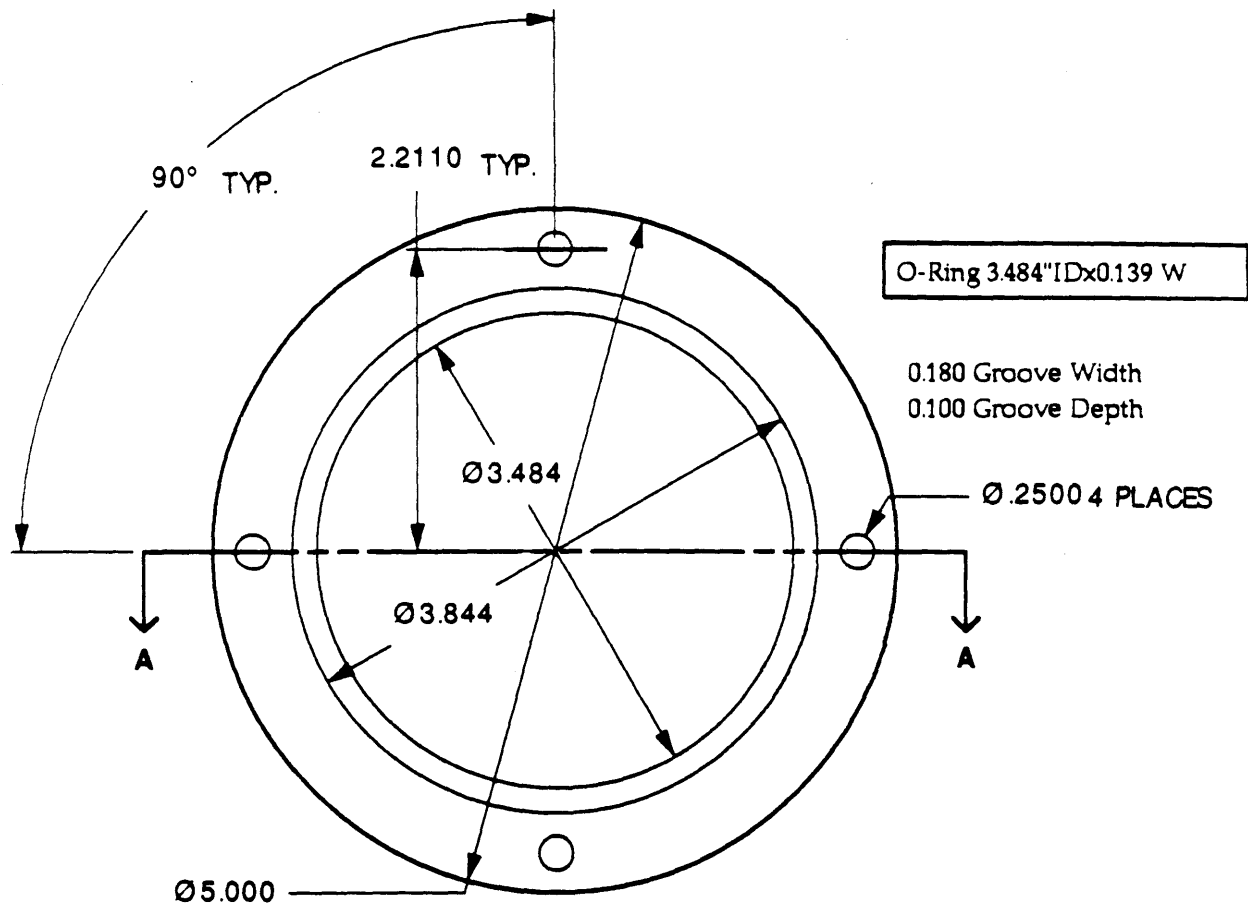


Figure A.4 Camera Housing Tube Flange



FRONT DISK - Make 1 of Lexan

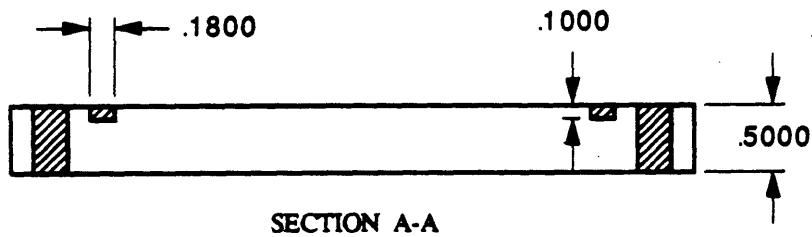
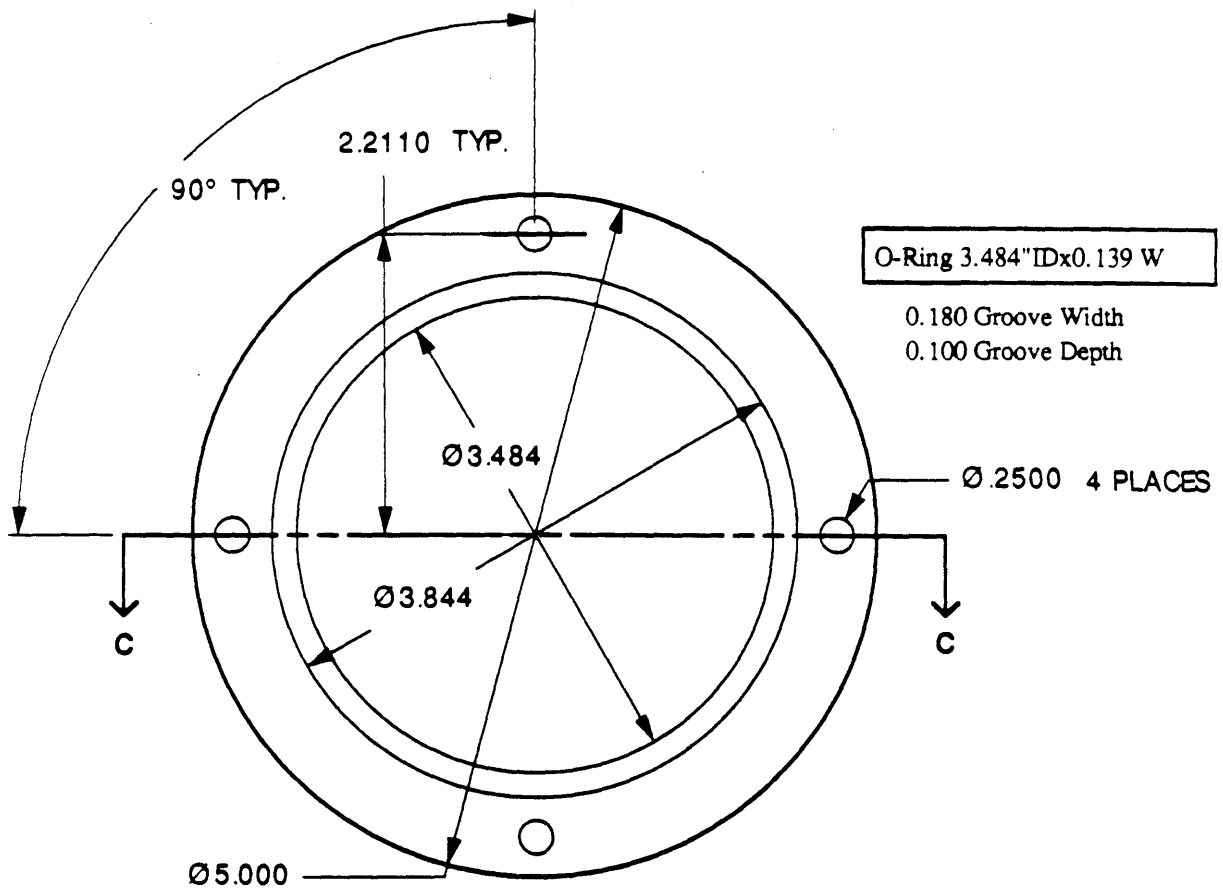


Figure A.5 Camera Housing Front Disk



BACK DISK - Make 1 of Aluminum

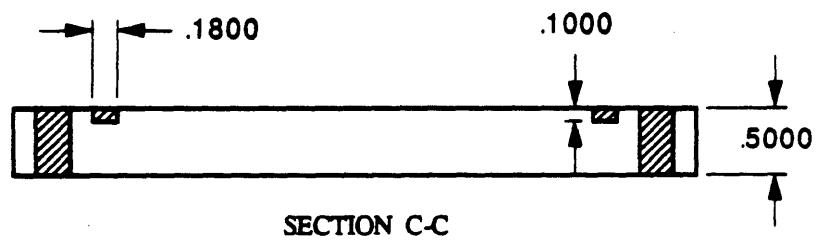


Figure A.6 Camera Housing Back Disk

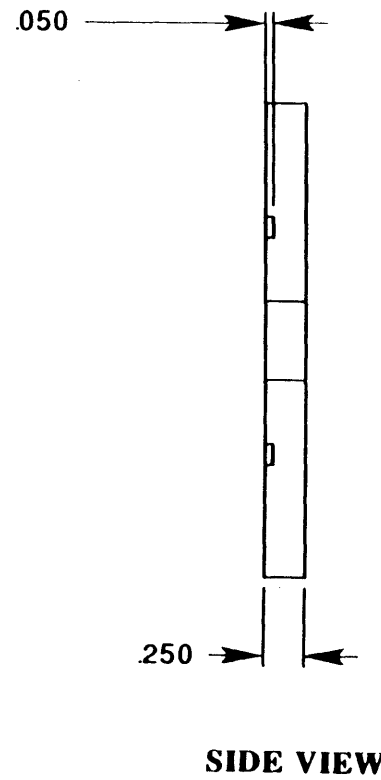
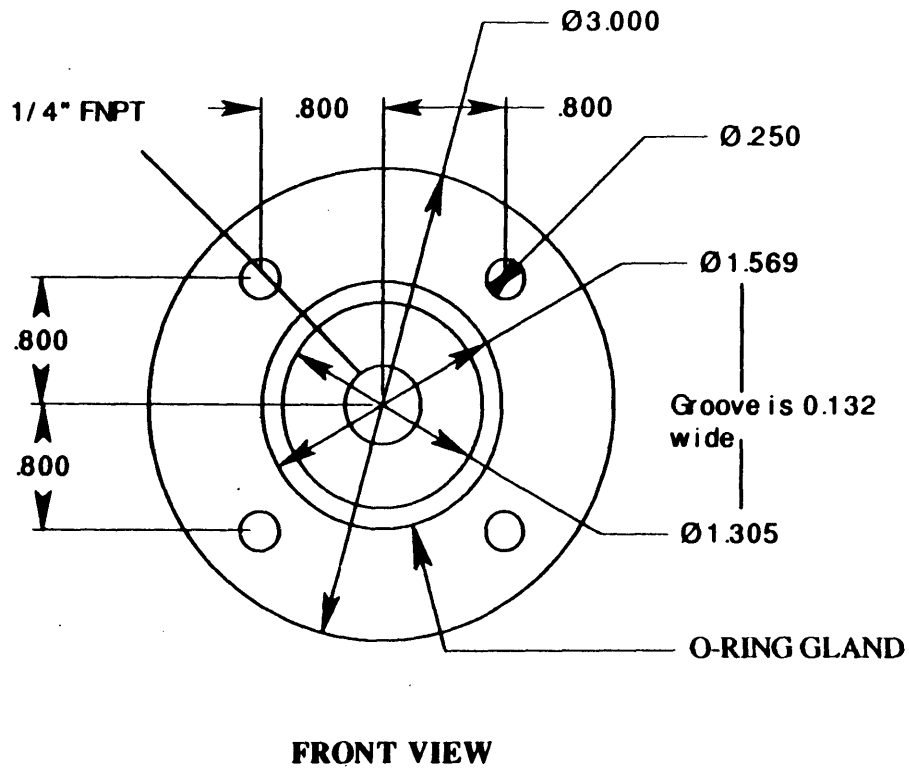


Figure A.7 Coaxial Pass-Through Plate for Electronics Door

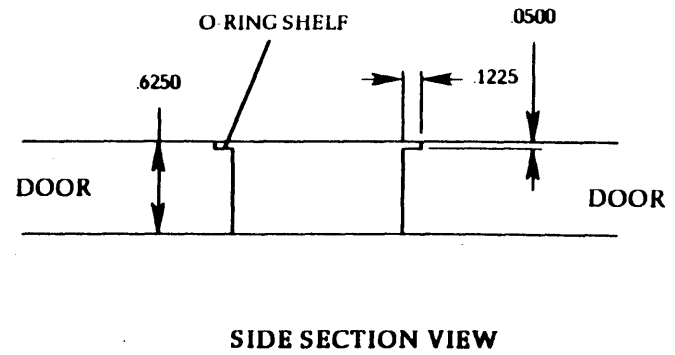
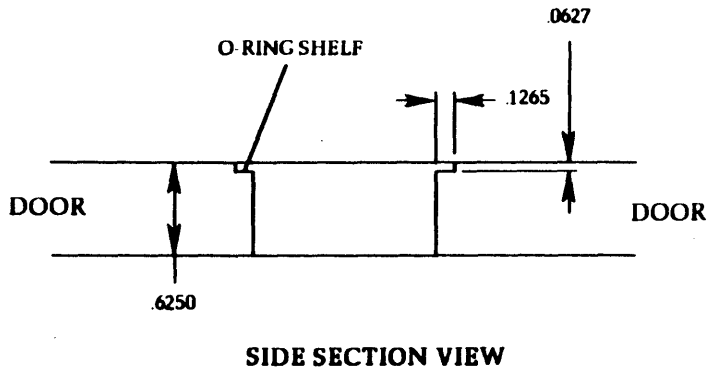
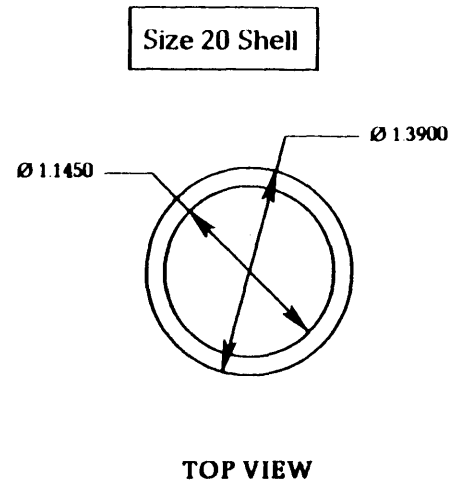
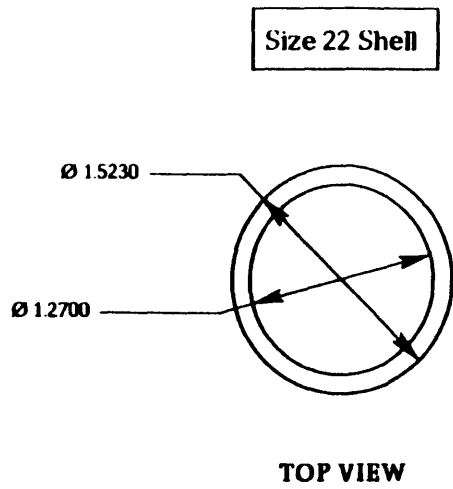


Figure A.8 Connector Hole Details

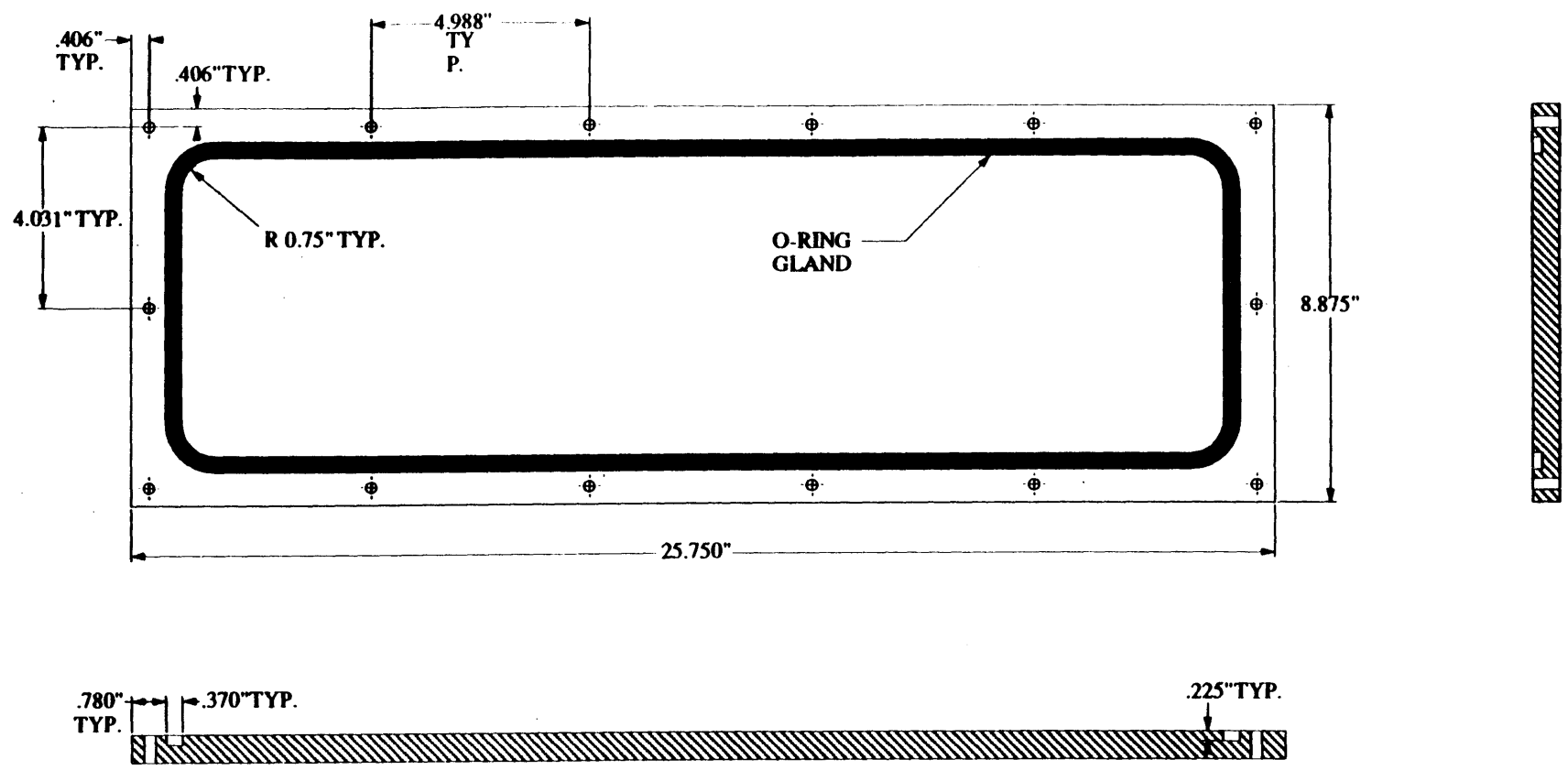


Figure A.9 Battery Compartment Door

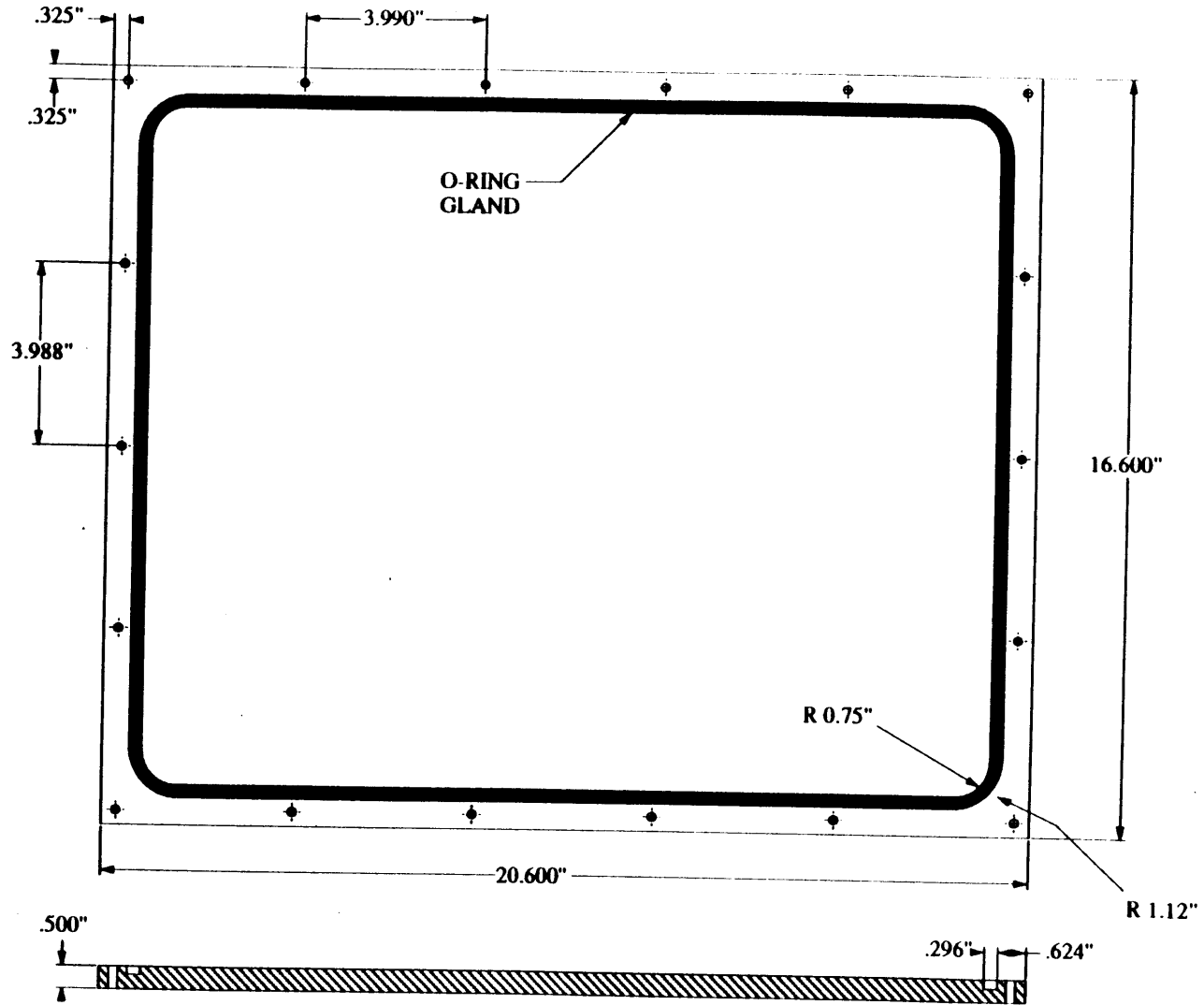


Figure A.10 Electronics Compartment Door

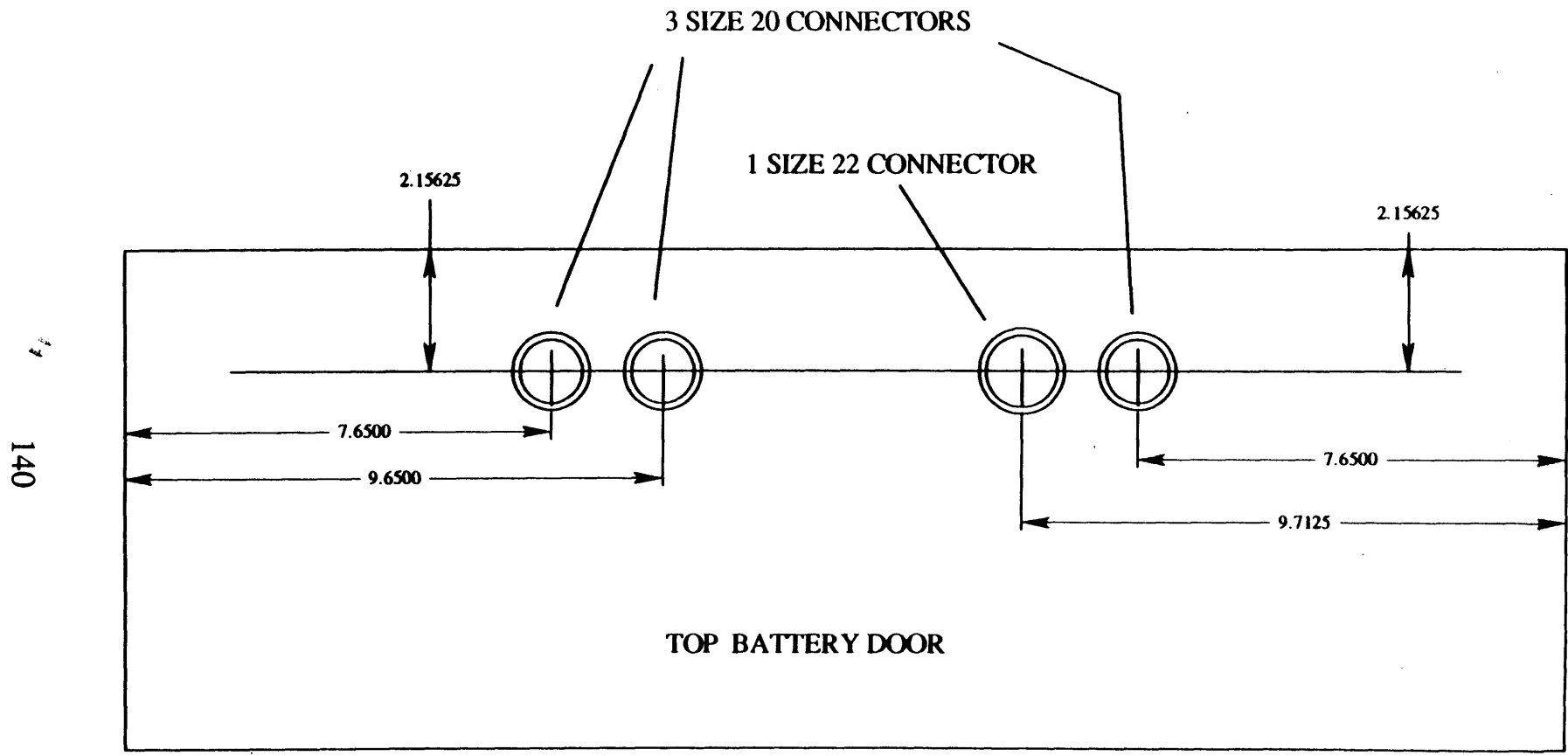


Figure A.11 Top Battery Door Connector Hole Layout

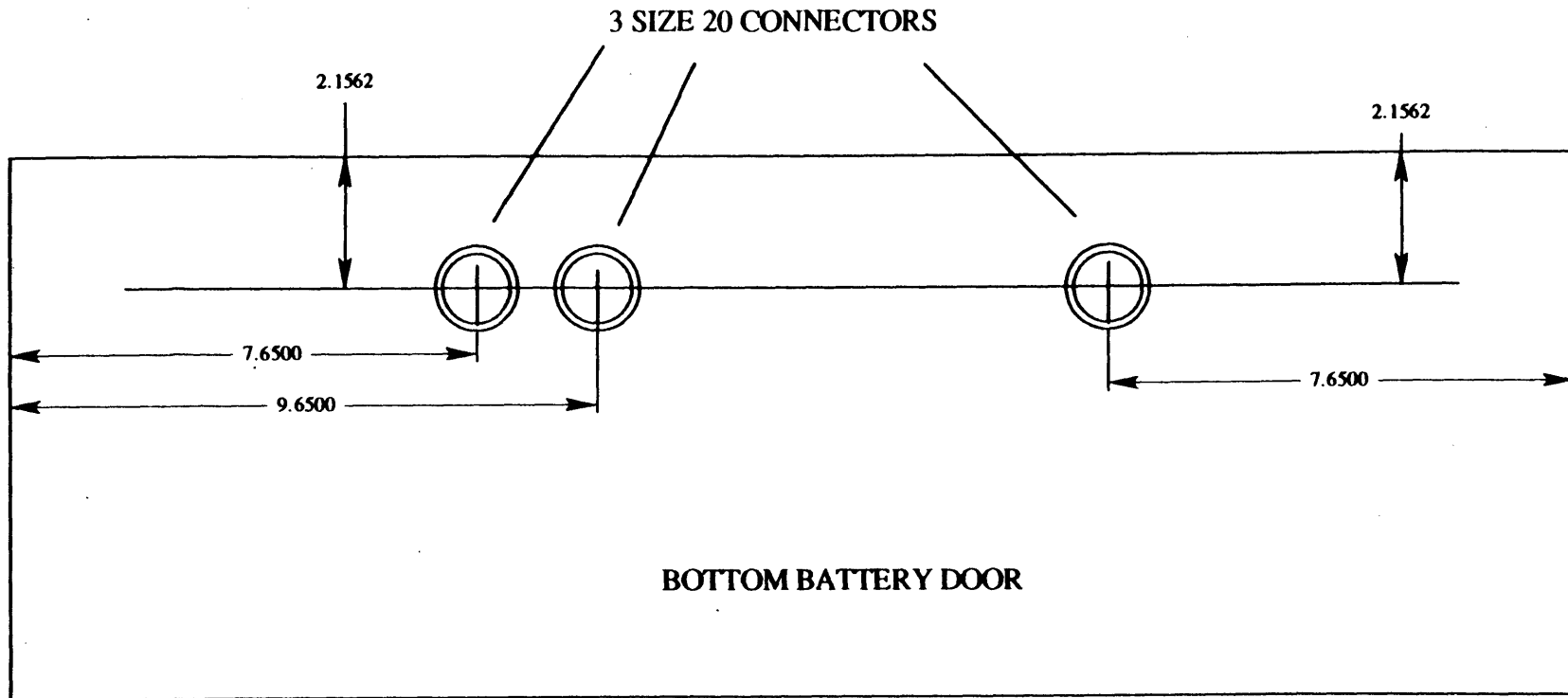


Figure A.12 Bottom Battery Door Connector Hole Layout

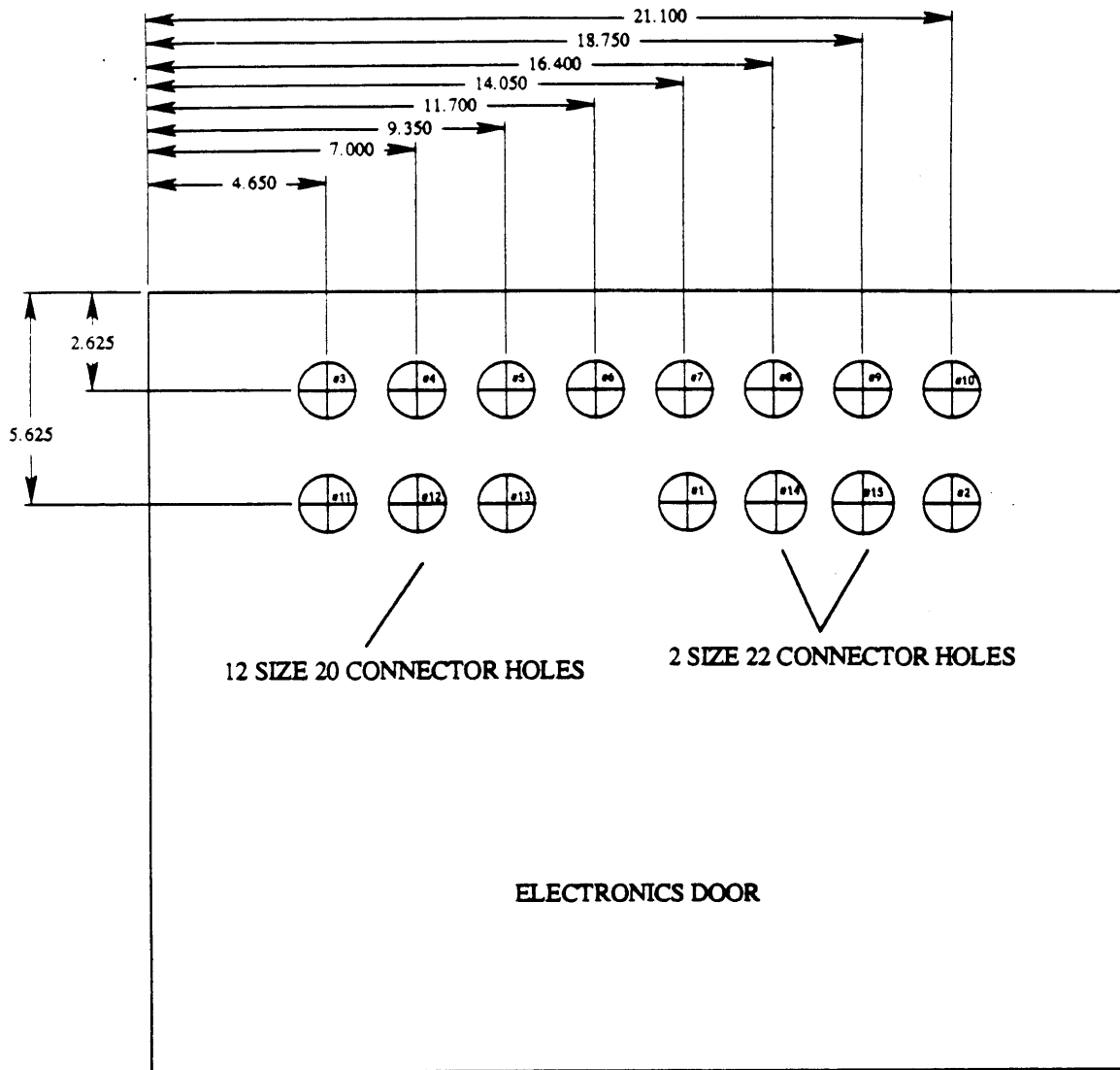


Figure A.13 Electronics Door Connector Hole Layout

B.1 STD - Bus

BX-SERIES CARD RACKS

INTRODUCTION

This section contains detailed specifications and guidelines for installation and use of the Pro-Log BX-Series card racks. All 711X-Series motherboard information in Section 1 of this guide applies to the card racks in this section.

CARD RACK FEATURES

- Uses Pro-Log's 711X-Series motherboards and retains their features
- Available in 3-, 6-, 9-, 12-, 15-, 18-, 21-, 24-, and 26-slot sizes
- Table- and rack-mounting versions in all sizes
- Rugged plated-steel construction
- Slot positions numbered at front of each rack
- Low profile
- Optional card restraint available for each size
- Multiple 711X motherboards can be mounted within a card rack
- End plates have large access windows
- Screws and washers provided for reversing end plates and their mounting flanges
- Open design provides maximum air circulation for cooling

CARD RACK SPECIFICATIONS

Environmental

- Free-Air Operating Temperature: -40°C to +90°C
- Storage Temperature: -40°C to +100°C
- Operating Noncondensing Relative Humidity: 5% to 95%

Electrical

All 711X-Series motherboard electrical specifications in Section 1 apply to the BX-Series card racks.

Mechanical

All 711X-Series motherboard mechanical specifications in Section 1 apply to the motherboards in BX-Series card racks.

- STD BUS Compatibility: No exceptions
- Connector Spacing: $\frac{3}{8}$ " (15.875 mm)
- Sheet Metal Type: Cold rolled steel
- Sheet Metal Thickness
 - Top and Bottom: 0.05" (1.2 mm)
 - End Panels: 0.09" (2.2 mm)
- Sheet Metal Finish: Zinc plate with clear chromate
- Weight (X = number of slots)
 - Table-Mount Models: 11.4 + X(2.43) oz; (approx.) 323 + X(68.9) g
 - Rack-Mount Models: 26.2 + X(2.43) oz; (approx.) 744 + X(68.9) g
- Maximum Card Weight: Loading every slot with cards of the following weights causes less than 0.05-inches (1.3-mm) deflection of the card rack's bottom side.
 - BX26 Racks: 1.5 lb (0.68 Kg) per card
 - BX12 Racks: 7 lb (3.2 Kg) per card
- Rack-Mount End Panel Load: 100 lb (445 N) max (With panel mounted using tapped holes and load applied to end of cantilever.)
- Dimensions (Table-Mount Models)
 - Overall: See Figure 5
 - End Panel: See Figure 6
 - Top and Bottom: See Figure 7
- Dimensions (Rack-Mount Models)
 - Overall: See Figure 8
 - End Panel: See Figure 9
 - Top and Bottom: See Figure 7
- Card Position Numbering: Top, front edge, L to R

B.2 A/D Card SPECIFICATIONS

(typical @ 25°C with nominal supply voltage unless otherwise noted)

RTI-1260 ANALOG INPUT CARD

Number of Input Channels	16 Single-Ended or 8 Differential (Jumper Selectable) Expandable to 32 Single-Ended or 16 Differential Using Two Plug-In Multiplexers (ADI Part #OA10)
Input Overvoltage Protection ¹	± 35V (Dielectrically Isolated)
Input Impedance	> 10 ⁸ Ω
Input Bias Current	± 50nA
Analog Connector	3M #3433, 50 pin
A/D Input Ranges ²	0 to +10V, ± 10V
A/D Resolution	12 Bits (4096 Counts)
A/D Output Codes ²	Binary, Offset Binary, Two's Complement
Instrumentation Amplifier Gain Ranges	1 to 1000V/V (Resistor Programmable Gain)
Gain Equation	$G = 1 + \frac{20k\Omega}{R_G}$
A/D Conversion Time	25μs
System Throughput ³	25,000 Channels/sec (G < 150) 20,000 Channels/sec (150 < G < 300) 11,000 Channels/sec (G = 1000)
Common Mode Voltage (CMV)	± 10V min
Common Mode Rejection (CMR)	78dB
Linearity	± 1/2LSB
Differential Nonlinearity	± 1LSB
Total System Error (Adjustable to Zero)	± 0.01% of FSR (Gain = 1 to 10) ± 0.05% of FSR (Gain = 100) ± 0.1% of FSR (Gain = 1000)
Temperature Coefficient	
Gain	± 30ppm/°C of FSR (G = 1)
Offset	± 100ppm/°C of FSR (G = 1000) ± 10ppm/°C of FSR (G = 1) ± 100ppm/°C of FSR (G = 1000)
INTERFACE PARAMETERS	
Compatibility	Meets all Electrical and Mechanical STD Bus Specifications
Implementation	Memory Mapped I/O Compatible with All CPU Types Port Mapped I/O Compatible with 8080, 8085, 8086 and Z-80 Family of CPUs
Address Selection	3 Contiguous Bytes in a 16 Byte Block. (Jumper Selectable in Any One of 256 Locations in 64K of Memory Space.)
Port Selection	3 Contiguous Ports in a 16 Port Block (Jumper Selectable on Any 16 Port Boundary in Either an 8-Bit or 16-Bit Port Image.)
Expansion Options	MEMEX and IOEXP Fully Supported with Jumper Selectable Enable High, Enable Low or Ignore Expansion Options.
POWER REQUIREMENTS	
	+ 5V ± 5% @ 450mA (On-Board dc/dc Converter Generates an Isolated ± 15V to Power the Data Acquisition Components.)
TEMPERATURE	
Operating	0 to +70°C
Storage	-55°C to +85°C
RELATIVE HUMIDITY	
	Meets or Exceeds MIL-STD 202 Method 103

B.3 D.C. Driver Card

ELECTRICAL AND ENVIRONMENTAL SPECIFICATIONS

7501 Medium Power DC Output Card Electrical Specifications

MNEM.	PARAMETER	RECOMMENDED OPERATING LIMITS			ABSOLUTE NON-OPERATING LIMITS		
		MIN.	TYP.	MAX.	MIN.	MAX.	UNIT
V _{CC}	Supply voltage	4.75	5.00	5.25	0.0	7.00	Volt
T _A	Free air temp	0	25	55	-40	75	°C
R _H	Humidity ①	5		95	0	95	%RH

User Electrical Characteristics over Recommended Operating Limits

MNEM.	PARAMETER	MIN.	TYP.	MAX.	UNIT
V _{OL}	Low level user output voltage		45	0.8	volt
V _{OH}	High level user output voltage			50	volt
I _{OL}	Low level user output current			225	mA
V _c	User-supplied clamp voltage			50	volt
	User output current duty cycle			100	%

STD BUS Electrical Characteristics over Recommended Operating Limits

MNEM.	PARAMETER	MIN.	TYP.	MAX.	UNIT
I _{CC}	STD BUS supply current		600	1000	mA
	STD BUS input load		See STD BUS Edge Connector Pin List		
	STD BUS output drive		See STD BUS Edge Connector Pin List		

Switching Characteristics over Recommended Operating Limits

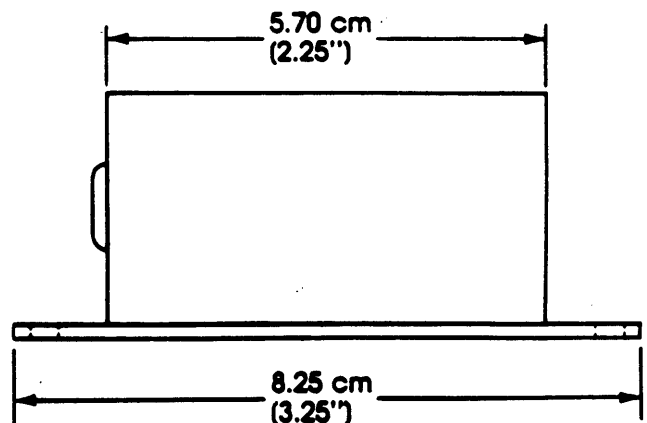
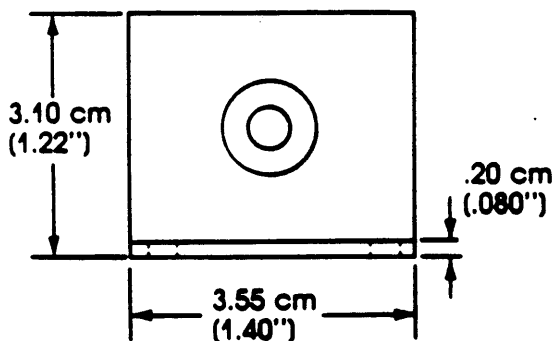
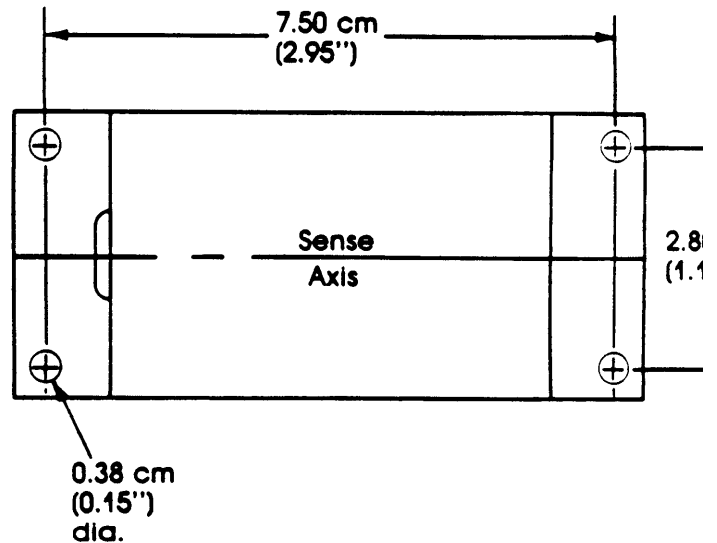
MNEM.	PARAMETER	FROM	TO	MIN.	TYP.	MAX.	UNIT
T _{PHL}	PROPAGATION TIME	STD DATA BUS	USER IFC		110		nsec.
T _{PLH}	PROPAGATION TIME	"	"		110		nsec.
T _{PHL}	PROPAGATION TIME	USER IFC	STD DATA BUS		110		μsec.
T _{PLH}	PROPAGATION TIME	"	"		110		μsec.

B.4 Rate Sensors

ANGULAR RATE SENSOR SPECIFICATIONS ONE AXIS UNITS Models ARS-C121-1A, ARS-C131-1A, ARS-C141-1A

• Power supply requirements:	+15 VDC \pm 5% 20 mA maximum -15 VDC \pm 5% 20 mA maximum
• Output	0 VDC at zero angular rate \pm 10 VDC at full scale angular rate
• Sensitivity	ARS-C121-1A \pm 30°/second full scale ARS-C131-1A \pm 100°/second full scale ARS-C141-1A \pm 300°/second full scale
Output current:	\pm 10 mA maximum
• System frequency:	360 Hz nominal
Scale factor error:	2%
Resolution:	Limited by noise
Linearity:	< 0.1% full scale
Hysteresis:	Negligible
Temperature offset:	0.5% full scale/°C maximum
Warm up drift:	Less than 1% full scale
• Frequency response:	DC to 50 Hz
• Output noise:	15mV RMS maximum
• Operating and storage temperature range:	-20°C to +50°C
Storage and operating altitude:	Unlimited
• Shock:	200 G
Life:	50,000 HRS. MTBF minimum
• Dimensions:	See drawing
• Weight:	110 grams (4 oz.)
• Note:	Custom units with variation in these parameters are available. Note: Above units optionally available with digital output.

Specifications subject to change without notice.



B.5 Accelerometers

SPECIFICATIONS				NAS SERIES				
GENERAL				ENVIRONMENTAL				
<u>Parameter</u>	<u>Value</u>	<u>Units</u>	<u>Notes</u>	<u>Parameter</u>	<u>Abbr.</u>	<u>Value</u>	<u>Units</u>	<u>Notes</u>
Input Range*	± 2	g		Temperature Range				
Output	0.5	Vdc	grounded load	Operating	T _o	-40° to +100°	°C	-40° to +212° F
Acceleration Limits	1500	g	any direction	Compensated	T _c	0° to +70°	°C	+32 to +158° F
ELECTRICAL (@ 12 Vdc, 25° C unless stated otherwise)				MECHANICAL				
Excitation	E _i	8-16	Vdc	Weight		10	grams	without cable
Supply Current	I	5	mA	Case		Valox thermoplastic polyester		
Output Impedance	Z _o	50	Ω					
Insulation Resistance	R _{iso}	100	MΩ					
			@ 50 Vdc					
<i>* Other ranges ±1 g to ±100 g are available for OEM applications; please consult factory</i>								
PERFORMANCE								
<u>Parameter</u>	<u>Value</u>	<u>Units</u>	<u>Notes</u>					
Zero Acceleration Output	2.50 ± .10	Vdc	Reverse polarity protected					
Sensitivity	1.25 ± .03	V/g	gravimetric calibration					
Non-Linearity	±1.0 (Max)	%FSO						
Frequency Response	0-200	Hz	±5% max, ref 100 Hz					
Mounted Resonant Frequency	550	Hz	typical					
Damping Ratio	0.7		typical					
Cross Axis Sensitivity	±3.0 (Max)	%FSO	±1% typical					
Thermal Accuracy - Offset	±2.0	%FSO*						
Thermal Accuracy - Full Scale Output	±2.0	%FSO*						
Notes: 1. All values are maximum. 2. Positive acceleration gives positive voltage; negative voltage for negative acceleration. 3. All values measured in reference to 12 Vdc, 25° C (77° F). 4. 0 to 70° C in reference to 25°C.								

A.1 Balancer Control Code

```
/* THIS FILE IS BAL.C */
/* by Captain Kurt and the Harald Meister */
/* based on detailed code by Mike "bit-shift" Valdez */
/* and the original balancer control software kurtgo.c */
/* updated by Harald 8/14/91 */

#include <stdio.h>
#include "balcommand.h"

#define OFFSET 0x000f
#define TRUE 1
#define BASE 0x250
#define BUSYBIT 0x01
#define MAXCNT 32000
#define WUPPER 0xff00
#define WLOWER 0x00ff
#define LUPPER 0xffff0000
#define LLOWER 0x0000ffff
#define CENTER 7000

/* read LM628 status register */
unsigned short rdstatus(n)
    int n;
{
    unsigned short status;
    status = io_in(BASE + 2*n - 2);
    return(status);
}

/* wait until LM629 is ready */
void ready(n)
```

```

int    n;
{
    unsigned loop_cntr;
    unsigned short status;

    for(loop_cntr = 0;loop_cntr<MAXCNT; loop_cntr++) {
        status = rdstatus(n);
        if (!(status & BUSYBIT))
            break;
    }
    if(loop_cntr == MAXCNT) {
        printf("\nBoard not responding \n");
        printf("last status read - %x\n\n", status);
        exit(-1);
    }
}

```

/* write command byte to LM629 */

```

void wrcmd(code,n)
    char code;
    int n;
{
    void wrbyte();

    ready(n);
    io_out(BASE + 2*n - 2, code);
}

```

/* write data byte to LM629 */

```

void wrbyte(byte, n)
    char byte;
    int n;
{
    io_out(BASE + 2*n - 1, byte);
}

```

/* read data byte from LM629 */

```

char rdbyte(n)
    int n;
{

```

```

    char byte;

    byte = io_in(BASE + 2*n - 1);
    return(byte);
}

/* write data word (2 bytes) to LM629 */
void wrword(word, n)
    unsigned word;
    int n;
{
    ready(n);
    wrbyte((word & WUPPER) >> 8, n);
    wrbyte(word & WLOWER, n);
}

/* read data word from LM629 */
unsigned rdword(n)
    int n;
{
    unsigned high,low;

    ready(n);
    high = (((unsigned) rdbyte(n)) << 8) & WUPPER;
    low = ((unsigned) rdbyte(n)) & WLOWER;
    return(high | low);
}

/* write double data word (4 bytes) to LM629 */
void wr2words(words, n)
    long words;
    int n;
{
    wrword(((unsigned)((words&LUPPER) >> 16), n);
    wrword(((unsigned)(words&LLOWER), n);
}

/* read double data word from LM629 */
long rd2words(n)

```

```

int n;
{
    long top,bottom;

    top = ((long)rdword(n) << 16) & LUPPER;
    bottom = (long)rdword(n) & LLOWER;
    return(top | bottom);
}

/* load filter parameters */
void loadfilt(kp,ki,kd,li,dsi,n)
    unsigned kp,ki,kd,li;
    unsigned short    dsi;
    int n;
{
    unsigned ctrlwd;
    unsigned short status;
    ctrlwd = (((int)dsi<<8) | 0x000f);

    wrcmd(LFIL,n);
    printf("\n\tLatest Status - %02x\n", rdstatus(n));
    wrword(ctrlwd,n);
    printf("\n\tLatest Status - %02x\n", rdstatus(n));

    wrword(kp,n);
    printf("\n\tLatest Status - %02x\n", rdstatus(n));
    wrword(ki,n);
    printf("\n\tLatest Status - %02x\n", rdstatus(n));
    wrword(kd,n);
    printf("\n\tLatest Status - %02x\n", rdstatus(n));
    wrword(li,n);
    printf("\nFilter Parameters Just Written to LM629\n");
    status = rdstatus(n);
    printf("\n\tLatest Status - %02x\n", status);
    wrcmd(UDF,n);
    printf("\nFilter Just Updated - UDF Command\n");
    status = rdstatus(n);
    printf("\n\tLatest Status - %02x\n", status);
}

```

```

}

/* ----- */

main()
{
    int offset, n, i, choice; /* n is number of LM629 to test */
    int go,ans,goneg,blah,wait;
    unsigned kd,kp,ki,li;
    unsigned short dsi, status, limit, bitter, ender;
    unsigned cmdwrđ;
    long newpos,pos,vel,acc;

    printf("\nEnter motor number--> ");
    scanf("%d", &n);
    wrcmd(RESET, n); /* Reset the chip */
    status = rdstatus(n);
    wrcmd(DFH,n);
    kd = 400;kp = 500; ki = 0; li = 0;
    dsi = 0x0000;

    loadfilt(kp,ki,kd,li,dsi,n); /* Load control gains to chip*/
    printf("\nFILTER PARAMETERS LOADED");
    status = rdstatus(n);
    printf("\nLatest Status - %02x", status);

    pos = 0; newpos = 0;
    choice = 0;go = 1; /* Initialize loop control variables */
    vel = 0x01010c6f;
    acc = 0x0001008c;

    while(go){
        if (choice ==1){ /* <-----Want to change the filter parameters */
            printf("\nLatest Status - %02x", status); /*Input Control Gains*/
            printf("\nInput Proportional gain ---->(%d) ",kp);
            scanf("%d",&kp);
            printf("\nInput Derivative Gain ----->(%d) ",kd);
            scanf("%d",&kd);
            printf("\nInput Integral Gain ----->(%d) ",ki);
            scanf("%d",&ki);
        }
    }
}

```



```

printf("\nInput Anti-Reset Windup ---->(%d) ",li);
scanf("%d",&li);

loadfilt(kp,ki,kd,li,dsi,n); /* Load control gains to chip*/
printf("\nFILTER PARAMETERS LOADED");
status = rdstatus(n);
printf("\n\tLatest Status - %02x", status);
}
else if(choice == 2){ /* Read Motor Position */
wrcmd(RDRP,n);
printf("\nReading Motor %d Position",n);
pos = rd2words(n); /* read where LM629 thinks the motor is */
printf("\n\tPosition %x\t%d", (int) pos, pos);
status = rdstatus(n);
printf("\n\tLatest Status - %02x", status);
}
else if(choice == 3){ /* Want to move the motor or change traj. */
printf("\nDo you want to change trajectory? Enter #(y=1/n=0)");
scanf("%d",&ans);
if (ans){
printf("Input new acceleration --->(%d)",acc);
scanf("%d",&acc);
printf("Input new velocity ----->(%d)",vel);
scanf("%d",&vel);
}
wrcmd(RDRP,n);
printf("\nReading Motor %d Position",n);
pos = rd2words(n);

printf("\n\tPosition - %x\t%d", (int) pos, pos);
status = rdstatus(n);
printf("\n\tLatest Status - %02x", status);
printf("\nInput the Desired Absolute Position --> ");
scanf("%d",&offset);
newpos = offset;
wrcmd(LTRJ,n);
printf("\nLTRJ Command Issued");

cmdwrd = 0x002a;
wrword(cmdwrd, n); /* pos, veloc and accel data to be loaded */
wr2words(acc, n);

```

```

    wr2words(vel,n);
    wr2words(newpos,n);
    printf("\nNEW TRAJECTORY DATA LOADED\n");
    wrcmd(STT,n);          /* start trajectory command */
    printf("\nTRAJECTORY COMMANDED\n");
    status = rdstatus(n);
    printf("\n\tLatest Status - %02x", status);
}
else if(choice == 4){ /* Reset motor and redefine encoder zero*/
    wrcmd(DFH,n);
}
else if(choice == 5){ /* Reset motor and quit program */
    wrcmd(RESET,n);
    go = 0;
    status = rdstatus(n);
    printf("\n\tLatest Status - %02x\n", status);
}
else if(choice == 6){ /*Read status of switches with fake */
    limit = rdstatus(12); /* motor number 12 */
    printf("%02x",limit);
}
else if(choice == 7){ /* Move weight to end, then to center */
    limit = rdstatus(12);
    if(n == 9){ /* X-balancer Motor #9 */
        bitter = limit & 0x0030;
        printf("\nMoving weight toward limit switch..");
        if (bitter != 0x0010){
            wrcmd(LTRJ,n);
            wrword(0x002a,n);
            wr2words(acc,n);
            wr2words(vel,n);
            wr2words((long) -15000,n); /* Move weight to neg end*/
            wrcmd(STT,n);
            while(1){
                limit = rdstatus(12) & 0x0030;
                if(limit == 0x0010){ /* Weight has arrived!! */
                    wrcmd(DFH,n);
                    printf("\nWeight has hit limit switch -- Position=0");
                    printf("\nWeight now travelling to center...");
                    break; /* Stop checking switch */
                }
            }
        }
    }
}

```

```

    }
}

    }
wrcmd(LTRJ,n);
wrword(0x0002,n);
wr2words((long) CENTER,n);    /* Move weight to center */
wrcmd(STT,n);
}

else if(n == 10){    /* Y-Balancer Motor #10 */
    bitter = limit & 0x000c;
    printf("\nMoving weight toward limit switch..");
    if (bitter != 0x0004) {
        wrcmd(LTRJ,n);
        wrword(0x002a,n);
        wr2words(acc,n);
        wr2words(vel,n);
        wr2words((long) -15000,n);    /* Move weight to neg end*/
        wrcmd(STT,n);
        while(1){
            limit = rdstatus(12) & 0x000c;
            if(limit == 0x0004){    /* Weight has arrived!! */
                wrcmd(DFH,n);
                printf("\nWeight has hit limit switch -- Position=0");
                printf("\nWeight now travelling to center...");
                break;    /* Stop checking switch */
            }
        }
    }

    }
wrcmd(LTRJ,n);
wrword(0x0002,n);
wr2words((long) CENTER,n);    /* Move weight to center */
wrcmd(STT,n);
}

else if(n=11){    /* Z-balancer motor 11 */
    bitter = limit & 0x0003;
    printf("\nMoving weight toward limit switch..");
    if (bitter != 0x0001){
        wrcmd(LTRJ,n);

```

```

        wrword(0x002a,n);
        wr2words(acc,n);
        wr2words(vel,n);
        wr2words((long) -15000,n); /* Move weight to neg end*/
        wrcmd(STT,n);
        while(1){
            limit = rdstatus(12) & 0x0003;
            if(limit == 0x0001){ /* Weight has arrived!! */
                wrcmd(DFH,n);
                printf("\nWeight has hit limit switch -- Position=0");
                printf("\nWeight now travelling to center...");
                break; /* Stop checking switch */
            }
        }
        wrcmd(LTRJ,n);
        wrword(0x0002,n);
        wr2words((long) CENTER,n); /* Move weight to center */
        wrcmd(STT,n);
    } /* End of z-bal else */
    while(1){ /* check to see if traj. is done */
        wrcmd(RDRP,n);
        ender = CENTER - rd2words(n);
        if (ender < 5){ /* if traj. almost complete*/
            printf("\n\nThe Weight is Centered(BAM!)...Have a nice day");
            wrcmd(RDRP,n);
            pos = rd2words(n);
            printf("\n\nPosition %x\t%ld", (int) pos, pos);
            break; /* stop checking status byte */
        }
    } /* End of centering loop */
} /* End of choice 7 */

if (go) {
    printf("\n\nChoose a Control Option:");
    printf("\n\n\t(1) Change Filter Parameters");
    printf("\n\n\t(2) Read Current Real Position");
    printf("\n\n\t(3) Move Motor to New Position and/or Change Traj.");
    printf("\n\n\t(4) Zero Encoder Position");
    printf("\n\n\t(5) Reset Motor and Quit Program");
}

```

```
printf("\n\t(6) Read switch status");
printf("\n\t(7) Center Balancer");
printf("\nEnter Option----> ");
scanf("%d",&choice);
    }          /* End of if statement for choices*/
}          /* End of while loop */
} /* end main */
```

A.2 Attitude Control Code

```
                /* THIS FILE IS ATTITUDE.C */
/* program to do preliminary feedback control using the
angular rate sensors */

/* */
#include <stdio.h>
#include <math.h>
#include <io.h>
#include <dev.h>
#include <timer.h>
#include "mocofprot.h"

#define RED 0x8440
#define CYAN 0x8340
#define GREEN 0x8240
#define BRIGHT 0x2
#define FAIL 10.
#define MAXROW 120 /* maximum rows for data array */

/*****
/* screen_init() is a function to set up the computer screen */
/* displaying information
*/

void screen_init()
{
    int e_attr, c_attr, s_attr, d_attr;
    int shadow, blank;

    set_option(stdin, get_option(stdin) & ~(EDIT|ECHO));
    set_option(stdout, get_option(stdout) & ~(EDIT|ECHO));

    if (term_load(stdout))
    {
        term_clear(0);
        term_box_fill(0,0,80,25,(0x80 | 7) << 8,0,0xdb);
        e_attr = (4 | 0x80) << 8 | 0;
    }
}
```

```

        c_attr = (0x80 | 2) << 8;
        s_attr = (0x80 | 5) << 8;
        d_attr = (0x80 | 1) << 8;
        blank = 0x80 << 8;
        shadow = 0x80 << 8 | 0x2;
    }
}

main()
{
    int          i,j;
    float  roll_gain, pitch_gain, yaw_gain;
    float  roll_bias, pitch_bias, yaw_bias;
    float  int_roll, int_pitch, int_yaw;
    float  roll_r, pitch_r, yaw_r;
    float  roll_igain, pitch_igain, yaw_igain;
    float  rollrate, pitchrate, yawrate;
    float  rcmd, pcmd, ycmd;
    float  yaw_cmd;
    float  dt[MAXROW][3];
    char   ch;
    int          endflag, dataflag;

    shell("slice 1 1");
    term_clear(0);
    screen_init();
    term_printf(2,2,CYAN,"STEADY THE VEHICLE PRESS RETURN\n");
    scanf("%c", &ch);
    term_printf(2,2,CYAN,"GETTING SENSOR BIAS VALUES  \n");
    get_bias();
    term_printf(2,2,CYAN,"READING IN SENSOR BIAS VALUES  \n");
    while((fp = fopen("sensor_bias", "r")) == 0);
    fscanf(fp, "%f", &roll_bias);
    fscanf(fp, "%f", &pitch_bias);
    fscanf(fp, "%f", &yaw_bias);
    fclose(fp);
    term_printf(2,2,CYAN,"SENSOR BIAS VALUES READ  \n");

    term_printf(3,2,RED,"NOW GETTING SENSOR CONTROL GAINS \n");
    while((fp = fopen("gain_file", "r")) == 0);

```

```

fscanf(fp, "%f", &roll_gain);
fscanf(fp, "%f", &pitch_gain);
fscanf(fp, "%f", &yaw_gain);
fscanf(fp, "%f", &roll_igain);
fscanf(fp, "%f", &pitch_igain);
fscanf(fp, "%f", &yaw_igain);
fscanf(fp, "%f", &yaw_cmd);
fclose(fp);
term_printf(3,2,RED,"CONTROL GAINS READ IN \n");
term_clear(0);
resetallmot();
printf("MOTORS RESET\n");
loadfiltall();
printf("FILTERS VALUES LOADED\n");
zerooffsetall();
printf("MOTORS INITIALIZED\n");
printf("%+4.3f\n", roll_gain);
printf("%+4.3f\n", pitch_gain);
printf("%+4.3f\n", yaw_gain);
printf("%+4.3f\n", roll_igain);
printf("%+4.3f\n", pitch_igain);
printf("%+4.3f\n", yaw_igain);

term_printf(10, 32, CYAN, "ROLL");
term_printf(11, 32, CYAN, "PITCH");
term_printf(12, 32, CYAN, "YAW");
term_printf(13, 32, CYAN, "ROLL CMD");
term_printf(14, 32, CYAN, "PITCH CMD");
term_printf(15, 32, CYAN, "YAW CMD");
dataflag = 0;
endflag = 1;
int_roll=0;
int_pitch=0;
int_yaw=0;
i = 0;
term_printf(1, 32, CYAN, "'d' to take data");
term_printf(2, 32, CYAN, "'e' to end program");
while(endflag) {
    while(char_waiting(stdin)) { /* check for key press */
        ch = getchar();

```



```

        if(ch == 'e')
            endflag = 0;
        else if(ch == 'd') {
            dataflag = 1;
            term_printf(3, 32, CYAN, "Taking data!!!!");
        }
    }

    /* force this task ready after 33 time slices */
    /* slice should be set to 1 msec */
    set_timer(TIMER_WAKEUP, FRELATIVE, 33);
    if((rollrate=roll_rate(roll_bias))!=FAIL)    roll_r = rollrate;
    if((pitchrate=pitch_rate(pitch_bias))!=FAIL)    pitch_r = pitchrate;
    if((yawrate=yaw_rate(yaw_bias))!=FAIL)    yaw_r = yawrate;

    int_roll=int_roll+(roll_r/30.);
    int_pitch=int_pitch+(pitch_r/30.);
    int_yaw=int_yaw+(yaw_r/30.);
    rcmd = -roll_gain*roll_r - roll_igain*int_roll;
    pcmd = -pitch_gain*pitch_r - pitch_igain*int_pitch;
    ycmd = -yaw_gain*yaw_r - yaw_igain*int_yaw;
    roll_tq(rcmd);
    pitch_tq(pcmd);
    yaw_tq(ycmd);

    term_printf(10, 40, RED, "%+3.2f", roll_r);
    term_printf(11, 40, RED, "%+3.2f", pitch_r);
    term_printf(12, 40, RED, "%+3.2f", yaw_r);
    term_printf(13, 41, RED, "%+3.2f", rcmd);
    term_printf(14, 41, RED, "%+3.2f", pcmd);
    term_printf(15, 41, RED, "%+3.2f", ycmd);

    if(dataflag) {
        if(i==15)int_yaw=int_yaw+yaw_cmd;
        dt[i][0] = yaw_r;
        dt[i][1] = int_yaw;
        dt[i][2] = ycmd;
        i++;
        if(i == MAXROW){
            term_printf(3, 32, CYAN, " ");
        }
    }

```

```

        i=0;
        dataflag = 0;
    }
}
resetallmot();
term_clear(0);
/* write data to a file */
while((fp=fopen("cdat", "w")) == 0);

fprintf(fp, "%4s\t%4s\t%4s\t%4s\t%4s\n", "rate", "int", "cmd", "", "", "");
for(i = 0; i < MAXROW; i++) {
    for(j = 0; j < 3; j++) {
        fprintf(fp, "%+9.6ft", dt[i][j]);
    }
    fprintf(fp, "\n");
}
fclose(fp);
term_printf(12, 20, RED, "MOTORS RESET: PROGRAM ENDED");
term_printf(24, 0, RED, "\n");
}

```